RARE EARTH ELEMENTS (REE) AS GEOCHEMICAL CLUES TO RECONSTRUCT HYDROCARBON GENERATION HISTORY.

by

DANIEL RAMIREZ-CARO

B.S., Universidad Autónoma de Chihuahua, 2008

A THESIS

submitted in partial fulfillment of the requirements for the degree

MASTER OF SCIENCE

Department of Geology
College of Arts and Sciences

KANSAS STATE UNIVERSITY
Manhattan, Kansas

2013

Approved by:

Major Professor
Dr. Matthew Totten

Copyright

Abstract

The REE distribution patterns and total concentrations of the organic matter of the Woodford shale reveal a potential avenue to investigate hydrocarbon maturation processes in a source rock. Ten samples of the organic matter fraction and 10 samples of the silicate-carbonate fraction of the Woodford shale from north central Oklahoma were analyzed by methods developed at KSU. Thirteen oil samples from Woodford Devonian oil and Mississippian oil samples were analyzed for REE also. REE concentration levels in an average shale range from 170 ppm to 185 ppm, and concentration levels in modern day plants occur in the ppb levels. The REE concentrations in the organic matter of the Woodford Shale samples analyzed ranged from 300 to 800 ppm. The high concentrations of the REEs in the Woodford Shale, as compared to the modern-day plants, are reflections of the transformations of buried Woodford Shale organic materials in post-depositional environmental conditions with potential contributions of exchanges of REE coming from associated sediments. The distribution patterns of REEs in the organic materials normalized to PAAS (post-Archean Australian Shale) had the following significant features: (1) all but two out of the ten samples had a La-Lu trend with HREE enrichment in general, (2) all but two samples showed Ho and Tm positive enrichments, (3) only one sample had positive Eu anomalies, (4) three samples had Ce negative anomalies, although one was with a positive Ce anomaly, (5) all but three out of ten had MREE enrichment by varied degrees. It is hypothesized that Ho and Tm positive anomalies in the organic materials of the Woodford Shale are reflections of enzymic influence related to the plant physiology. Similar arguments may be made for the Eu and the Ce anomalies in the Woodford Shale organic materials. The varied MREE enrichments are likely to have been related to some phosphate mineralization events, as the

Woodford Shale is well known for having abundant presence of phosphate nodules. The trend of HREE enrichment in general for the Woodford Shale organic materials can be related to inheritance from sources with REE-complexes stabilized by interaction between the metals and carbonate ligands or carboxylate ligands or both. Therefore, a reasonable suggestion about the history of the REEs in the organic materials would be that both source and burial transformation effects of the deposited organic materials in association with the inorganic constituents had an influence on the general trend and the specific trends in the distribution patterns of the REEs. This study provides a valuable insight into the understandings of the REE landscapes in the organic fraction of the Woodford Shale in northern Oklahoma, linking these understandings to the REE analysis of an oil generated from the same source bed and comparing it to oil produced from younger Mississippian oil. The information gathered from this study may ultimately prove useful to trace the chemical history of oils generated from the Woodford Shale source beds.

Table of Contents

List of Figures

List of Tables

Acknowledgements

I'd like to firstly thank Dr. Matthew Totten, and Dr. Sambhudas Chaudhuri for their passion and determination to build the Petroleum Geology program at K-State. I am grateful to both of you for taking me as a graduate student and patiently sharing your experience and knowledge. Thanks to Dr. Saugata Datta for his insight while collaborating as a committee member in this research project. I'd like to thank the OGS (Oklahoma Geological Survey) for their disposition to help me, and being accessible when collecting core samples from them. Thanks to Vy Jordan at the OPIC for opening doors into the core library. Thanks to Brian Cardott (OGS) for his availability and openness to share data. I am indebted to Greg Riepl whose commitment and love to K-State is reflected towards the Petroleum Geology grad students, as he showed to me by providing oil samples for this study. I want to thank KSU for accepting me into coming to pursue my Master's degree and offering a TA position. I also acknowledge the NSF EIDRoP Fellowship which through their vision I was trained to communicate research to different audiences. Thanks to Bill Barret whom year after year supports a Petroleum Geology student at KSU through the AAPG grant in aid, your contribution made my research possible. Thanks to UNISTRA for analyzing my samples and using their time and effort to make the results of this study possible, thanks to Dr. Norbert Clauer, Rene Boutin and K. Semhi. I appreciate Dr. Eric Maata's willingness to open up a lab space for my sample processing at the Chemistry-Biochemistry department. Thanks to Weatherford labs for providing quick services and supporting university students. Dereck Ohl, thanks for introducing me to the Petroleum Geology world. Luis Carlos Caro, thank you for sharing your vision of education and talking me into pursuing a Master's degree.

I'd like to acknowledge the K State AAPG Student Chapter for believing we can become young Petroleum Geologists who will be active in the industry. And special thanks to K-State alumni for their continual support to the Petroleum Geology program.

Dedication

I dedicate this work to my family who has always supported me. Thanks Mariah for bearing through the times I was away. Thank you God for guiding my ways, opening doors for me and walking me through places I never thought I would be at.

Preface

Energy is the driving force behind everything in our daily lives. It makes our everyday possible, even if we have no time to think about it. Simple things like our clothing, entertainment, to basic needs like transportation, communication and food require energy. Society subsists and finds most of its energy coming from hydrocarbons. Oil has made the world move for the past 100 years, influencing the global flow of business and commerce in our society.

More than 20,000,000 barrels of oil are consumed in the United States daily, and 750,000 barrels of oil are consumed in the world every thirteen minutes (Switch). As the global demand for transportation and commodities increases, the oil industry must constantly find, explore and improve technologies and methods to extract and recover oil. As oil supply in conventional resources starts to run low, the industry is diving quickly into the study and benefit of unconventional resources.

I believe new methods and new insights will be very important as we move into a future where demand for oil will keep rising and where scientific understanding of hydrocarbons will be needed. Early geologists turned to practical uses of geochemistry using the carbon ratio theory introduced by David White in 1915, and geochemistry has remained a powerful tool to understand generation, migration and correlation of hydrocarbons. This research project focuses on analyzing rare earth elements in the source rock, and oil produced from it, opening a new approach on geochemical studies for hydrocarbons, making viable the study of Rare Earth Elements in the organic matter.

Chapter 1 - Introduction

The geochemical analysis of the Woodford Shale and its produced oil is approached in this study by focusing on the REE. REE have been proved to be useful tracers in many geological and geochemical investigations and demonstrate important applications in igneous, sedimentary and metamorphic petrology (Rollinson, 1993). The potential of these elements is yet to be assessed in hydrocarbon generation. To date, studies by Abanda and Hannigan (2006), and the one by Dao-Hui et al., 2013 are the only ones that have examined the REE content in the organic matter, but they did not address the REE geochemical potential in the investigation of organic source bed and crude oil connection. In my study, REE geochemical investigations were targeted on oils generated in the Woodford shale and overlaying Mississippian formation located in the Anadarko Basin, north-central Oklahoma. This is the first study that takes a holistic approach to get an additional insight about oil generation using REE as an analytical means. Particular attentions have been given to correlations among the oils within the same general source beds, and to correlation between the Mississippian and Devonian oils to see the potential REE offer to do gecoehemical fingerprinting between the oils and their source beds.

Every hydrocarbon play originates from a source rock. Each play's viability, whether it would be conventional or unconventional is dependent primarily on the play's source rock. The other variables for oil and gas generation and accumulation comprise the petroleum system. In a conventional petroleum system, the source rock is buried to depths where oil is generated, the thermally mature source rock generates petroleum and it's expelled and transported through migration into a porous rock, the reservoir rock. This rock needs to be stratigraphically or structurally trapped beneath an impermeable rock layer called the seal. The foundation for a petroleum system is its source rock; all the other components of the system become irrelevant if the source rock is not present.

This project targets the Devonian Woodford Shale which is an organic-rich black shale formation of the Anadarko Basin located in the state of Oklahoma. This organic-rich shale is known to be a prolific source bed for the generation of gas and oil, due to its geological setting, thermal maturity, and total organic carbon percentages ranging from 2-14 (Cardott, 2008), and estimates indicate that as much as 85% of the oil produced in central and southern Oklahoma

originated in the Woodford (Jones and Philp, 1990). Exploration and interest in the Woodford shale has rapidly increased, this shale has shown thermal maturity at relatively shallow depths compared among other basins. Its high silica content allows it to generate fractures easily and responds well to fracturing techniques. The Woodford shale is not only the primary source bed, but it is also the drilling objective from where the oil is being extracted. According to Comer, The Woodford Shale contains high concentrations of marine organic matter, with mean organic carbon concentrations of 5.7 % weight for the Anadarko Basin (Oklahoma and Arkansas).

Exploration and Production companies are aware of the global challenge when finding and developing the remaining oil resources. Unconventional resources are becoming the option when producing oil, and studying the capacity of oil generation in source rocks finds its building block in petroleum geochemistry. Would there be an advantage on understanding the chemical interactions among different components such as organic matter and inorganic sediments in the source rock while this is being transformed through maturation? Would understanding the processes a source rock undergoes on its way to yielding hydrocarbons give us geochemical insight about the interactions occurring during transformation, which could possibly tell us about what to observe in a rock when looking for a rich organic source rock? These questions are sought to be answered through the study of the REE in the organic matter and the silicate-carbonate fraction of the Woodford shale separately, along with the study of crude oil produced in an unconventional way from this same source rock. The REE are also studied in the oil generated from the Woodford Shale. Calculated compositions of retained and expelled petroleum show evidence of oxygen's presence in petroleum (Sandvik et al., 1992), and knowing the affinity that REEs have for oxygen allows us to study them in hydrocarbons. Woodford shale associated oil is especially attractive because oil generated hasn't gone through migration beyond the source bed. Source rocks generate oil through maturation of organic matter. Conventionally the generated oil migrates into an overlaying reservoir rock which has good porosity or fractures able to hold the migrated hydrocarbons. Now with unconventional methods of hydrocarbon production, the source rock can be directly targeted for production, eliminating the migration effect into a reservoir rock, which allows us to see the behavior of REEs in such a closely related oil-source rock interconnection providing a clearer insight of organic matter transformation through maturation. This presents a great advantage when studying oil-source rock correlation, due to the elimination of variables like numerous geochemical interactions through migration

processes. Oils generated from a Mississippian formation and from the Woodford shale are analyzed in this study giving us insight of REE behavior in oils from different formations by doing oil-oil correlation.

1.1 Rare Earth Elements

The REEs or lanthanides (Ln) are a group of 14 elements from lanthanum (La) with atomic number 57, to lutetium (Lu) with atomic number 71. They are located in block 5d of the periodic table (Figure 1). Rare earth elements have completely filled $5s^2$, $4d^{10}$, $5p^6$, and $6s^2$ orbitals. The elements differ from each other in their electronic configurations based on electron filling at the next higher energy orbitals beyond $6s^2$, namely, either at 4f orbitals or a higher-energy 5d orbital. All the lanthanides are present as trivalent ions (Ln^{+3}), with the exceptions of europium (Eu) which also occurs as a divalent (Eu^{2+}),and the exception of cerium (Ce) which can also have a valence of 4 (Ce^{4+}).

There are several well-known coherent chemical properties of Ln atoms or ions in their interactions with compounds. These properties are shown on Table 1, where the atomic number and ionic radii's values are shown for the individual REE. A major property of the Ln is the well-known "lanthanide contraction", that is the progressive decrease in the size of the atom, or decrease in the ionic radius, with increasing atomic number (Smith, 1963; Evans, 1990). This

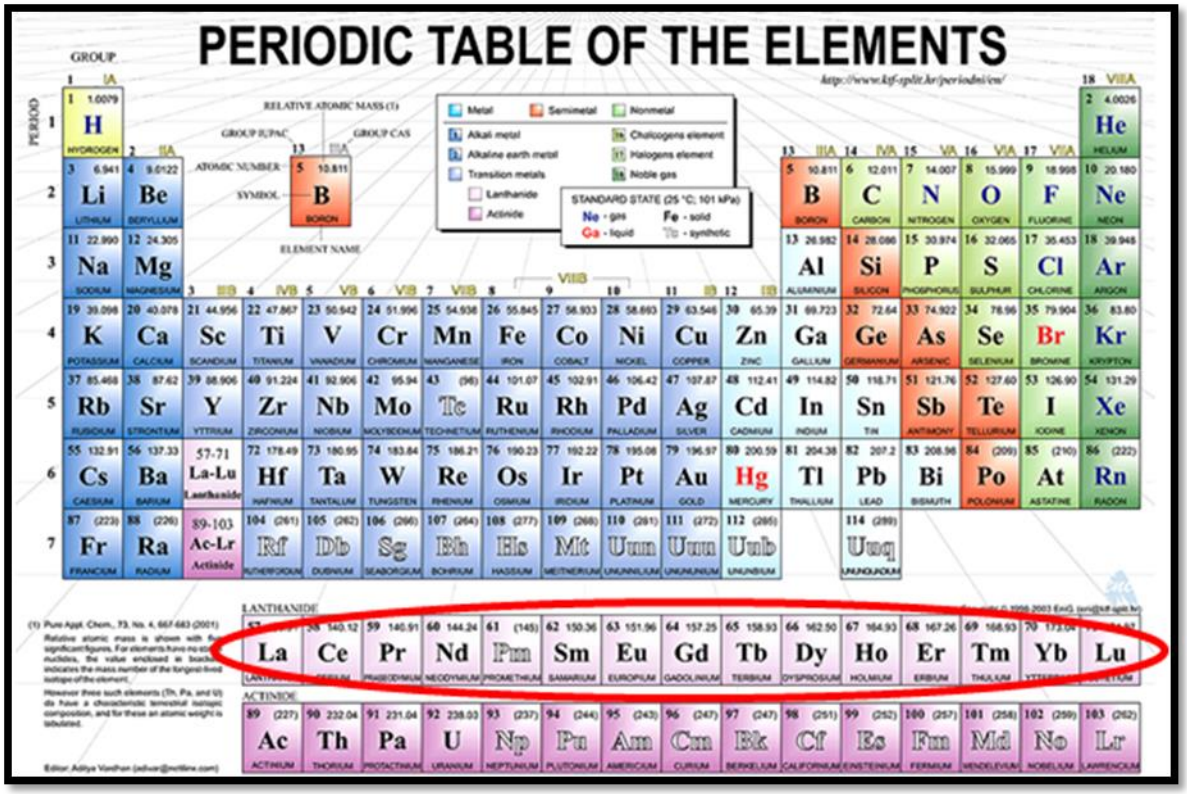

Figure 1 Rare Earth Elements or Lanthanides in the Periodic Table

property makes them good tracers for defining many different natural inorganic and organic geological processes.

Table 1 Atomic number and Ionic Radii for the REE.

Element	La	Ce	Pr	Nd	Pm	Sm	Eu	Gd	Tb	Dy	Ho	Er	Tm	Yb	Lu
Atomic electron configuration (all begin with [Xe])	$5d^1 6s^2$	$4f^1 5d^1 6s^2$	$4f^3 6s^2$	$4f^4 6s^2$	$4f^5 6s^2$	$4f^6 6s^2$	$4f^7 6s^2$	$4f^7 5d^1 6s^2$	$4f^9 6s^2$	$4f^{10} 6s^2$	$4f^{11} 6s^2$	$4f^{12} 6s^2$	$4f^{13} 6s^2$	$4f^{14} 6s^2$	$4f^{14} 5d^1 6s^2$
Atomic number	57	58	59	60	61	62	63	64	65	66	67	68	69	70	71
Ln^{3+} radius (pm) (6coordinate)	103.2	101	99	98.3	97	95.8	94.7	93.5	92.3	91.2	90.1	89	88	86.8	86.1
		+3,+4				+2,+3									

The lanthanide contraction, or the progressive decrease in size with increase in the atomic number for the lanthanides, arises from insufficient shielding of the increasing nuclear attractive force with each additional proton at the nucleus and accompanying additional electron that fills the 4f orbital, as the atomic number increases. The imperfect shielding thus causes a reduction in size of the entire 4f sub shell and a general steady contraction in the ionic radii (Cotton and Wilkinson, 1962).Because Ln vary primarily in the number of 4f electrons, these elements are very similar in chemical properties and are always found occurring together in natural materials. However, their occurrence together in natural materials does not imply that they respond equally to chemical changes of natural systems. In fact, the Ln ions separate to some degree when optimum atomic radii for accommodation in mineral structures are available or when they are in solution and become involved in complex ligands having different stabilities, especially in the formation of chelates (the same ligand offering two donor atoms to form bonds with the REEs). In some mineral structures, such as those in amphiboles and garnets, REE with smaller ionic radii (or the heavier REE) are accommodated, whereas in some other mineral structures, such as in the feldspars, REE with larger ionic radii are favored. In solutions, some degree of separation among REE occurs because the stability constants of many different REE-ligand complexes are typically varied in a gradual or steady fashion, but not necessarily in a smooth pattern, across the REE series.

The observed trends in REE distribution patterns among samples of interest may cast light on similarities or dissimilarities of their chemical evolutionary process or processes. The REE relative distribution patterns of natural materials fall into a small number of broad categories. The variations that have been observed in natural materials have led studies on REE to subdivide the elements into three groups (Figure 2):

Light REEs (La, Ce, Pr, Nd, Sm, and Eu – from atomic number 57 to 63)

Middle REEs (Sm, Eu, Gd, Tb – from atomic number 62 to 65)

Heavy REEs (Gd, Tb, Dy, Ho, Er, Tm, Yb, and Lu – from atomic number 64 to 71).

The middle REE group includes the two end-members (Sm and Eu) of the light REE group and the first four members (Gd, Tb, Dy, and Ho) of the heavy REE group (Topp, 1965).

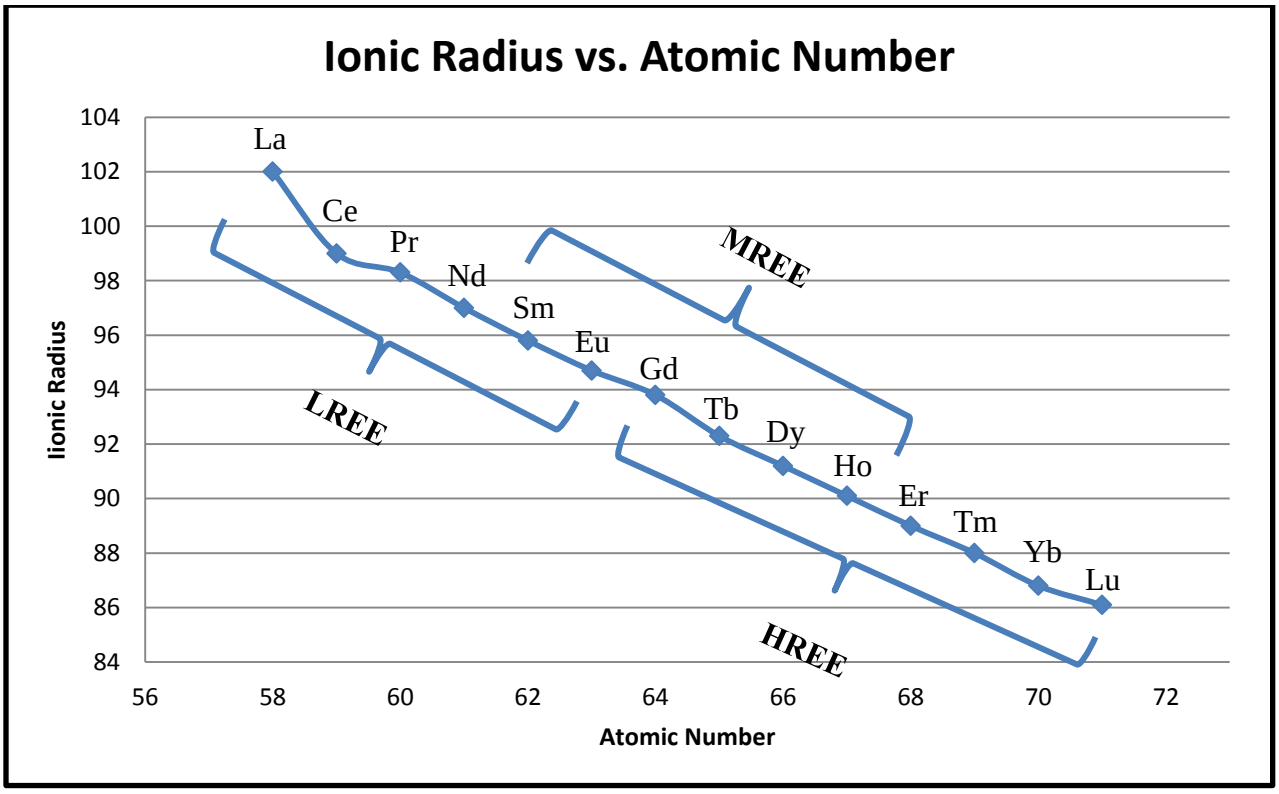

Figure 2 Lanthanide Contraction

In Pearson's (1963) terminology, the Ln^{3+} ions are classified as "hard" ions, which causes them to bond preferentially with "hard" base ligands such as H_2O, OH^-, CO_3^{2-}, NO_3^-, SO_4^{2-}, PO_4^{3-}, O^{2-}, F^-, CH_3COO^-, R-OH (alcohols). Ln, like many other "hard" acid ions, have strong preference for O donor atoms. Bonding to Cl^- ion has been known, but it is relatively weak compared to bonding to O^{2-} and F^- anions. Complexes solely with NH_3, R-

NH_2 (amines), HS^- and CN^- are extremely weak (Evans, 1990, Wood, 1990). In general, the Ln ion preference for donor atoms is O > N > S (Thompson, 1979).

Wood (1990) gave a comprehensive review of the stability constants of Ln-complexes with many common inorganic anions or ligands. Thompson (1979) and Evans (1990) provided data on stability constants of Ln-complexes with a number of different organic ligands. The sulfate ligands cause very little fractionation between the light Ln^{3+} ions (LREE) and the heavy Ln^{3+} ions (HREE). Fluoride complexation can cause fractionation of the Ln ions in dilute fluoride solutions. Similar to that of fluoride complexations, the stability of Ln-CO_3^+ complexes also progressively increases with increasing atomic number of the Ln. In general, the stability of chloro complexes decrease with increasing atomic number, a trend that is opposite of the behavior of the fluoro complexes (Wood, 1990). Several studies have noted that precipitation of phosphate minerals from solutions causes the minerals to have a relative enrichment of the middle Ln across the series, displaying a convex relative distribution pattern often marked by the highest enrichment of Sm and the corresponding equilibrium solutions to have a relative depletion for the middle Ln, displaying a concave upward relative distribution pattern with the most depletion of Sm (Byrne et al., 1996).

Variations in the ionic size of the Ln, charges for the two Ln ions (namely Eu^{2+}—Eu^{3+} and Ce^{3+}—Ce^{4+}) and the stability of the complexes very often impose some distinctive geochemical characteristics on the Ln compositions of natural materials. The two REE that have multiple valences may themselves be fractionated, if either reducing (Eu^{2+}) or oxidizing (Ce^{4+}) conditions are present. Increased values above the expected trivalent abundance based upon their closest neighbors are considered positive anomalies, lower values are negative. Crystallographic controls on these elements are fairly well known, ie. the affinity of feldspars for Eu^{2+}. Enzymatic effects are not as well known.

Variations within their coherent chemical properties make the Ln group a good tracer for the differentiation of inorganic and organic processes. Subtle differences in the chemical history of a group of solids, solutions, or solid-solution reactions may be best revealed through an examination of the relative distribution of the REEs for each substance of interest when compared with a known standard or reference material.

On moving across the rare-earth series with increasing atomic number, a distribution pattern of the REEs for a given substance is shown as the ratio of the concentration of each

individual REE of the substance to the concentration of the same element of a chosen standard or reference material. REE studies in igneous petrology use chondrite as reference material. Sedimentary studies with REE use the Post Archean Australian Shale (PAAS) or the North American Shale Composite (NASC). When analyzing a specific sample, the reference material used should be convenient to the material analyzed. Using chondrite as a reference material for the REE study in oil might not be appropriate. The PAAS is the reference material used throughout this study. When normalizing REE concentrations to a reference material, in this case the PAAS, typically, but not always, an apparently smooth distribution pattern within the LREEs may be interrupted at Ce and Eu. Europium positive or negative anomalies may be linked to a crystallo-chemical or solution-chemistry effect, for example, feldspars that accommodate Eu^{2+} over Eu^{3+}. This effect might not be applicable in all materials, particularly when studying organic matter. Europium can be biochemically controlled by enzymatic effect in a living system. Cerium anomalies can also be attributed to crystallographic effects, as is the case of Manganese oxide precipitation, like the observed cerium negative anomalies in solution being developed through oxidation of Ce(III) onto the manganese oxide surface. This reaction occurs in a large scale in marine environments, associated to the formation of the previously mentioned manganese oxides. The consequence of this reaction is the cerium depletion and the equilibrium of the precipitated phases with sea water (McLennan, 1989). It is important to note that cerium has also been found with anomalies in plants. Anomalies are identified in these elements if their observed relative concentrations are in excess of relative concentrations that could be predicted from the relative distribution trend defined by their two immediate respective neighbors, or negatively anomalous if the observed relative distribution values are short of the predicted values determined by the trend line that connects their two respective immediate neighbor REEs.

The REE distribution patterns and total concentrations of the organic matter in the whole rock reveal potential to investigate organic matter maturation processes in the source rock. The overall expansion of the geochemical knowledge of crude oil through REEs is another objective of this research, providing a signature to better understand oil generation and migration. This investigation provides a window of opportunity where the REEs might be used as correlation tracers in the study of genesis and migration of crude oil, and as source rock maturity indicators.

1.2 Composition of crude oil

Petroleum is composed almost completely of hydrogen and carbon, with 1.85 more hydrogen atoms than carbon. Sulfur, nitrogen and oxygen constitute less than 3 percent of petroleum. From kerogen to the asphalt to the oil, an increase can be observed in hydrogen and a decrease in sulfur, nitrogen and oxygen relative to carbon.

Table 2 Elemental Composition of Natural Materials (Hunt, 1995)

ELEMENT	VOLUME PERCENT		
	Oil	Asphalt	Kerogen
Carbon	84.5	84	79
Hydrogen	13	10	6
Sulfur	1.5	3	5
Nitrogen	0.5	1	2
Oxygen	0.5	2	8
Total	100	100	100

Table 2 from Hunt shows average composition levels for oils worldwide. Hydrocarbons vary in their structural forms comprising different molecular arrangements. Paraffins are alkanes (open-chain molecules with single bonds between the carbon atoms), they are the second most common constituents of crude oil, and they comprise most of the gasoline fraction of crude oil. Naphthenes are cycloalkanes (alkane rings), they are the most common molecular structures in petroleum. These rings usually contain 5 or 6 carbon atoms in them. The average crude oil contains 50% naphthenes approximately, with more of them in the heavier fraction and less in the lighter fraction. Aromatic hydrocarbons contain at least one benzene ring (a ring with 6 carbons and 6 hydrogens attached to each carbon). They rarely make up more than 15% of total crude oil, and they concentrate mostly in the heavy fractions of petroleum. Crude oil also contains molecules other than hydrogen and carbon. These molecules include nitrogen, sulfur and oxygen. These are present through the entire boiling range of crude oil. The compounds which contain oxygen are of particular interest due to the REEs affinity to oxygen.

Since REE may be found bound to oxygen bearing sites, it's important to note some compounds which have oxygen molecules in them (Figure 3). Oxygen compounds are made up of chain or ring acids. Phenols and Carboxylic acids encompass these compounds which consist of chains or ring acids.

Naphthol $C_{10}H_7OH$ Fatty Acid R=straight paraffin chain Benzofuran $C_8H_6OC_6H_5$ COOH Benzoic Acid

Figure 3 Compounds found in oil containing Oxygen molecules

Compounds containing Nitrogen, Sulfur and Oxygen and Aromatics represent about 75% of the residuum part of crude oil. Residuum entails approximately 18% of the total volume of an average 35˚ API gravity crude oil (Table 3). Residuum is the least understood fraction of petroleum and it is the most complex one. The main components of residuum are heavy oils, resins, asphaltenes, and high molecular-weight waxes.

Table 3 Composition of a 35 ˚ API Gravity Crude Oil (Hunt, 1995)

Molecular Size	Volume Percent
Gasoline (C_5 to C_{10})	27
Kerosine (C_{11} to C_{13})	13
Diesel Fuel (C_{14} to C_{18})	12
Heavy Gas Oil (C_{19} to C_{25})	10
Lubricating Oil (C_{26} to C_{40})	20
Residuum (>C_{40})	18
Total	100

Asphaltenes are dark brown to black amorphous solids. In going from oils to resins to asphaltenes, the molecular weight, the aromaticity, nitrogen, oxygen and sulfur content increases. Asphaltenes exist in petroleum as colloidal particles dispersed in an oily medium. As the oily medium is removed by distillation, the particles become more concentrated to form an asphalt, which at room temperatures is highly viscous, resembling a hard solid. According to Hunt (1995) an asphaltene molecule consists of 10 to 20 condensed aromatic and naphthenic rings with paraffin and naphthenic side chains. These condensed aromatic structures also contain space for free radicals, where highly reactive an unpaired electrons are emplaced. Some of these sites are capable of complexing metals.

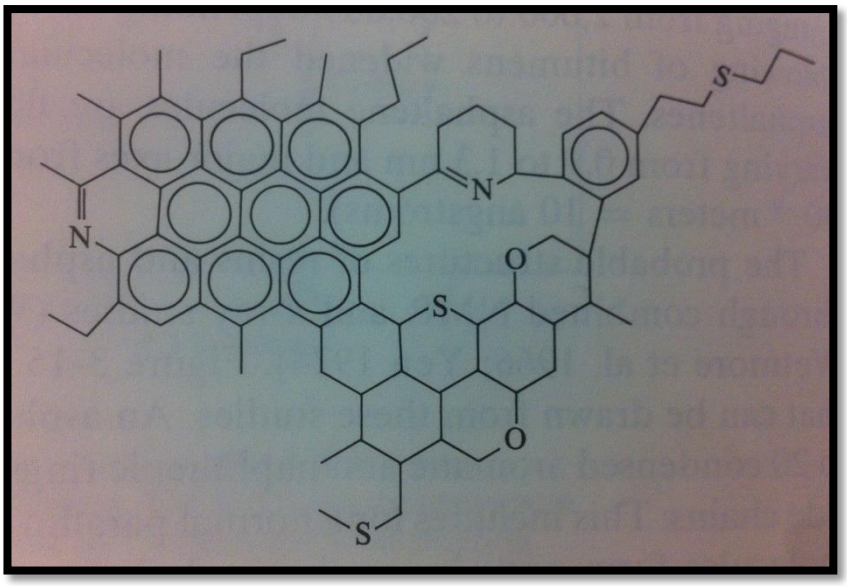

Figure 4 Schematic Asphaltene Molecule (Hunt, 1995)

The next table displays the percent of resins and asphaltenes in various crude oils.

Table 4 Resins and Asphaltenes in Crude Oils (Erdman and Saraceno, 1962)

Crude Oil	Source	Weight percent	
		Resins	Asphaltenes
Ellenburger	W. Texas	4.2	0.24
Ragusa	Sicily	9	0.28
Grozni	USSR	8	1.5
Karami	China	14	1.8
Wilmington	California	14	5
N. Beldridge	California	18	5
Khaudag	USSR	33	8
Belaim	Egypt	20	13
Boscan	Venezuela	29	18
Athabasca	Canada	24	19

Heavy crude oils have more oxygen with residue containing over 5 % oxygen most of the times (Hunt 1995). It is important to note that Oxygen is present in the composition of crude oil. Analysis of REE is possible due to the previously mentioned characteristic of REE, the affinity REE have to create ligands with oxygen.

1.3 Geological Setting

The Anadarko basin is a northwest-southeast trending sedimentary structural basin that is axially asymmetric (Fig 5) and of Paleozoic age in western Oklahoma and the Texas Panhandle (Cardott and Lambert, 1985). The Greater Anadarko basin describes the previously mentioned area, plus the southwestern part of Kansas and the southeastern corner of Colorado, comprising an area of approximately 60,000 mi^2 (Davis and Northcut 1989). This basin is the deepest sedimentary basin in the cratonic interior of North America, having Paleozoic sedimentary rocks ranging in thickness from 40,000 ft near the southern margin of the basin, to 10,000 ft in the northern shallower parts (Kennedy et al., 1982)

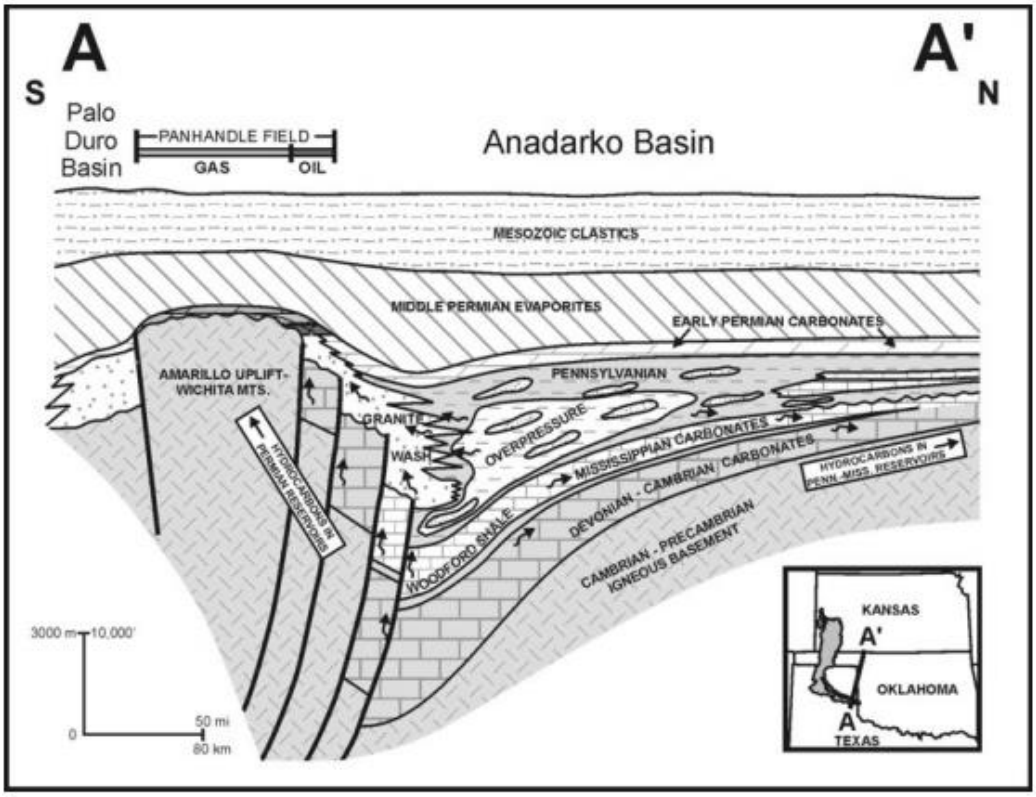

Figure 5 South-north cross section AA' through Anadarko Basin (Sorenson, 2005).

The main early Paleozoic tectonic and depositional provinces of Oklahoma include: 1) the Oklahoma Basin, 2) the Southern Oklahoma Aulacogen, and 3) The Ouachita trough. Figure 6 shows the location of the depositional provinces of Oklahoma. The Oklahoma Basin is an expansive thick shallow marine carbonate shelf that is interbedded with marine sandstones.

(Johnson and Cardott, 1992).The name aulacogen was proposed by Hoffman in 1974 in place of the southern Oklahoma Geosyncline. Aulacogens are thick sedimentary sequences extending at high angles from orogenic belts. They are generally considered favorable locations for oil and gas accumulations. Aulacogens form as the failed arm of a three or four armed rift system during crustal doming over a mantle plume (Walper, 1977). Aulacogen evolution typically includes 1) rifting or extension, 2) subsidence, and 3) compression (Hoffman et al., 1974).

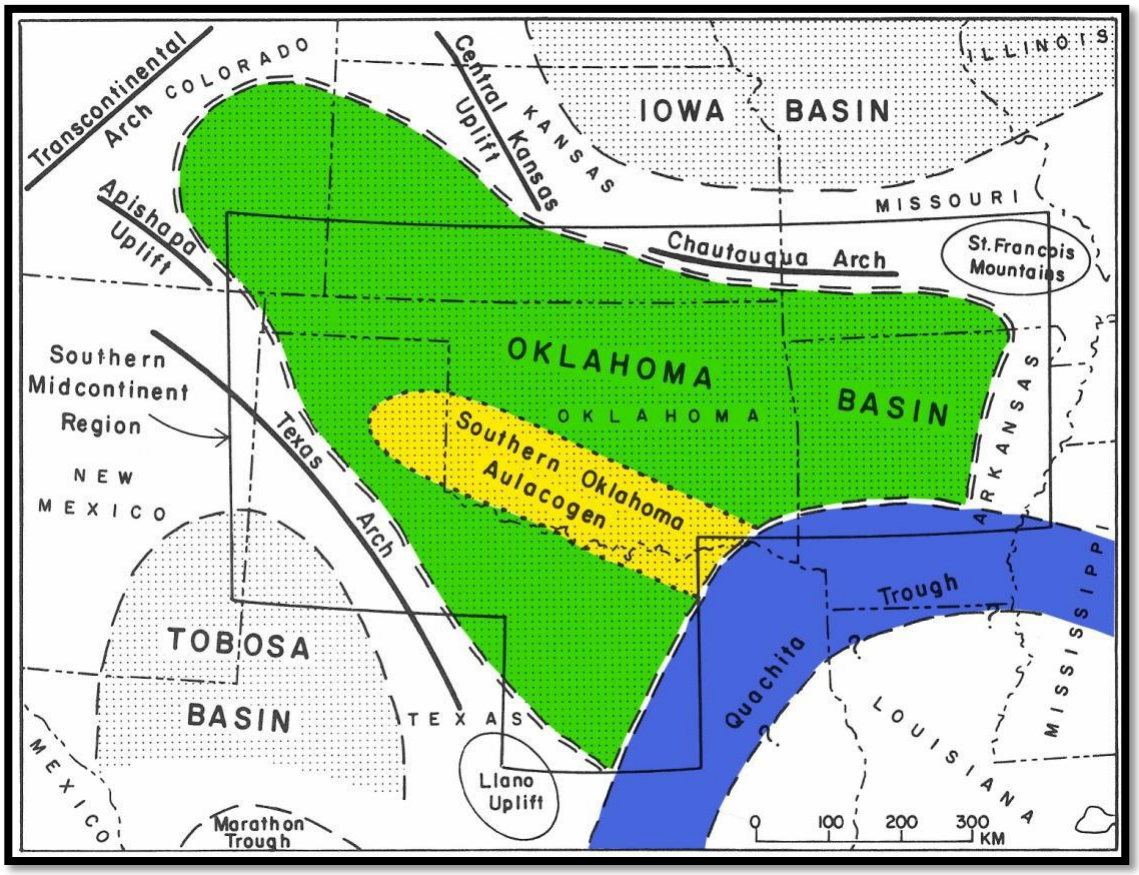

Figure 6 Paleogeography of the southern mid-continent, early to middle Paleozoic showing the Oklahoma basin and Ouachita trough depositional provinces as well as the southern Oklahoma Aulacogen tectonic province. Modified from Johnson et al., 1988.

The southern Oklahoma aulacogen began as an intratectonic rift during the late Precambrian to Early Cambrian . From there it developed into a trough shaped depocenter for the Oklahoma Basin (Johnson and Cardott, 1992). This extension produced normal faults and igneous rocks were emplaced in the deepest part of the present day Anadarko basin. By the middle Cambrian igneous activity ceased. The Wichita fault zone was only active in the early

phase of the rifting, but was inactive during the shelf stable carbonate phase of the early Paleozoic (Ham et al., 1964).

The second step, subsidence, occurred in several phases beginning in the late Cambrian and into the early Mississippian. The subsidence was ascribed to cooling after thermal events that were associated with crustal thinning that took place in the Cambrian (Feinstein, 1981; Garner and Turcotte, 1984). In 1984, Garner and Turcotte proposed crustal and lithospheric thinning as a model to explain accelerated isostatic subsidence during the late Mississippian. This implies that the upper crustal extension and faulting were accompanied by a rise in heat flow during the late Mississippian.

During the early Pennsylvanian, the Wichita Orogeny region saw intense crustal shortening. This shortening was most likely associated with the late Paleozoic collision involving the Ouachita orogenic belt, raised vertical blocks in the Amarillo-Wichita uplift and reactivated zones of weakness associated with the initial graben stage (Ham et al., 1964; Walper, 1977). Reverse faults produced in the frontal Wichita fault zone and the adjacent deep Anadarko Basin typically had throws of more than 30,000 feet. The Northern area of the region saw less intense activity (Brewer et al., 1983). Finally, Figure 6 also shows the Ouachita through. This trough accumulated deep-water sediments due to earlier rifting of the North American Craton. These basins formed due to down-warping and were thus differentiated from earlier Paleozoic basins in Oklahoma (Johnson and Cardott, 1992).

1.3.1 Woodford Shale

Source rocks have to undergo a physical, biochemical and geologic process that produce a fine-grained sedimentary rock with high content of hydrogen and carbon in its organic matter. The environmental and depositional conditions of the Woodford Shale are a key factor for the amount of organic material in it.

The Woodford consists mostly of organic-rich siliceous shale with varying amounts of carbonate and interbedded chert beds. Andrews (2009) reported that the organic-carbon-rich units of the Woodford Shale occur in black shale with cherty beds and some phosphatic nodules as can be seen in Figure 7.

Figure 7 Phosphatic Nodules in the Woodoford Shale present in Newfield Exploration's core.

According to Comer, The Woodford Shale contains high concentrations of marine organic matter; with mean organic carbon concentrations of 5.7 % weight for the Anadarko Basin's portion in Oklahoma and Arkansas. Organic carbon concentrations range from less than 0.1 % weight in some chert beds to 35 % weight in black shale and the organic matter is mostly oil-prone Type II kerogen (Comer and Hinch, 1987). This kerogen, which is rich in hydrogen and low in carbon generates oil or gas with the right process of heating and maturation. Type II kerogen is derived from the remains of plankton that have been reworked through bacteria (McCarthy et al., 2011).This kerogen type is typically generated in reducing environments found in moderately deep marine settings. The Woodford shale was deposited over the Hunton Group (Figure 8) in a similar environment to the previous one described, a euxinic, shallow epicontinental sea, under a chemically reducing and quiet environment (Sullivan, 1983).

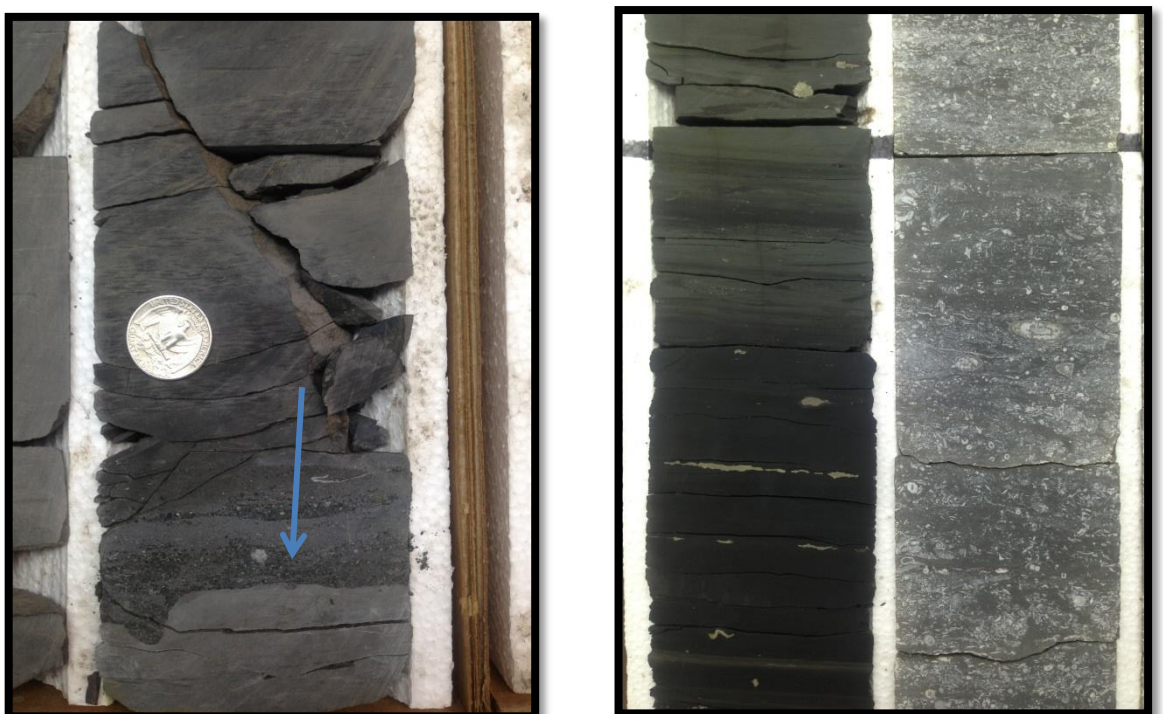

Figure 8 Woodford/Hunton Contact, and stratigraphic change in Newfield Exploration's Woodford Core

The Woodford Shale is widely believed to be the major hydrocarbon source rock in the Anadarko Basin (Rascoe and Hyne 1988), and exploration and interest in the Woodford shale has rapidly increased in the recent time, due to its good thermal maturity at relatively shallow depths compared among other basins, and its high silica content which allows it to generate fractures easily and responds well to fracturing techniques. The Woodford Shale is mostly late Devonian, but ranges in age from middle Devonian to early Mississippian (Figure 9). The Paleozoic stratigraphic column of the Anadarko Basin is linked to a type log of the basin showing the Gamma Ray and Resistivity properties for the Woodford shale and immediate underlying formations. The Woodford Shale shows organic rich shale properties on this log with Gamma Ray values above 150 API and Resistivity higher than 15 ohm-m. Age-equivalent strata include the Chattanooga Shale, Misener Sandstone, Sycamore Sandstone, the middle division of the Arkansas Novaculite, upper part of the Caballos Novaculite, Houy Formation, Percha Shale and the Sly Gap Formation. These units were deposited over a major regional unconformity (Amsden, 1967).

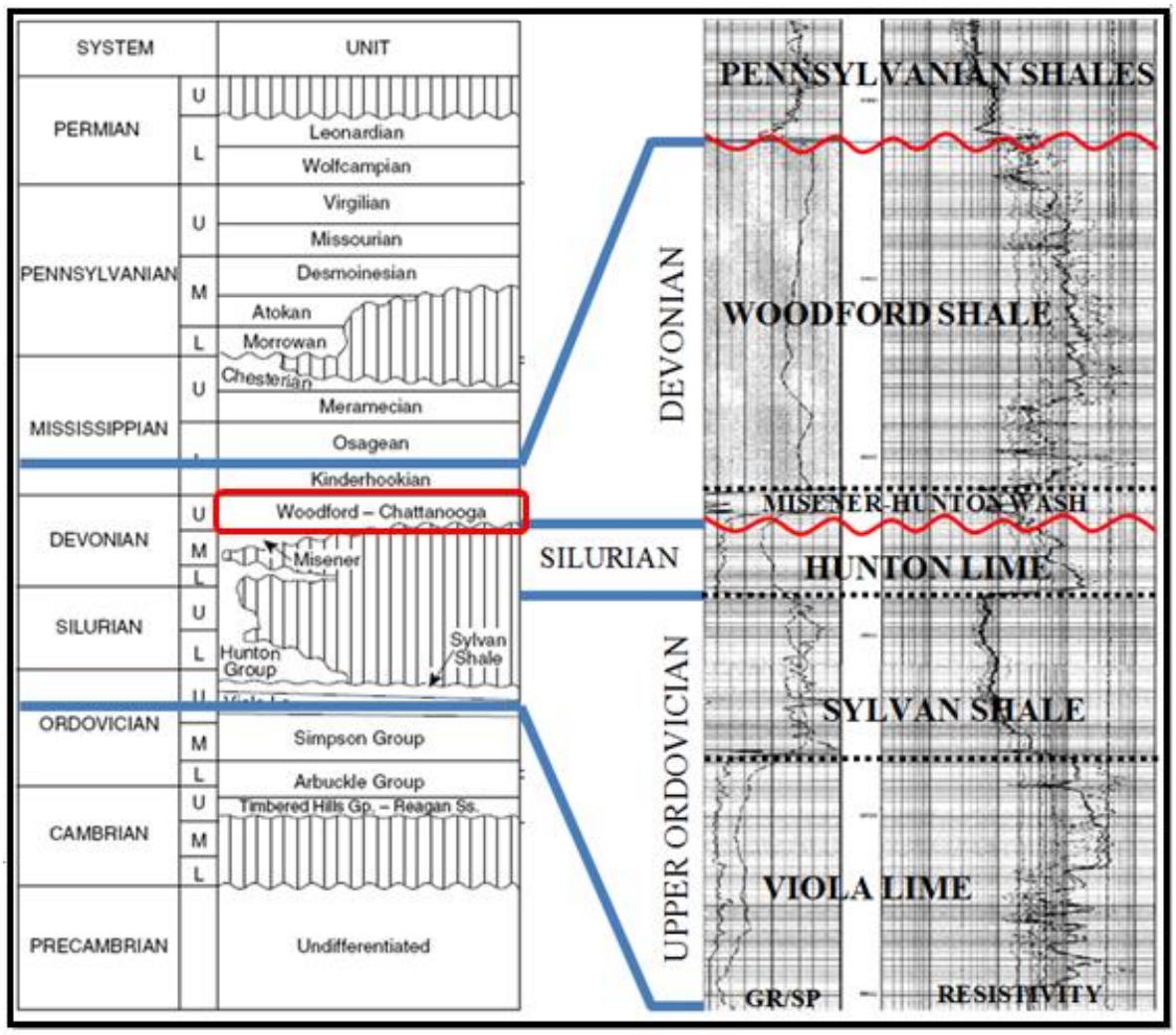

Figure 9 Regional Paleozoic Stratigraphic column in the Anadarko Basin.

In the southern midcontinent, these units are the stratigraphic record of worldwide late Devonian marine transgression (Figure 10). During this marine transgression the Woodford sediments were being deposited in an inland sea as anaerobic and dysaerobic biofacies, where high concentrations of marine organic matter coexisted with abundant biogenic silica. An arid paleoclimate is suggested by Comer, 2008 as he recorded hypersalinity as anhydrite in burrows. Plate-tectonic reconstructions confirm an arid paleoclimate in the study area. Water evaporation in the area allowed ocean water to flow into the inland seas, supplying an influx of oceanic nutrients with high biologic productivity. Taking into account the arid paleoclimate with a lack of rainfall, suggests river discharge was minimum, having a low contribution of terrestrial derived biological material.

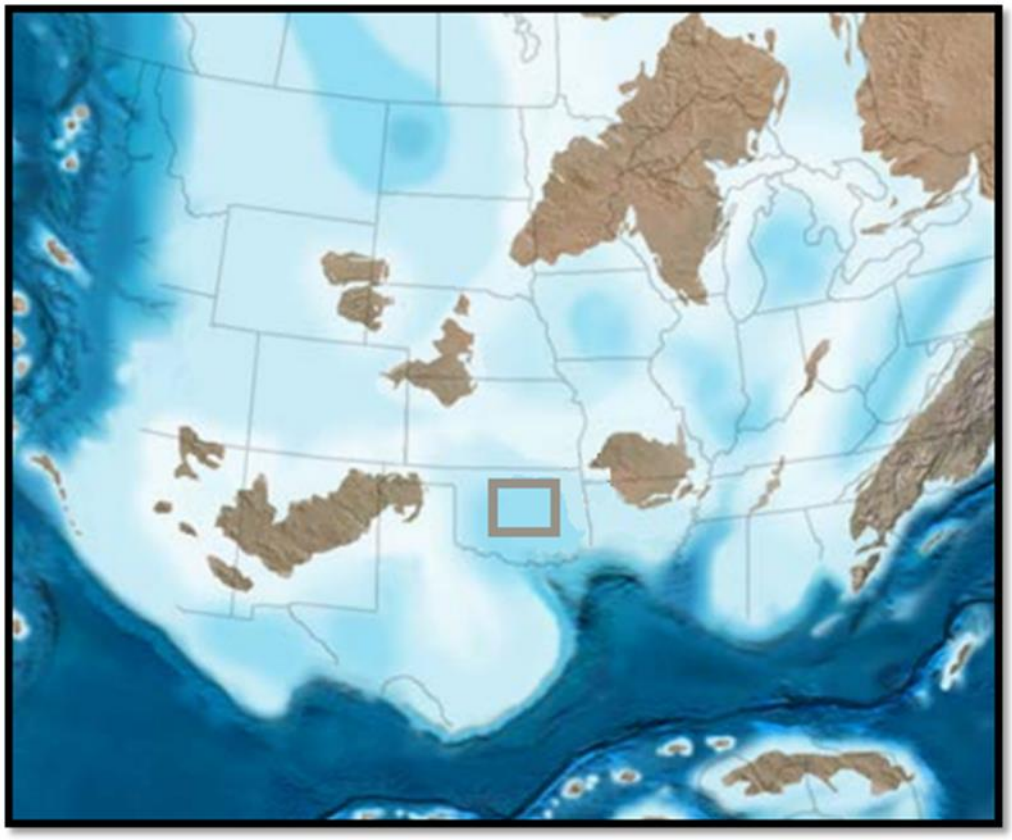

Figure 10 Late Devonian (360 mya) Paleogeography showing study area location, modified from Blakley, 2013

The Woodford shale is stratigraphically equivalent to several North American Devonian black shales (Figure 11) with active and potential unconventional oil and gas production, including the Antrim Shale in the Michigan Basin, Marcellus Shale in the Appalachian Basin, New Albany Shale in the Illinois Basin, Bakken Shale in the Williston Basin and Exshaw Formation in the Western Canada Basin (Comer, 2008). The geological settings present in Oklahoma are different from the geological settings where stratigraphically equivalent black shales to the Woodford are present; this is reflected on the thermal maturity of the Woodford shale. The Woodford shale structure is followed by thermal maturity, being able to observe a pattern where the highest maturities are found in the deep basins and the lowest maturities are found on structural highs.

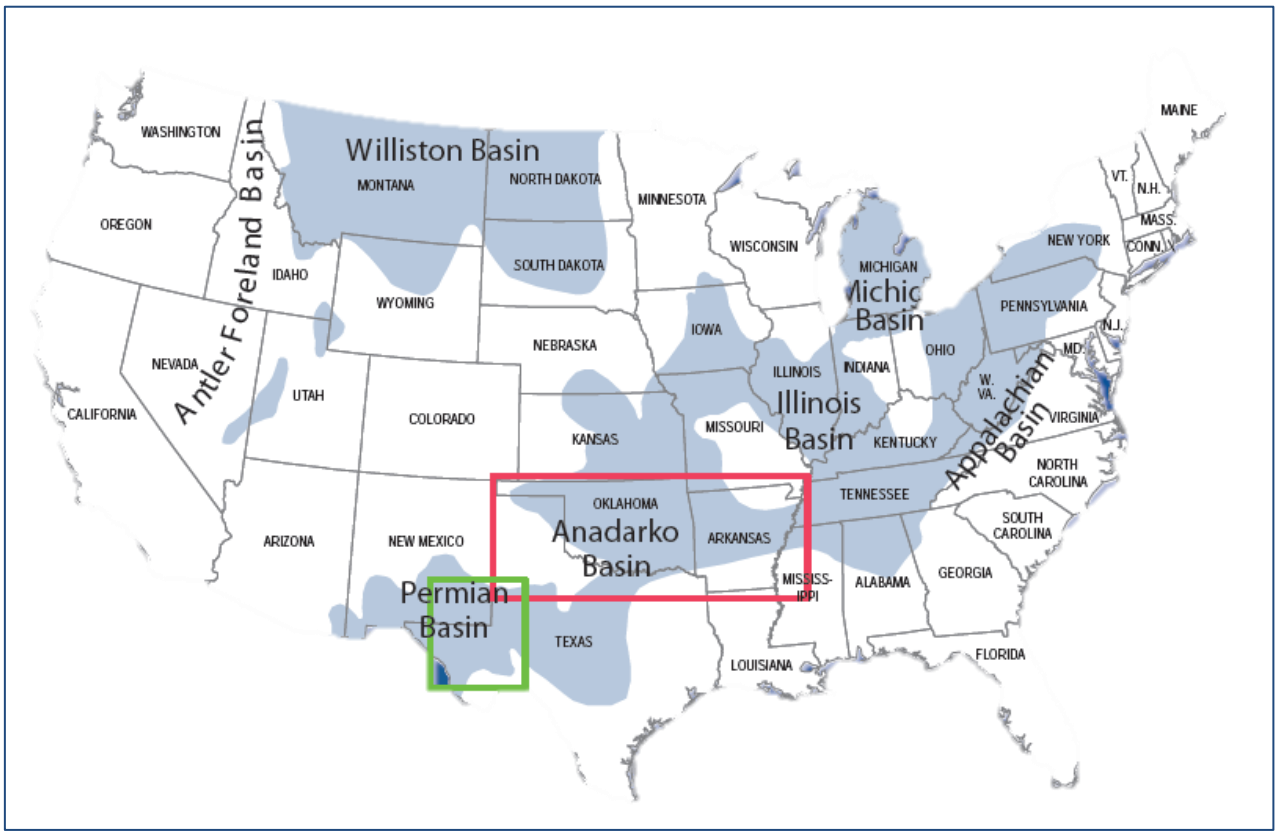

Figure 11 Distribution of Devonian Black Shales in the USA, modified from Comer, 2008

The organic rich siliceous shales in the Woodford shale are well developed in the southeastern portion of the basin. The Woodford thickens rapidly to the southwest of the state and exceeds 600 feet in thickness in southern Oklahoma (Figure 12). Large areas of Oklahoma are underlain by significant thicknesses of Woodford shale that is well into the oil window. It is the primary source for oil and gas in Mississippian, Siluro-Devonian and Ordovician units.

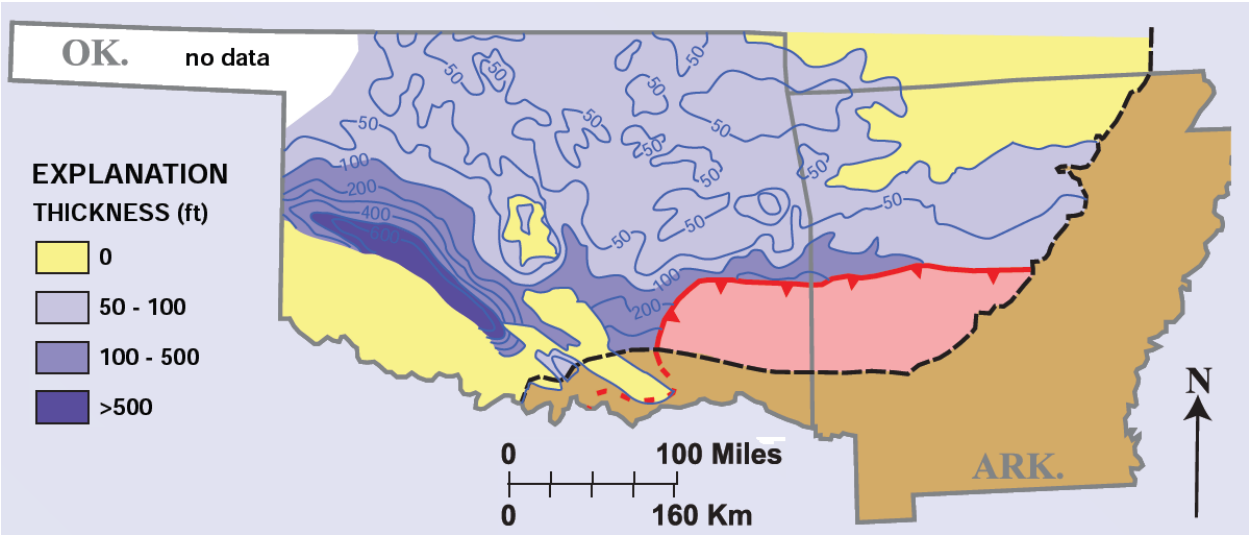

Figure 12 Regional Isopach of the Woodford Formation, Comer 2008

In most of south-central and southeastern Oklahoma, The Woodford consists of three members, the Upper, Middle and Upper Woodford, which are identified in outcrop, but may not be evident in the subsurface (Figure 13). The upper member contains cherty beds from 1 to 3 inches thick, which if not interlaid by black to gray-siliceous shale, constitutes the majority of the strata. An abundance of pyrite crystals in the formation causes limonitic staining in fractured surfaces. This upper member contains phosphatic nodules. Radiolarian's siliceous skeletons make the beds that are described as "cherty". This member and its cherty consistency is hard to drill into because of its weather resistant nature. The middle member consists mainly of black to gray fissile shale. The strata in this member can be very silty and normally doesn't contain phospahtic nodules. The lower member is similar to the upper member composed of interbedded black-gray siliceous shale and cherty beds, but lacking the phosphate nodules which characterize the upper member. Most of the drilling completions for hydrocarbon production in the Woodford Shale are landed in the Middle Member of the Woodford.

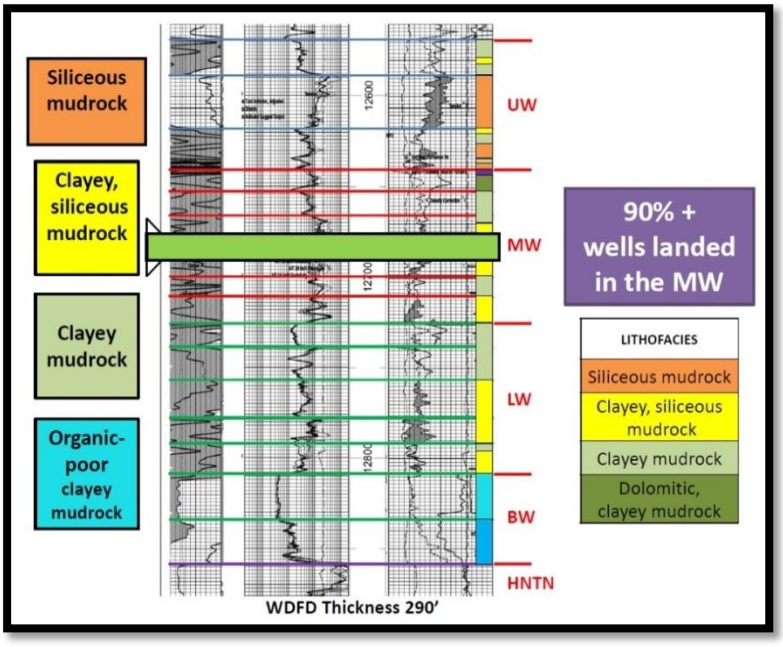

Figure 13 Andarko Basin type log, indicating the three members of the Woodford Shale, Caldwell and Johnson, 2013

1.3.2 Production in the Anadarko Basin: Woodford Shale's Potential

The Anadarko Basin is one of the giant oil and gas provinces of North America, with exploration and development activities having started more than 75 years ago(Wang, 1997) Brenneman's Oil-to-rock correlation studies show that the Woodford Shale is a prolific oil source (Brenneman and Smith, 1958), and estimates indicate that as much as 85% of the oil produced in central and southern Oklahoma originated in the Woodford (Jones and Philp, 1990). Hycrude (1986) analyzed the oil yield of the Woodford Shale in an exposure in the Arbuckle Mountains. After hydroretorting the samples, the oil yield in the samples ranged from 22.9-46.8 gallons per short ton of rock, clearly exceeding the minimum limit of 10 gallons of oil per ton of shale. In the main oil-producing region of central and southern Oklahoma, 22 billion bbl of bitumen and 16 billion bbl of saturated hydrocarbons were estimated to have been expelled from the Woodford formation (Comer and Hinch, 1987).

The Woodford shale being such a rich source rock in the Anadarko Basin, is not only the source for different hydrocarbon reservoirs in Oklahoma, it is now being targeted as an unconventional resource. As technologies advance and new completion techniques are being applied to extract oil, the Woodford shale, as a source rock has become a completions target. Combining different conventionally used techniques like horizontal drilling and hydraulic fracturing, oil extraction has been made viable and economical in Shale Oil and Shale Gas which are among the sources for unconventional hydrocarbon production. Unconventional energy resources are considered the next energy frontier, and the Woodford Shale is renown among these types of resources.

Over four thousand horizontal wells have been completed in the basin to date at vertical depths as great as 15,000 feet. In central and southern Oklahoma, Upper Devonian black shales are rich oil source rocks, from which seventy to eighty five percent of the commercial oil reserves of the region are estimated that have provenance from the Woodford. Since 2004 the number of completed wells in this formation has increased three hundred percent. This increase is due to hydraulic fracturing technologies being developed providing a feasible economic completion. There have been 2,461 wells produced in the Woodford Shale from the years 2004 to June of 2012, and about two thirds of these wells were completed horizontally (Figure 14).

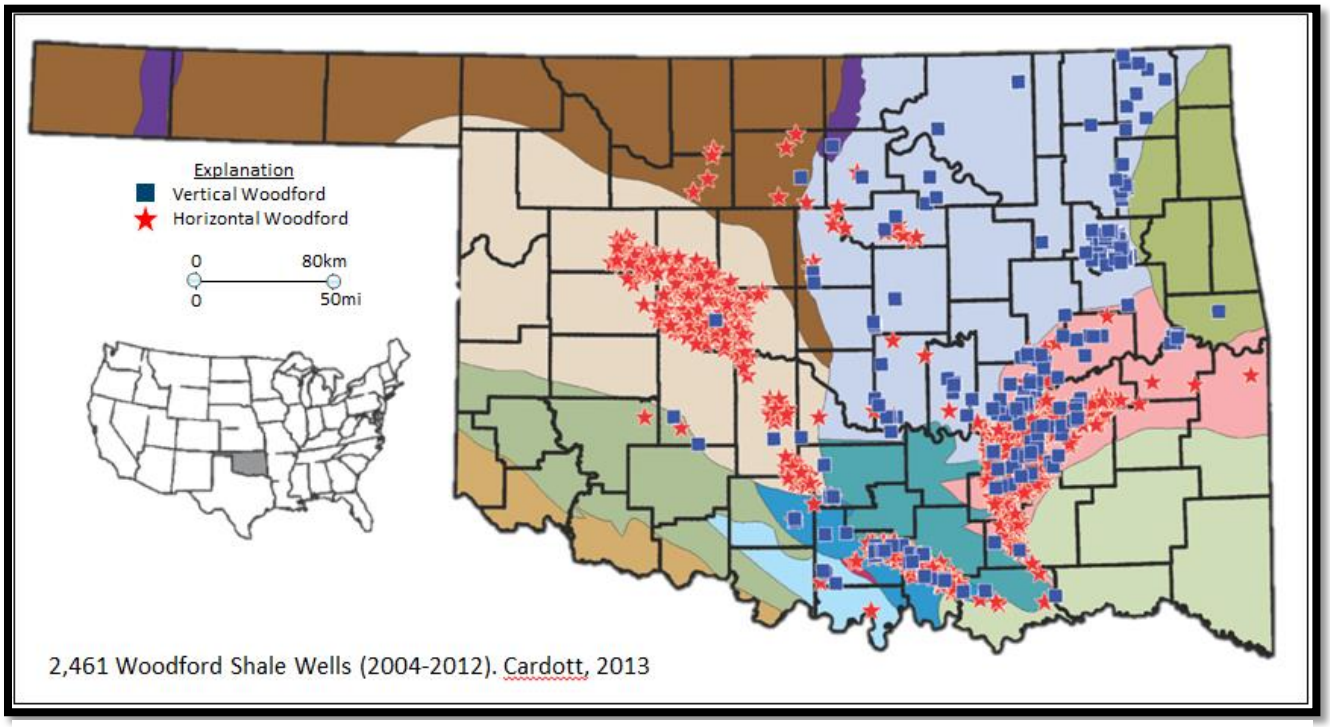

Figure 14 Location of Vertical and Horizontal Woodford Shale Completions in Oklahoma from 2004-2012. Cardott, 2013

Chapter 2 - Methodology

2.1 Study Area and Sample Locations

The study area comprises the Greater Anadarko Basin, focusing on the north central part of Oklahoma. Ten Woodford Shale samples were collected for analysis in this research project. The samples were collected from the core library at the OPIC (Oklahoma Petroleum Information Center) in the OGS (Oklahoma Geological Survey). Samples were collected according to availability, looking to have a wide spatial distribution in north central Oklahoma. The target number of samples was originally twenty five Woodford Shale samples, but due to limited core availability, and poor core conditions (delaminated, desiccated), the best 10 samples were collected, with an average weight of 90 grams per sample. Sampling consisted of choosing intervals in the Woodford shale core existing in good conditions, which represented the most organic portion of the Woodford shale, basing the organic matter content inference by physical observation, picking samples that depicted the cleanest black shales. Some of the core sections existing in the OPIC had only 9 ft of Woodford core present, and other wells had larger intervals of Woodford core. Approximately 90 grams of sample were collected for each of the core plugs. Examples of sections chosen are seen on Figures 15 and 16.

Figure 15 Sampling location in blue arrow of WF#5 Mobil Dwyer MT, Plug Depth 17581 ft.

Figure 16 Sampling location in blue arrow of WF#9 Jones and Pellow, NE Alden Un, Plug Depth 6793 ft.

Oil samples were obtained from eight oil wells in Payne County, OK. The wells are operated by Truevine Operating LLC. These wells were drilled to depths ranging from 3,200 ft to 5,500 ft approximately, being completed by hydraulic fracturing. The samples were collected following the high pressure injection of fracturing fluids. Flow-back fluids were collected, catching a total of thirteen oil samples from eight different wells. The initial sampling began in October of 2011 from four wells that are producing from the Woodford Shale, those same wells were sampled 5 months after their initial production. Another four wells were sampled at the same initial date of October from wells producing in the overlaying formation, the Mississippian. Again the same sampling procedure was processed for the Mississippian oil, collecting samples in March of 2012, with 5 months difference between the samples. The name of the samples was differentiated with a (1) for the oil sample from an earlier date and a (2) for the same sample for the later date of collection. When sampling oil, the fluid sampled comes with brine associated to the oil, which was collected along with the oil samples. Three to five liters of sample were collected from each well, collecting enough sample amounts to complete the sample preparation which is explained in the next section.

The location of the Woodford shale samples is listed in Table 5, showing a distribution for the samples in eight counties in north central Oklahoma. The depths of the samples vary from

4,100 ft. to 17,000 ft. approximately, although most of the samples are not in the deepest portion of the basin, where depths of the Woodford reach 26,000 ft. Oil samples from Devonian and from Mississippian oils are located in Payne County, OK. The sample location can be found in Figure 17, where the Woodford shale samples are represented by a black dot and the oil samples are represented by a green dot.

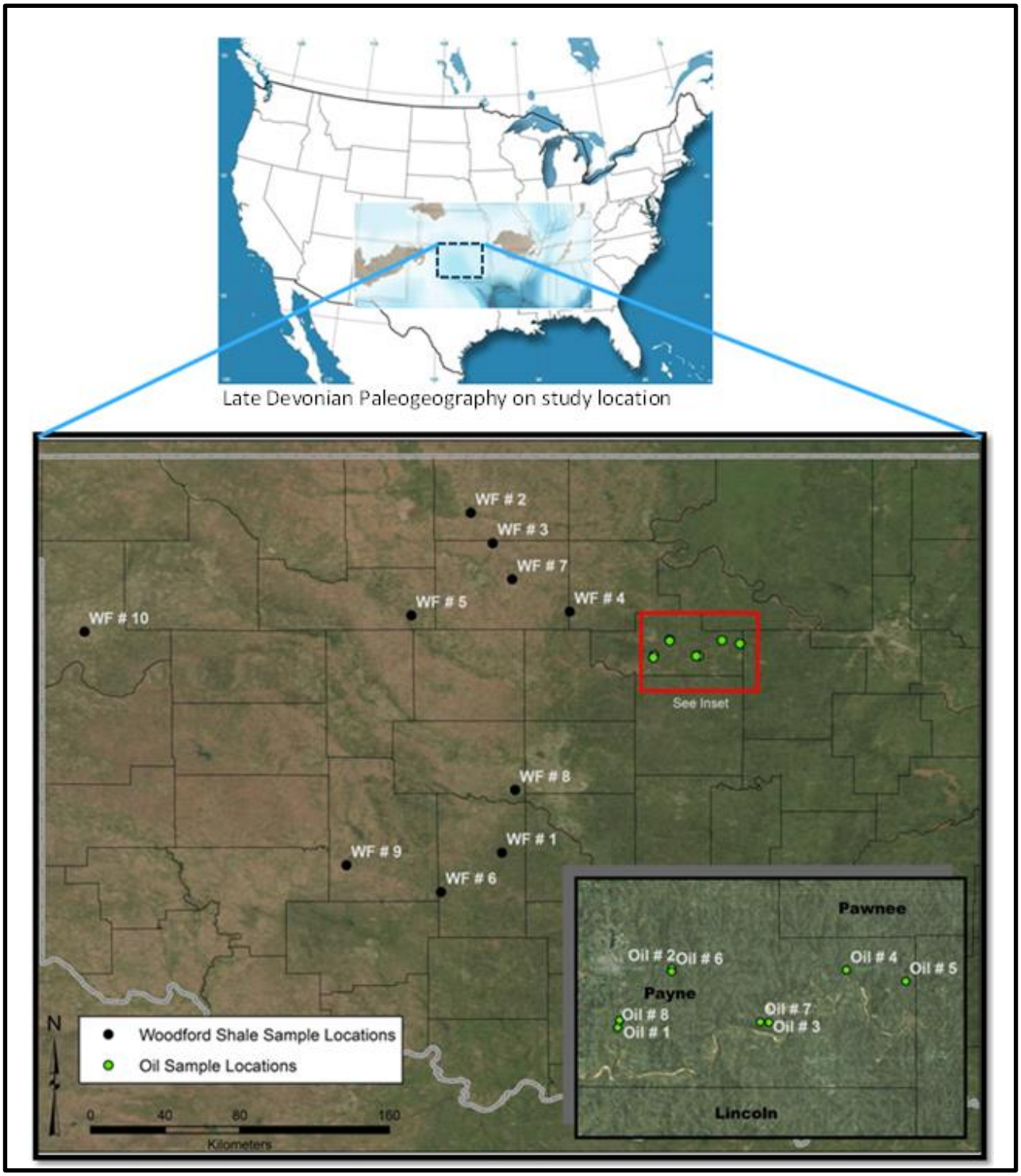

Figure 17 Regional map showing study area and sample locations

Table 5 Location of Samples and their Stratigraphic Units

Sample Name	Latitude	Longitude	Section	TWP	RNG	County	Sample Depth(ft)	Formation
WF # 1 Shell McCalla Ranch	35.0912	-97.78539	12	07N	06W	GRADY	12309	Woodford
WF # 2 Mobil Sara Kirk	36.72669	-97.93513	15	26N	07W	GRANT	5567	Woodford
WF # 3 Mobil Rahm Lela	36.5809	-97.82898	03	24N	06W	GARFIELD	6729	Woodford
WF # 4 Shell Guthrie	36.25138	-97.45871	31	21N	02W	NOBLE	4165	Woodford
WF # 6 Mobil Cement Ord	34.90223	-98.07862	18	05N	08W	GRADY	17581	Woodford
WF # 5 Mobil Dwyer Mt	36.23352	-98.22134	01	20N	10W	MAJOR	8716.5	Woodford
WF # 7 Amerada Chenoweth	36.40693	-97.73539	04	22N	05W	GARFIELD	6513	Woodford
WF # 8 Apexco Curtis	35.39349	-97.72205	27	11N	05W	CANADIAN	8520	Woodford
WF # 9 Jones and Pellow	35.03079	-98.53458	35	07N	13W	CADDO	6793	Woodford
WF # 10 Lonestar Hannah	36.15513	-99.79674	06	19N	24W	ELLIS	14323	Woodford
Oil # 1 Mehan 5-14	36.04037	-97.05213	14	18N	02E	PAYNE	4580-4600	Woodford
Oil # 2 Holstein 2-22H	36.11549	-96.97661	22	19N	03E	PAYNE	4140	Mississippian
Oil # 3 German 1-13H	36.03734	-96.83598	13	18N	04E	PAYNE	3923-5550	Mississippian
Oil # 4 Myers	36.11295	-96.72414	24	19N	05E	PAYNE	3510-3520	Woodford
Oil # 5 Jester 1-26	36.09673	-96.63842	26	19N	06E	PAYNE	3260-3290	Mississippian
Oil # 6 Holstein 1-22	36.11062	-96.97672	22	19N	03E	PAYNE	4274-4300	Woodford
Oil # 7 McGuire 1-14	36.03791	-96.84872	14	18N	04E	PAYNE		Mississippian
Oil # 8 Mehan 2-14H	36.02974	-97.05475	14	18N	02E	PAYNE		Woodford
Oil # 9 Mehan 5-14 (2)	36.04037	-97.05213	14	18N	02E	PAYNE	4580-4600	Woodford
Oil # 10 Holstein 2-22H (2)	36.11549	-96.97661	22	19N	03E	PAYNE		Mississippian
Oil # 11 German 1-13H (2)	36.03734	-96.83598	13	18N	04E	PAYNE		Mississippian
Oil # 12 Holstein 1-22 (2)	36.11062	-96.97672	22	19N	03E	PAYNE	4274-4300	Woodford
Oil # 13 McGuire 1-14 (2)	36.03791	-96.84872	14	18N	04E	PAYNE		Mississippian

2.2 Methodology for Source Rock Sample Preparation

2.2.1 Methodology for Organic Matter Separation and Analysis

The rock samples were pulverized using a manual mill, and stored in a 30 ml LDPE Narrow mouth Nalgene bottle. Plenty of rock sample was powdered to have remaining sample for future analysis. The sample was put on a Teflon beaker for the chemical preparation. High purity HF (Hydrofluoric Acid) was applied to each sample in a range of 12 to 15 ml, to dissolve the silicates. The sample was then put on a hot plate at 80˚C in a fume hood for slow evaporation. The sample was stirred from time to time until complete evaporation was achieved (12 to 14 hours). After cooling off of the sample thorough rinsing was performed several times with copious amounts of deionized water and evaporated overnight at low temperature. The sample was then put in reaction with 2-3 ml of highly purified HCl (Hydrochloric Acid) and then evaporation procedure was repeated, converting the solution into chlorides and dissolving the carbonates from the rock sample. Following the rinsing of the samples, a repeat step of HF dissolution was made to minimize the presence of silicate materials remaining attached to the organic fraction. After HF digestion and rinsing the samples in large amounts of deionized water, the acid digested sample then was put into water suspension for a collection of the organic fraction (Figure 18). The entire procedure was intended for obtaining sediment-free organic material, but there was no complete assurance that the procedure actually yielded the desired materials, although it is inferred the results of the separation are positive when observing the difference in REE concentrations between the organic matter and the silicate-carbonate fraction analyzed (Table 6A, Table 6B). The possibility of having fine inorganic particles remaining attached to the organic constituents is recognized, and the development of a careful sample preparation method is desirable. The organic matter samples collected after dissolution of the silicate-carbonate fraction were calcinated at 600˚C, then the calcinated product was dissolved in a known volume of HNO_3 (Figure 19)to finalize the samples preparation for their analysis by inductively coupled plasma mass spectrometry (ICP-MS) and inductively coupled plasma atomic emission mass spectrometry (ICP-AES).

The precision obtained for all elements was about ±10% expressed as relative standard deviation.

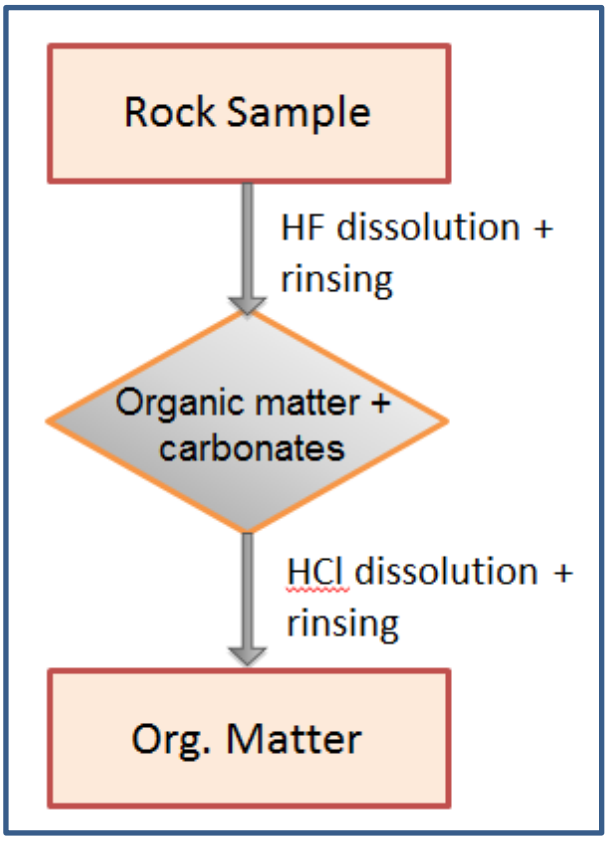

Figure 18 Organic Matter separation Flowchart

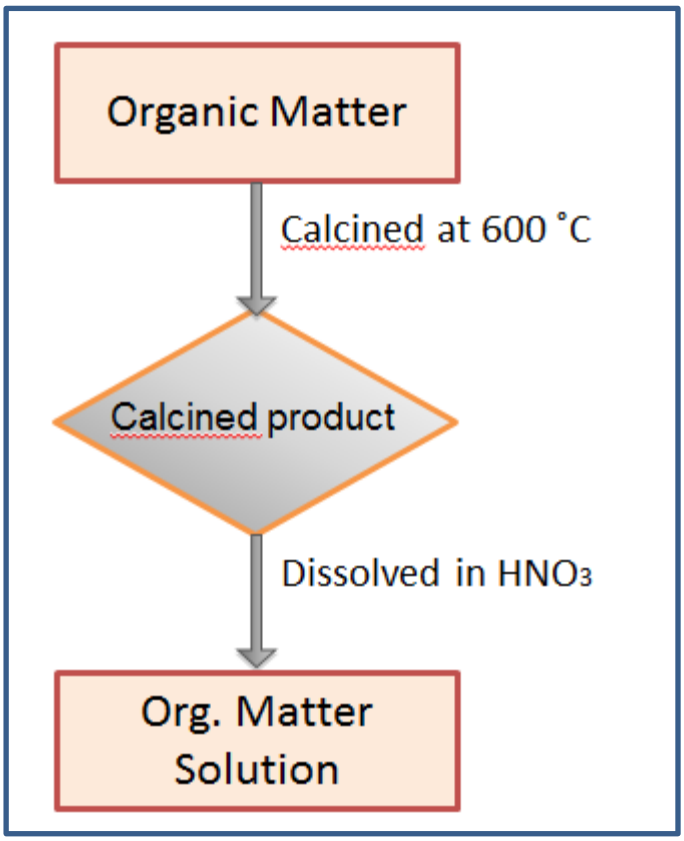

Figure 19 Organic matter solution for analysis

2.2.2 Methodology for Silicate-Carbonate fraction Analysis

Whole rock preparation for analysis through ICP-MS and ICP-AES was very similar to the separation process of organic matter. Having the samples grinded to powder started the process for separation of carbonates and silicates from the organic matter. The variation in the process was dissolving the rock sample in a mixture of HF and HCl. The solution was heated and filtered. Thorough rinsing followed the filtration and the samples were collected. The sample was then evaporated to dryness and finally re-dissolved in HNO_3 to obtain a final solution in nitric form (Figure 20).

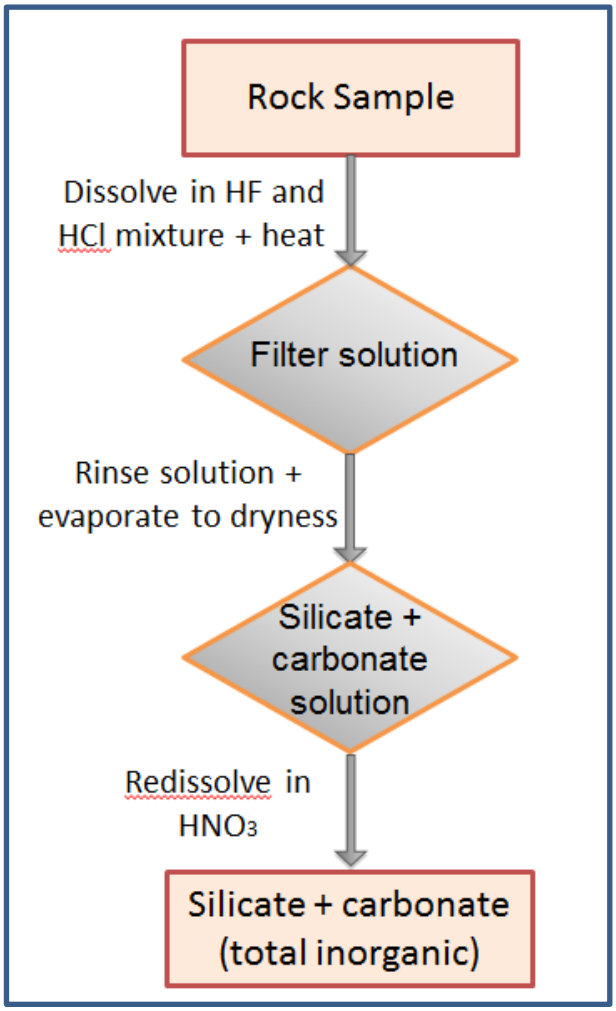

Figure 20 Silicate-carbonate fraction separation flowchart

2.3 Methodology for Oil Analysis

The oil samples were initially processed for analysis in the geochemistry laboratory in the geology department, and then the samples were later processed in the chemistry lab in the biochemistry department both in KSU.

The sample processing began by extracting pure oil sample from the crude bottles, which contained oil and brine associated to the oil. The oil was extracted by carefully pipetting out the oil, not extracting the whole oil sample leaving a frame of oil so there was no room for error in the extraction, staying away from the brine. This process was made for all the oil samples and each pipetted sample was collected in a clean Nalgene bottle. The pipetted oil sample was again processed for separation moving the sample into 50 ml centrifuge tubes. After the manual separation, each sample with an approximate of 250-300 ml of oil were centrifuged. This

mechanical separation of oil and water took over four hours for each of the samples. After each sample was centrifuged it could be observed in different samples that there was again some separation of brine and oil; this was observed as the remaining brine in the sample was at the bottom of the centrifuge tube. In some cases the remaining brine was very little, and in other cases the remaining brine was close to three milliliters. Each oil sample was then weighted by the milliliter, in an electronic scale to know the sample's mass in grams. This process was of notable importance as the density of the oil samples is needed to interpret the analytical results. After this separation process was completed, the evaporation process began for the oil samples.

The first five samples were experimentally processed in the geology lab. Those first five samples were ashed in s furnace oven at varying temperatures. The first sample was ashed initially at aprox. 400˚C. It was observed that after 20 minutes of being in the furnace at that temperature the sample caught on fire, and was left to burn. Learning through this experience, the samples were processed in the furnace with subtle temperature increments of 40 to 50 degrees Celsius every 40 to 60 minutes. The purpose of this procedure was to have the oil samples lose the lighter fraction, looking to have the oil residue as an end product of the process. The room preparation was not adequate to do heavy oil evaporation, the black fumes were very noticeable and the fume hood was not strong enough to take all the fumes out of the room, so a new process was implemented by Dr. Totten, Dr. Chaudhuri and me (Figure 21). This consisted of preparing a homemade slow evaporation furnace with complete isolation to the outside and a ventilation conduct to dispose of the fumes, all while being set up outdoors on a field in Wamego, KS, with the purpose of avoiding exposure to black heavy fumes from oil.

Figure 21 Outdoor furnace built for oil sample evaporation.

The initial evaporation started with the temperatures set on the hot plates at temperatures of 200 ˚C, at these temperatures the samples would not boil, but fumed heavily. The samples were monitored during their evaporation, always avoiding any boiling but having a high enough temperature for the samples to fume. Each oil sample took an average of 70 hours of slow evaporation, during which the temperature was gradually and slowly increased to cause the volatilization of the light fractions of the oil samples. As explained in the crude oil composition section, the residue in oil, or the heavy fraction is the residue with a high percentage of Oxygen and Nitrogen. The purpose of the evaporation of the oil samples was to separate the heavy fraction, which was very noticeable when the sample wouldn't evaporate anymore and the originally liquid oil had become a very viscous, pasty material, in some cases it was completely hardened. When the sample wouldn't fume anymore at temperatures close to 500˚C, the sample was removed and taken to the Chemistry lab to continue preparing the oil samples. The procedure continued by introducing the samples in the furnace where they were further ashed at a high temperature close to 600˚C. A solution was prepared with the ashed sample (residue) dissolving it in HNO3, for the metal analysis by ICP-MS and ICP-AES (Figure 22).

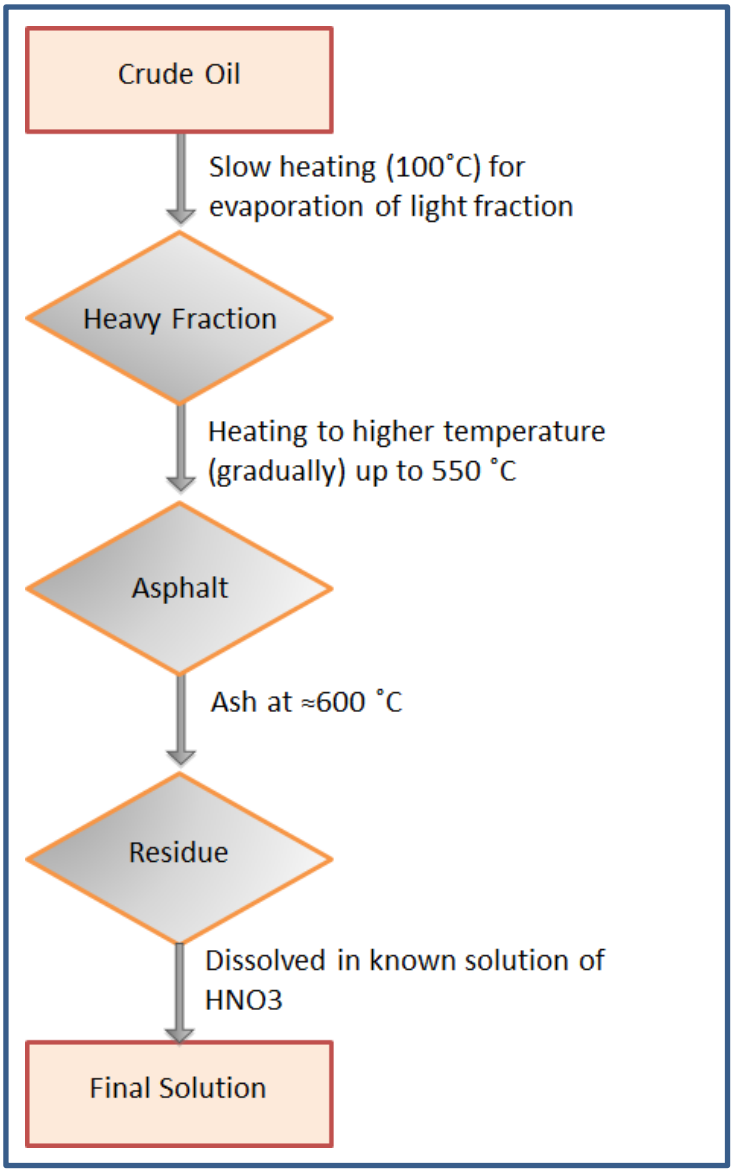

Figure 22 Oil sample preparation Flowchart

2.4 Methodology for Organic Geochemical Analysis.

The Woodford shale whole rock samples were analyzed for TOC (Total Organic Carbon). Elemental chemistry was also performed on four samples of the organic portion of the Woodford Shale. Carbon, hydrogen, oxygen, nitrogen and sulfur were analyzed in the organic portion of the Woodford shale to use the O/C and H/C ratios to identify the kerogen type in the four analyzed samples. The samples were prepared by using a manual ball mill and pulverizing them. The samples were then sent to the Weatherford Lab in Golden, CO for the elemental analysis and to the Weatherford Lab in Shenandoah, TX for TOC analysis. Rock Eval Pyrolysis is the method used to identify petroleum potential in sediments. This method consists of programmed temperature heating in an inert atmosphere with the sample of approximately 100 mg. The hydrocarbon and oxygen containing compounds (CO_2) are selectively determined during the cracking of the organic matter in the sample. When measuring TOC in the sample, the sample is oxidized to target the organic matter remaining in the sample after pyrolysis. The TOC is determined by adding the organic carbon that underwent pyrolysis and the residual organic carbon measured through the oxidation procedure.

Chapter 3 - Results

The Woodford Shale samples were prepared for analysis by separating the organic matter from the silicate-carbonate fraction. The organic matter and the rock matrix were analyzed separately and the results are shown in the following tables. Oil sample results are also shown in the following tables. The samples were sent to the Laboratory of Hydrology and Geochemistry in the University of Strasbourg, France, for the analytical examination by ICP-MS and ICP-AES.

3.1 Analytical Data of Woodford Shale's Organic Portion.

On Table 6A, the analytical data for the organic matter of the Woodford shale is represented. Major elements were analyzed by an Ion Coupled Plasma Atomic Emission Spectrometer (ICP-AES), showing the concentrations of the results in ponderated % of calcinated sample.

Table 6A Major element analytical results of Organic Portion of Woodford shale (WF) Samples

Woodford Shale (WF) Samples Organic Matter Analysis (weight %)										
Sample	**Si %**	**Al %**	**Mg %**	**Ca %**	**Fe %**	**Mn %**	**Ti %**	**Na %**	**K %**	**P %**
WF#1	<0,03	20.17	6.73	8.83	3.77	0.03	0.40	0.86	5.69	0.059
WF#2	<0,04	13.65	9.16	12.94	3.18	0.11	0.52	0.53	5.96	0.47
WF#3	0.047	18.97	6.72	5.27	11.01	0.047	0.61	0.88	7.56	0.093
WF#4	0.33	21.54	5.34	4.91	8.95	0.04	0.47	1.54	6.09	0.060
WF#5	0.16	11.09	2.89	1.70	5.34	0.023	0.56	0.65	5.37	0.069
WF#6	0.75	12.56	3.23	0.44	7.83	0.017	0.76	0.92	5.74	0.11
WF#7	0.096	23.85	6.74	0.37	4.86	0.055	0.48	0.84	10.14	<0,06
WF#8	0.87	17.54	4.74	2.52	5.71	0.035	0.92	1.35	5.76	0.17
WF#9	0.061	6.32	0.31	5.77	3.15	0.017	0.45	0.15	1.40	2.59
WF#10	0.044	16.82	8.23	9.89	3.80	0.037	0.18	0.42	7.48	0.052

The data represented in this table 6B was obtained by the sample analysis with an Inductively Coupled Plasma Mass Spectrometer (ICP-MS). Trace elements are included in the

analysis, with the REE included. The concentrations are represented in parts per million. Total REE concentration for each of the samples ranges from 300 to 800 ppm approximately. Vitrinite Reflectance values shown at the bottom of Table 6B are collected from two data sources. Brian Cardott directly analyzed five of the Woodford Shale samples for Vitrinite Reflectance (Ro). The samples directly analyzed for Ro are samples WF#4, WF#5, WF#8, WF#9, and WF#10. The five Ro values for the remaining samples are estimated from a regional maturity map for the Woodford Shale constructed by Cardott and Lambert (1985), through vitrinite reflectance data. Vitrinite Reflectance measures the thermal maturity of a source rock considering a sample is mature if its Ro values are higher than 0.5%, and considering a sample being post mature if the sample's Ro values range from 2% to 3%. Ratios of K/Rb, U/Th and V/Ni can also be found in the bottom section of Table 6B.

Table 6B REE and Trace Metals Analytical Results of Organic Portion of Woodford Shale (WF) Samples

Woodford Shale(WF) Samples Organic Matter Analysis										
Concentrations expressed in mg/g of organic matter (ppm)										
Location	**12-07N-06W,**	**15-26N-07W**	**03-24N-06W**	**31-21N-02W**	**01-20N-10W**	**18-05N-08W**	**04-22N-05W**	**27-11N-05W**	**35-7N-13W**	**06-19N-24W**
County	**Grady**	**Grant**	**Garfield**	**Noble**	**Major**	**Grady**	**Garfield**	**Canadian**	**Caddo**	**Ellis**
Plug Depth	**12309 ft**	**5567 ft**	**6279 ft**	**4165 ft**	**8716.5**	**17581 ft**	**6513 ft**	**8520 ft**	**6793 ft**	**14323 ft**
Element	**WF#1 SHELL MCCALLA RANCH**	**WF#2 MOBIL SARA KIRK**	**WF#3 MOBIL RAHM LELA**	**WF#4 SHELL GUTHRIE**	**WF#5 MOBIL DWYER MT**	**WF#6 MOBIL CEMENT ORD**	**WF#7 AMERADA CHENO WETH**	**WF#8 APEXCO CURTIS**	**WF#9 JONES AND PELLOW Ne Alden Un**	**WF#10 LONESTAR HANNAH**
V	183.82	153.94	257.21	393.71	329.49	5530.43	477.67	927.53	1446.93	108.22
Cr	107.84	117.02	139.53	490.07	57.14	86.96	109.59	141.18	273.74	88.89
Co	16.67	12.77	43.02	11.26	36.57	26.09	41.1	23.53	9.5	17.78
Ni	90.2	26.6	91.86	202.65	281.71	548.7	275.34	348.24	250.28	33.33
Cu	199.02	30.85	131.4	198.01	205.14	606.96	124.66	588.24	382.12	34.07
Zn	60.78	63.83	91.86	156.29	152	1991.3	167.12	278.82	262.01	37.04
As	39.61	14.04	145.35	76.16	90.86	216.52	73.56	43.88	64.8	33.26
Rb	415.69	290.43	408.14	486.75	544.57	650.43	689.04	409.41	136.31	405.19
Sr	226.76	228.4	179.3	320.53	188.4	377.91	259.32	605.18	509.11	145.41
Y	56.14	49.27	66.69	62.42	70.86	201.74	93.93	101.01	117.88	58.39
Zr	196.08	148.94	127.91	152.32	120	243.48	178.08	200	134.08	251.85
Cd	0.43	0.34	0.71	1.23	1.06	10.11	1.44	1.64	1.11	0.15
Sn	11.76	9.57	9.3	8.61	6.29	10.43	9.59	10.59	5.59	3.7
Sb	4.79	1.59	10.34	16.14	16.75	101.74	9.68	20.55	17.22	1.32
Cs	18.63	7.45	15.12	21.19	42.86	40.87	27.4	17.65	8.38	11.85
Ba	1686.27	641.49	920.93	834.44	720	5582.61	1054.79	1941.18	1519.55	762.96
La	93.19	66.36	89.69	109.27	67.43	173.04	114.25	108.49	81.56	88.89
Ce	165.69	120.21	181.4	164.24	124	247.83	224.66	203.53	106.71	193.33
Pr	19.34	14.62	21.43	18.08	15.77	43.75	26	25.8	19.51	20.41
Nd	70.78	54.26	82.21	59.34	62.29	176.52	95.34	101.41	80.45	77.78
Sm	11.67	9.68	15.81	9.4	11.89	34.87	17.4	19.29	16.42	13.93
Eu	2.09	1.8	3.15	1.9	2.5	6.87	3.34	3.82	3.31	2.66
Gd	9.9	9.15	15.12	9.21	12.06	33.91	16.16	18.71	16.98	12.67
Tb	1.42	1.24	2.01	1.35	1.69	4.78	2.36	2.55	2.36	1.76
Dy	8.92	7.68	12.1	9.17	10.39	29.76	15.47	15.66	15	10.7
Ho	2.16	1.7	2.79	2.32	2.51	7.13	3.56	3.76	3.52	2.44
Er	6.18	4.79	7.33	7.02	6.46	18.09	9.86	9.76	9.33	6.67
Tm	1.15	0.79	1.2	1.28	1.05	2.92	1.68	1.59	1.45	1.05
Yb	6.99	4.38	6.81	7.84	5.97	16.12	9.21	9.54	8.08	6.42
Lu	1.09	0.69	1	1.21	0.87	2.36	1.36	1.44	1.18	0.96
Pb	38.53	24.26	52.67	223.25	55.43	115.65	90.41	59.88	35.47	40.96
Th	33.73	17.55	25.47	34.83	21.14	35.04	39.32	30.94	15.81	30.52
U	7.64	4.28	42.92	17.41	47.3	131.3	35.62	41.99	50.73	4.03
Ce/Ce*	0.94	0.93	0.99	0.87	0.92	0.69	0.99	0.93	0.64	1.09
Eu/Eu*	1.03	1.01	1.08	1.08	1.11	1.06	1.06	1.06	1.05	1.06
K/Rb	13.71	20.52	18.52	12.51	9.86	8.82	14.71	14.06	10.27	18.46
U/Th	0.23	0.24	1.69	0.5	2.24	3.75	0.91	1.36	3.21	0.13
V/Ni	2.04	5.79	2.8	1.94	1.17	10.08	1.74	2.66	5.78	3.25
∑REE	400.57	297.35	442.05	401.63	324.88	797.95	540.65	525.35	365.86	439.67
Ro	0.75	0.51	0.55	0.67	0.68	1.25	0.52	0.53	0.47	2

3.1.1 REE Concentration on organic matter of Woodford shale.

Concentration levels of REE in the organic matter of the Woodford shale have a striking difference in abundance when comparing it to REE concentration levels in average shale, in modern day plants and in silicate rocks (Figure 23).

Total rare earth concentration in the organic portion of the Woodford show values from 300 to 800 ppm. Modern day plants contain ppb levels of TREE. Where are the high concentrations of REE present in organic matter of the Woodford Shale coming from? Silicate rocks show total rare earth concentrations according to Barrat, et al., in levels around 100 ppm. It can be suggested that as the source rock is being transformed through maturation, there is release of rare earth elements from the silicate rocks into the organic portion of the whole rock, due to dissolution of the silicate rocks.

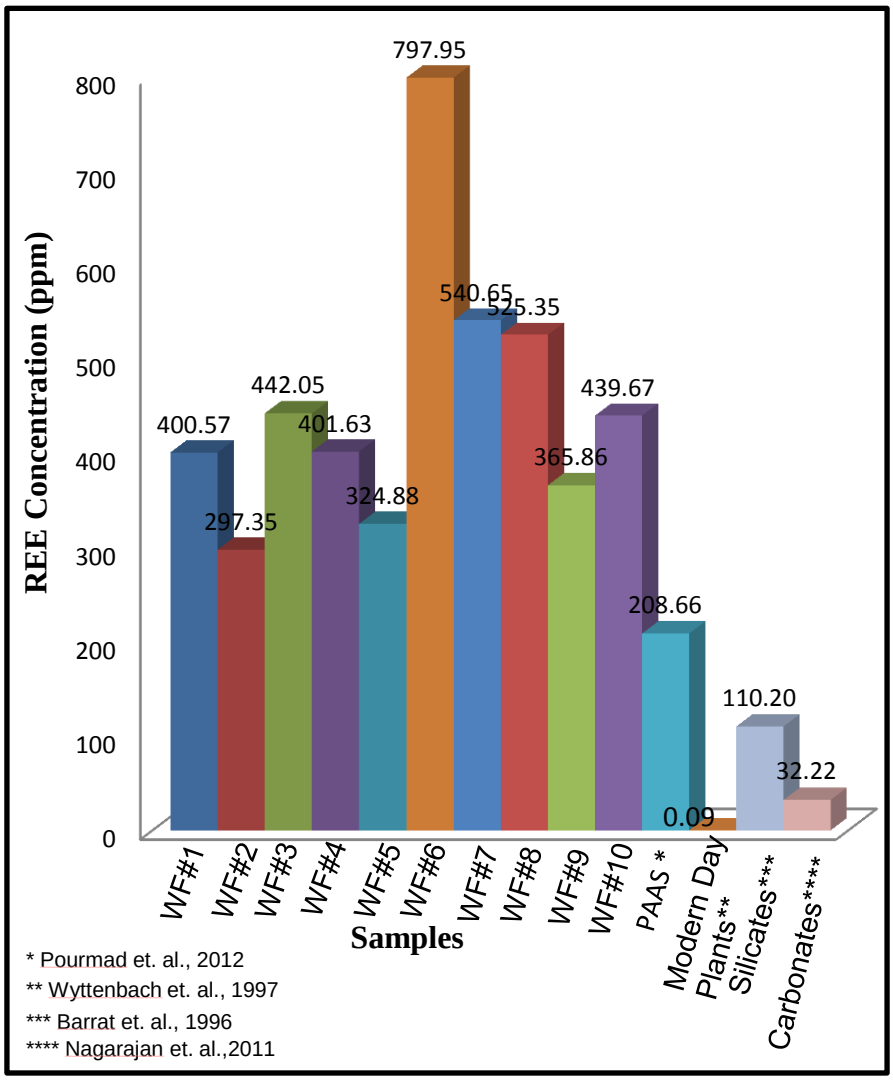

Figure 23 REE concentrations in the Woodford Organic Matter Samples and in reference materials

The concentration of REE in silicates is not being affected, as the provision of REE into the organic matter is influenced by dissolution of the rock, and that opens up a possibility of using concentration of REE in organic matter as a transformation indicator in the whole rock, having a higher concentration of REE in the organic matter when the rock has undergone maturation, and having lower concentration values of REE when the rock has not been matured.

3.1.2 REE Distribution Patterns of Organic Matter in the Woodford Shale

The general distribution patterns for PAAS show an enrichment in light rare earths (LREE: La to Nd), negative europium anomalies, flat middle rare earths (MREE: Sm to Ho) and also flat heavy rare earth abundance patterns (HREE: Er to Lu) as postulated by Rollison (1993). It has been stated that fractionation and mobilization of the rare earth elements happens during sedimentation and diagenesis (Condie, 1993). Release of rare earth elements occurs by breakdown of unstable minerals during early diagenesis, and the REE are complexed in organic-rich layers and phosphates (Kidder and Eddy-Dilek, 1994). The purpose of looking into the rare earth element distribution patterns normalized to PAAS in the organic, and the inorganic portion of the Woodford shale separately, the oil generated from this source rock and the brine associated to the oil, is to characterize these patterns and relate them to thermal maturation and diagenesis. Most studies on the effects of diagenesis on trace elements in organic rich sediments have only been studying the whole rock composition, but through this study the organic matter and the silicate-carbonate fraction is isolated to understand the effects of organic matter diagenesis through thermal maturation on the distribution of REE in the Woodford shale. As stated before the rare earth elements are useful provenance indicators in sedimentary rocks (Taylor and McLennan, 1985) The PAAS values used for this study are taken from a study by Ali Pourmand, et. al.,2012, and represented in Table 7.

Table 7 PAAS concentration values by Pourmand et. al. used as reference in this study

PAAS ppm(2012 Pourmad, et.al.)										
Element	AO-6	AO-7	AO-9	AO-10	AO-12	SC-7	SC-8	PL-1	PW-5	Mean (n=9)
La	37.87	40.3	38.65	45.69	44.59	43.08	44.52	42.77	63.53	44.56
Ce	75.23	78.27	74.56	87.48	82.5	87.61	91.38	90.4	126.8	88.25
Pr	8.6	8.96	8.66	10.14	10.02	9.9	10.29	10.02	14.72	10.15
Nd	31.46	32.29	31.5	37.01	37.01	36.75	38.28	36.82	54.78	37.32
Sm	5.728	5.878	5.759	6.935	6.149	6.835	7.141	7.24	10.29	6.884
Eu	0.99	1.031	1.002	1.264	1.115	1.211	1.192	1.21	1.917	1.215
Gd	4.911	5.127	4.944	6.102	5.388	5.983	6.218	6.588	9.127	6.043
Tb	0.72	0.761	0.72	0.861	0.857	0.867	0.895	1.013	1.328	0.8914
Dy	4.273	4.557	4.283	5.027	5.291	5.135	5.299	6.243	7.816	5.325
Ho	0.839	0.91	0.844	0.982	1.064	1.009	1.047	1.264	1.515	1.053
Er	2.446	2.687	2.477	2.865	3.121	2.911	3.044	3.814	4.314	3.075
Tm	0.36	0.4	0.365	0.421	0.456	0.421	0.442	0.578	0.617	0.451
Yb	2.419	2.703	2.459	2.819	3.064	2.774	2.926	3.916	4.03	3.012
Lu	0.354	0.399	0.36	0.412	0.451	0.4	0.425	0.569	0.578	0.4386
Eu/Eu*	0.56	0.57	0.57	0.59	0.58	0.57	0.54	0.53	0.6	0.57±0.02
LREE/HREE	9.73	9.44	9.67	9.61	9.16	9.45	9.44	7.81	9.21	9.28±1.17

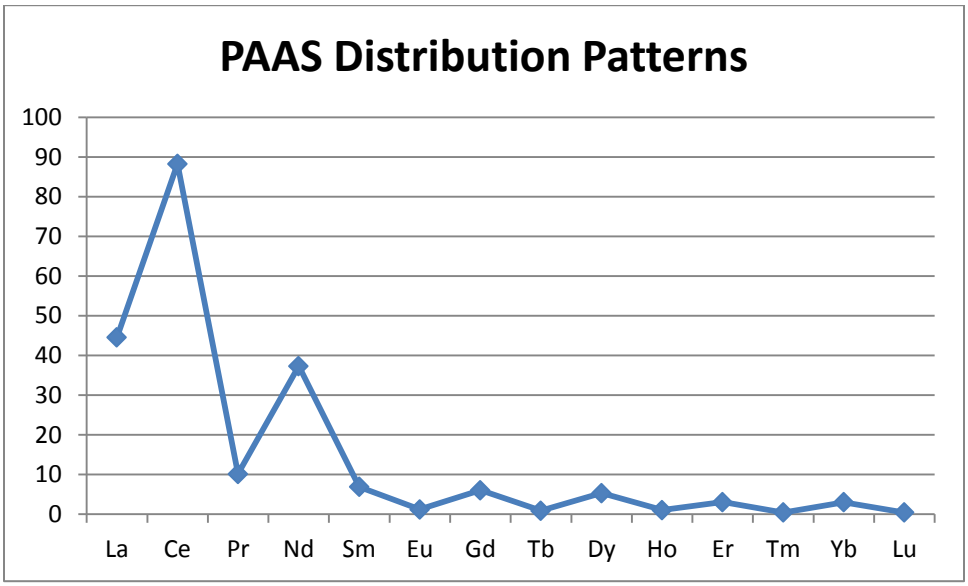

Figure 24 REE distribution pattern in PAAS according to Pourmand et. al.,

No uniquely broad distribution pattern can be the characteristics of all organic materials, but some common features in the REE distribution patterns may be repeatedly seen for organic materials deposited within a given sedimentary basin or part of a given sedimentary basin. Because the organic materials in a sedimentary basin can have multiple sources from both land and ocean, it will be highly unlikely to see any trend in correlation between the total REE and the REE distribution pattern. But what has been observed in our study of the REE in organic fractions of the Woodford Shale in the northern part of Oklahoma is that most of the organic fractions have their MREE (from Sm to Tb) distributions are anomalously similar. Characterizing the rare earth element distribution patterns normalized to PAAS in the organic matter of the Woodford Shale is part of this study with the objective of understanding the chemical interactions occurring diagenetically when the organic matter is undergoing maturation.

Cerium and europium anomalies are measured by finding the value of cerium or europium that the distribution pattern should follow if there was no depletion or enrichment, by interpolating between the normalized values of Lanthanum and Praseodymium for cerium anomaly, and interpolating between Samarium and Terbium for the europium anomaly. The calculated value is designated as Ce* or Eu* respective to the inquiry. To finally know the anomaly, the analytical value of Ce and Eu is divided by the Ce* and Eu* values respectively.

The cerium and europium anomalies for the individual Woodford Shale samples for the organic portion and the silicate-carbonate fraction are shown on the individual distribution pattern charts shown on the Appendix. Due to analytical error margin of 10% from the laboratories used, when calculating the anomalies, a standard is set where my value is considered an anomaly when having a value of ±10% for enrichment or depletion.

Figure 25 shows the REE distribution patterns normalized to PAAS for the entire Woodford Shale organic matter fraction samples. A consistent trend of heavy rare earth enrichment is noticeable when observing the patterns all together. The distribution patterns show more distinctive features and are described in the following sections.

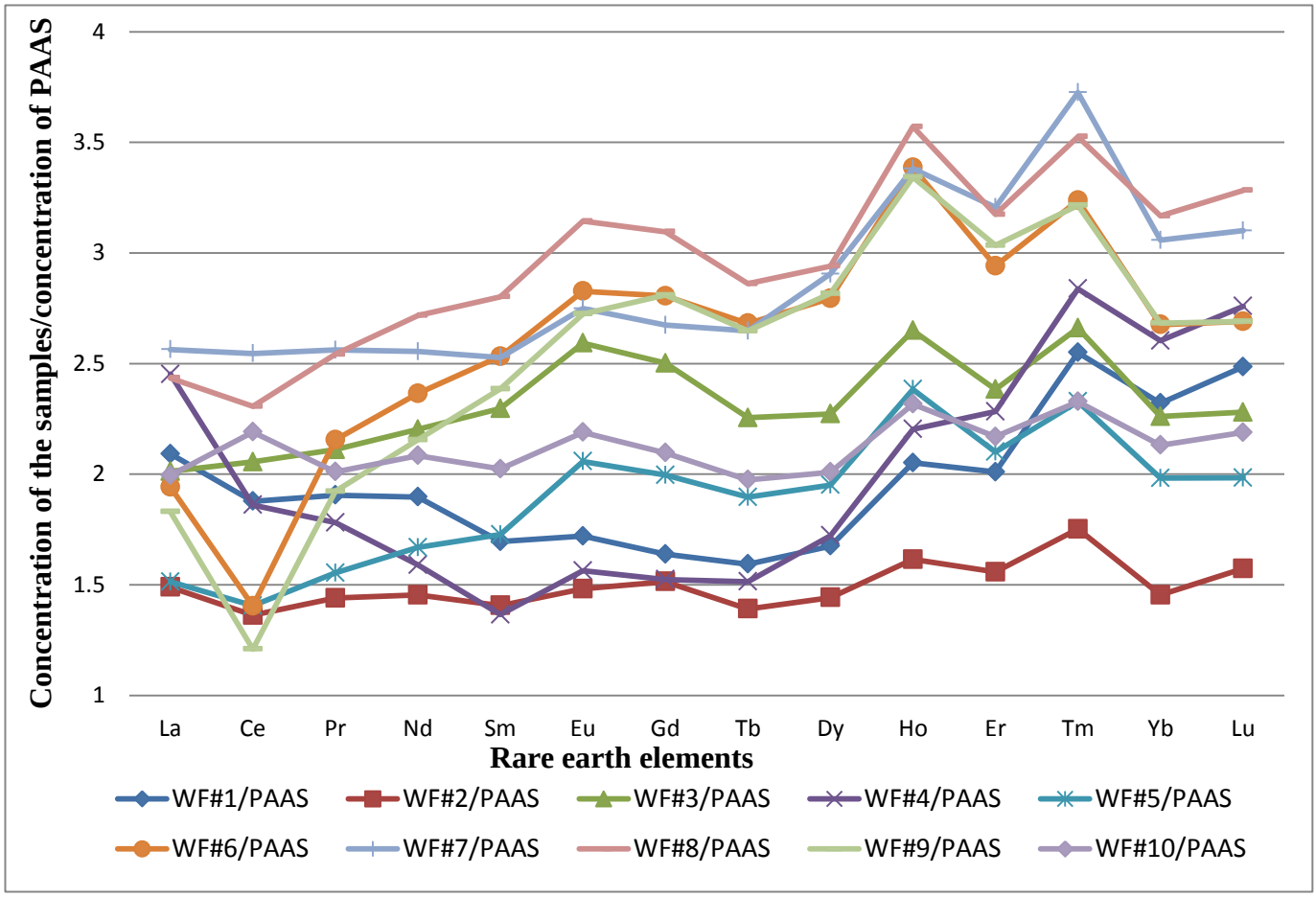

Figure 25 REE distribution patterns normalized to PAAS for the Organic portion of the Woodford Shale

Cerium Anomalies

One of the striking features of the PAAS-normalized REE distribution patterns of the organic fractions of the Woodford Shale is the presence of Ce negative anomalies in three out of the ten samples as can be seen in Figure 26. The rest of the samples show a low cerium anomaly which does not surpass 10% of anomaly (Figure 27). Only one of the samples (WF#10) shows a cerium positive anomaly although this anomaly again is not higher than 10% (Figure 28). A simple explanation for the widely variable Ce anomalies among samples from different localities may be that the differences are linked to organic material source variations. Several studies have demonstrated that Mn-oxyhydroxides partly controlled rare earth element fractionation and mobility in natural water, providing evidence that a negative cerium anomaly in solution is developed through oxidation of Ce (III) onto the MnO_2 surface (Davranche, et.al., 2005). The literature has also frequently reported Ce negative anomaly in terrestrial inorganic materials to manganese oxide precipitation effect, as manganese oxide materials, especially those Mn-nodules that have been found on ocean beds, have been seen with Ce positive anomalies. In fact, sea waters have been found with Ce negative anomalies. Thus, growth in marine environments may be traced for those organic fractions of the Woodford Shale that had been found with Ce negative anomalies, but that will not explain the one organic fraction with a light positive Ce anomaly and the rest of the samples with no considerable anomaly. Besides a mixing effect of inputs from different sources of organic materials with differing kinds of anomaly which could explain all the Ce trends observed in this study, inputs of Ce from associated sediments into organic materials under an environment of deep burial sediment-organic material interaction could be another explanation for the varied Ce anomalies among the organic fractions of the Woodford Shale.

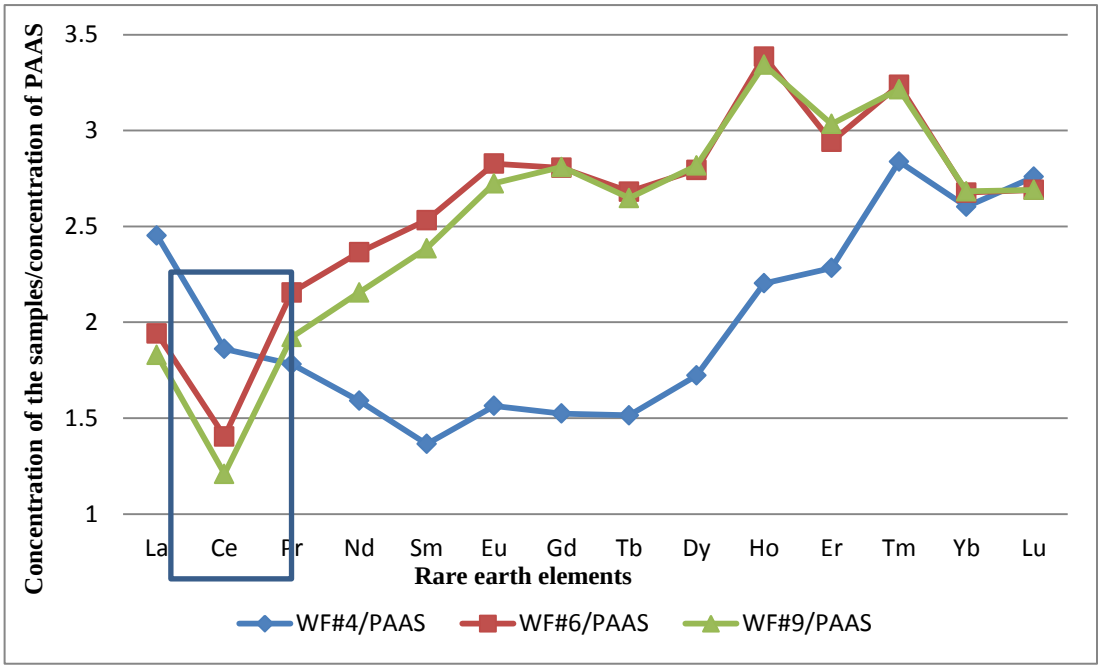

Figure 26 REE distribution patterns of organic matter fraction of the Woodford shale s having Ce depletion.

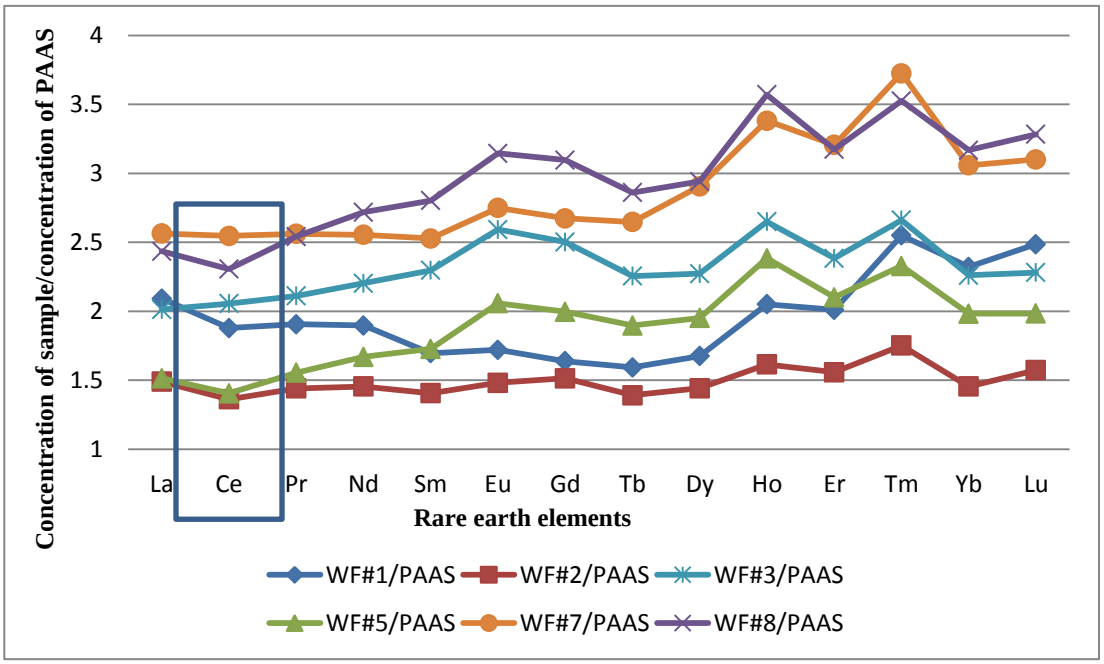

Figure 27 Distribution patterns of REE in 6 organic matter portion of the Woodford Shale without Ce anomalies.

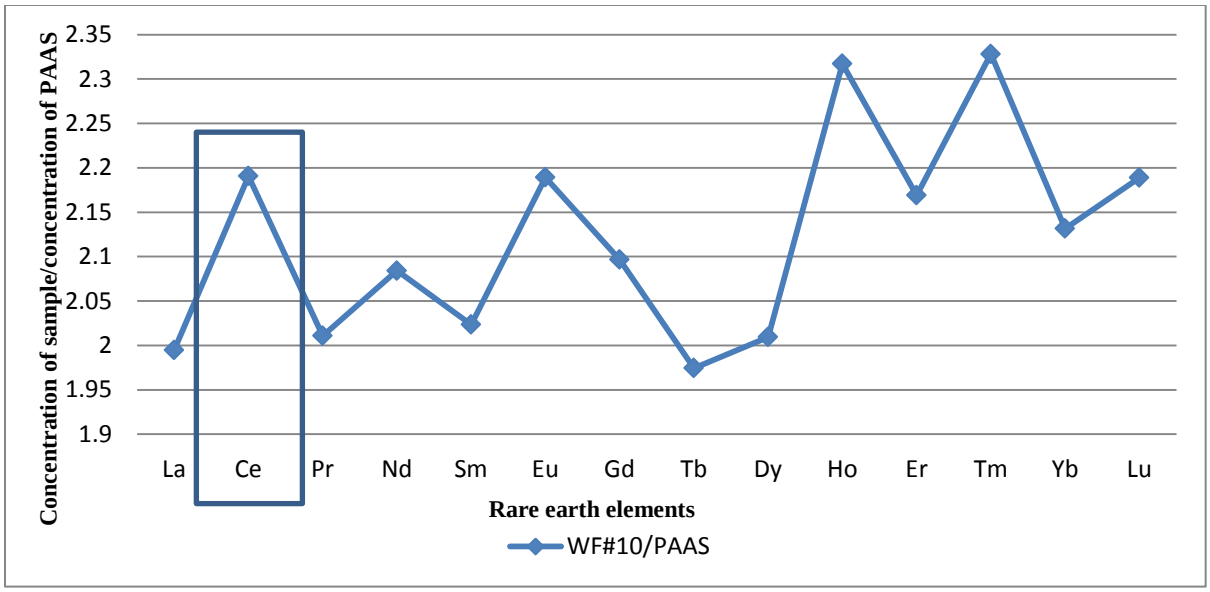

Figure 28 REE distribution pattern of sample WF#10, having cerium positive anomaly.

Europium Anomalies

The REE distribution patterns of the organic fractions of the Woodford Shale can be characterized by the lack of Eu anomalies, having only one sample (WF#5) with a Eu/Eu* value higher than 10% (Figure 29). The rest of the samples do not show any Eu anomaly higher than 10% (Figure 30). Most geochemists working on crustal inorganic materials have attributed positive Eu anomalies in such materials to crystallographic effects, especially feldspar minerals which favor accommodation of Eu^{2+} over a trivalent species. But those who have worked on modern plants, like Chaudhuri and Clauer, have found Eu positive anomalies in plants relative to their growth substrates. The evidence from such studies does not support the idea of a crystallographic effect. Often finding differences in Eu anomalies among different organs of the same plant, Chaudhuri and Clauer (2007) subscribe to the notion that plant enzymic effect plays a significant role in Eu anomalies in the organic materials. Hence, the observed Eu positive anomaly for the organic fraction of the Woodford Shale can be an evidence for the source difference. Again, a case for an influence of post-depositional alteration of sediments in association with the organics can be made for the range of Eu positive anomalies of the organic fractions.

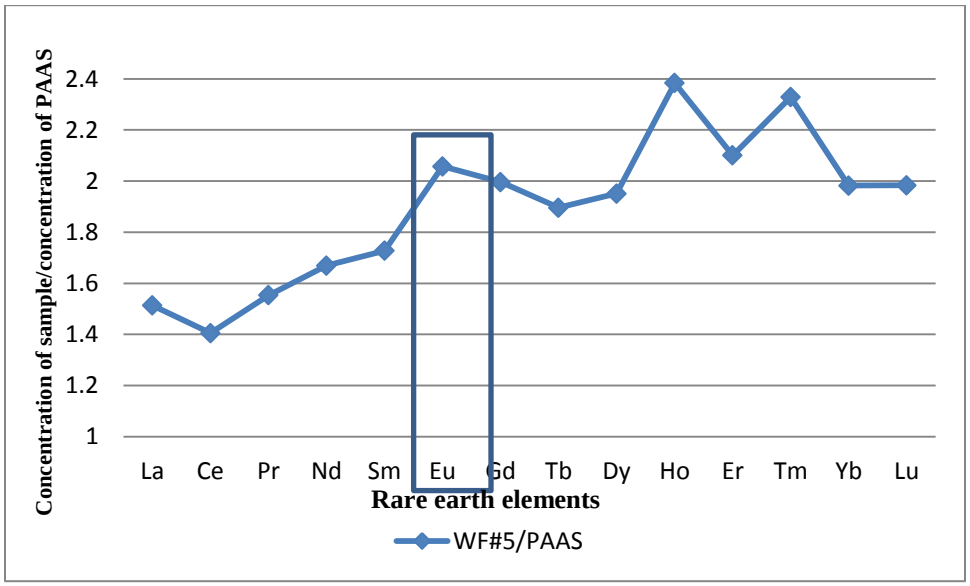

Figure 29 Europium positive enrichment in organic portion of Woodford shale sample

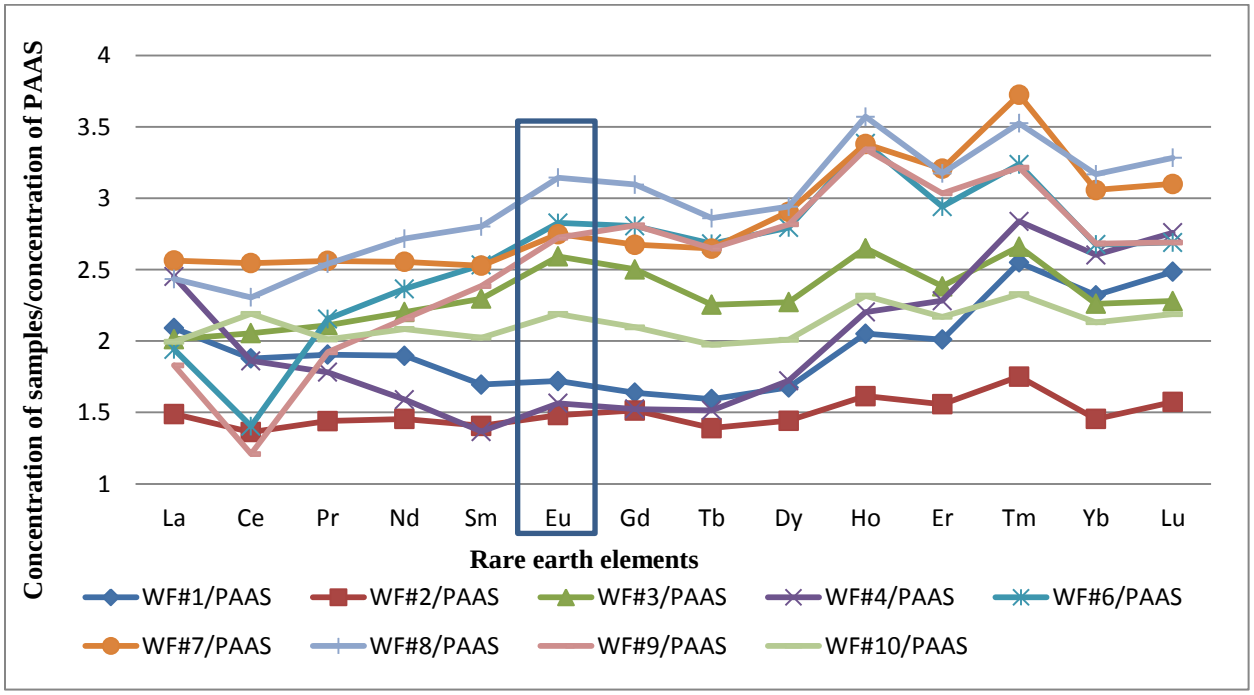

Figure 30 REE Distribution patterns for Woodford Shale Organic Portion, 9 out of the 10 samples don't have a europium anomaly.

Heavy Rare Earth Enrichment

Except for WF#2, and WF#10 (Figure 32), all other organic materials of the Woodford Shale were found with PAAS-normalized REE distribution patterns that can be broadly described as being HREE enriched as seen in Figure 31, even though the trends between La to Lu were interrupted by such attributes as Ce anomalies, Eu anomalies, MREE enrichment, and Ho and Tm positive anomalies. Because the stability constants of the REE-carbonate complexes and the REE-carboxylic complexes have been found to increase progressively with increasing atomic number, the HREE enrichments for the organic fractions of the Woodford Shale might have been caused by effects of REE-carbonate complexes or REE-carboxylate complexes or both. These effects could have been a post-depositional phenomenon.

Table 8 Lanthanum to Lutetium ratio showing HREE enrichment in all the samples except WF#2 and WF#10

Samples	La/Lu
WF#1/PAAS	0.84
WF#2/PAAS	0.95
WF#3/PAAS	0.88
WF#4/PAAS	0.89
WF#5/PAAS	0.76
WF#6/PAAS	0.72
WF#7/PAAS	0.83
WF#8/PAAS	0.74
WF#9/PAAS	0.68
WF#10/PAAS	0.91

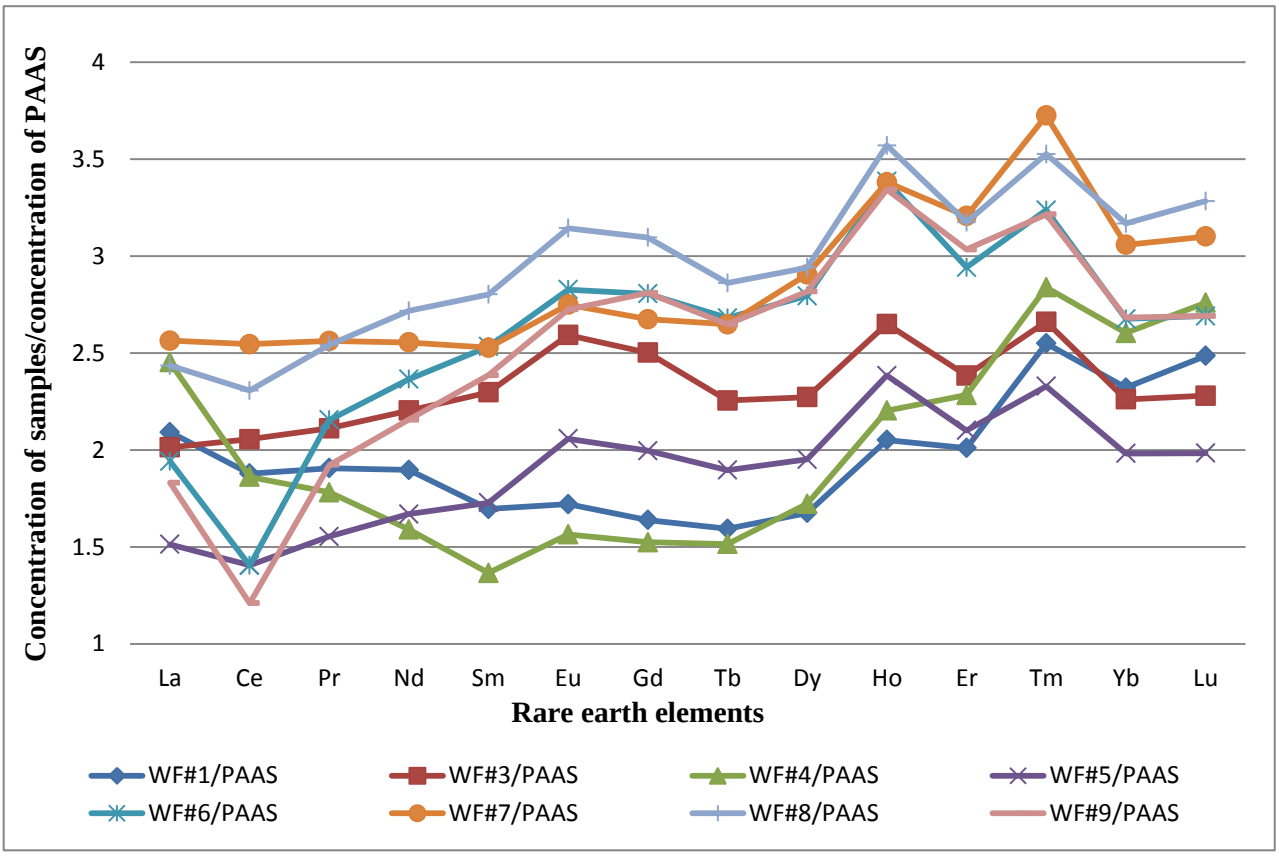

Figure 31 Heavy Rare earth enrichment on Woodford shale's organic matter samples.

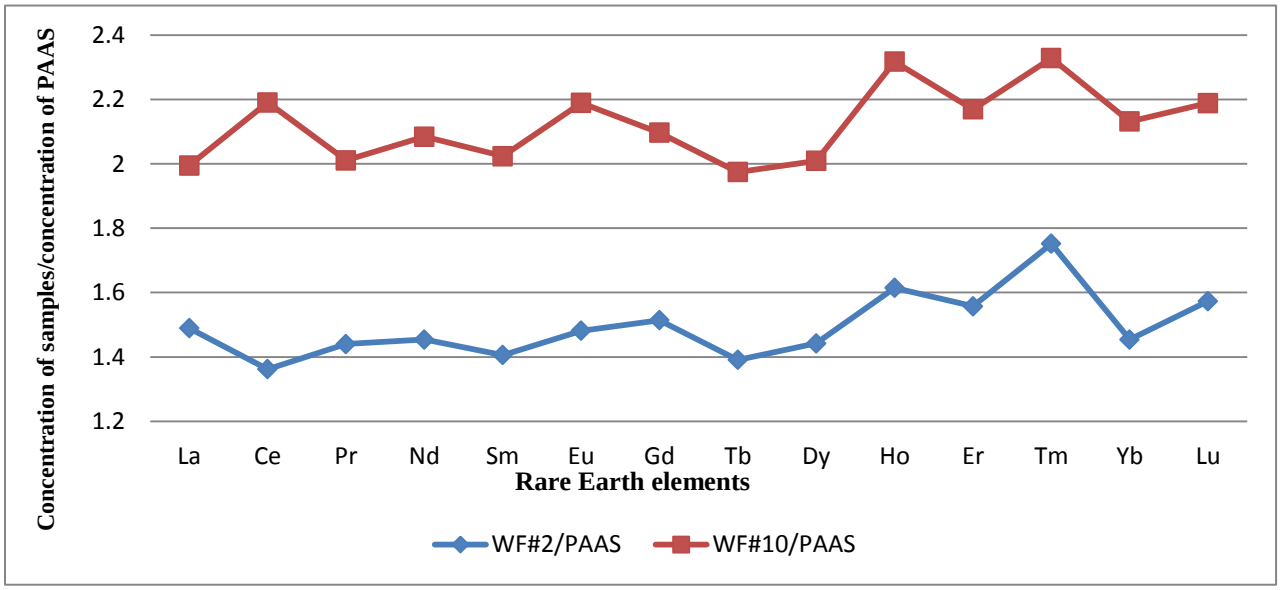

Figure 32 REE Distribution patterns of Organic portion samples from the Woodford shale with flat distribution from La to Lu.

Holmium and Thulium Enrichment

An aspect of the REE distribution patterns that was found to be common to all the samples, except for sample WF#2 and Wf#10, included the presence of Ho and Tm positive anomalies, and this can be observed on Figures 31 and 32 and on the ten individual distribution patterns of the Woodford shale organic matter (Appendix). Sample WF#2 shows a Thulium, but not Holmium enrichment, and sample WF#10 shows a Holmium but not Thulium enrichment. The anomalies have been common with Eu and Ce in natural materials because of the difference in the oxidation states from the natural (III) oxidation state for all the REEs. Thus, Ho and Tm anomalies, varied in different degrees among the samples, and these are reflections of the growth history of the organic source material, arising potentially from enzymatic influence during the growth of the organic materials.

Middle Rare Earth Enrichment

A significant fact about the REE distribution patterns of the MREE of the organic fractions of the Woodford Shale is that six samples (#3, #5, #6, #8, #9, and #10) out of ten had been found with MREE enrichments (or MREE with convex upward trends) by varied degrees and this is observed in Figure 34. Four other organic fractions (#2, #4, #7, and #10) of the Woodford Shale were without any apparent aberration in the distribution trend for the MREE (Figure 35). Phosphate nodules, in general of apatite composition, of different sizes, as large as about 3-4 cm diameter, have been known as secondary deposits in the Woodford Shale (Figure 33). As

Figure 33 Woodford Shale: Arbuckle uplift, Southern Oklahoma (1-35S). Phosphate nodules present, Puckette, 2013

apatite and other phosphate minerals have been well known to have enrichments in MREE, the organic fractions of the Woodford Shale might have been linked to the history of formation of the secondary phosphate minerals. Shales are constituted primarily by clay minerals and quartz, and secondarily by iron oxides and accessory minerals. Apatite is one of those accessory minerals which strongly influence the REE distribution pattern, affecting the concentration of the middle rare earth elements in a positive quantity, when apatite is present in the shale. If apatite has been removed from the samples, it will present a MREE depletion indicating the absence of apatite in the sample.

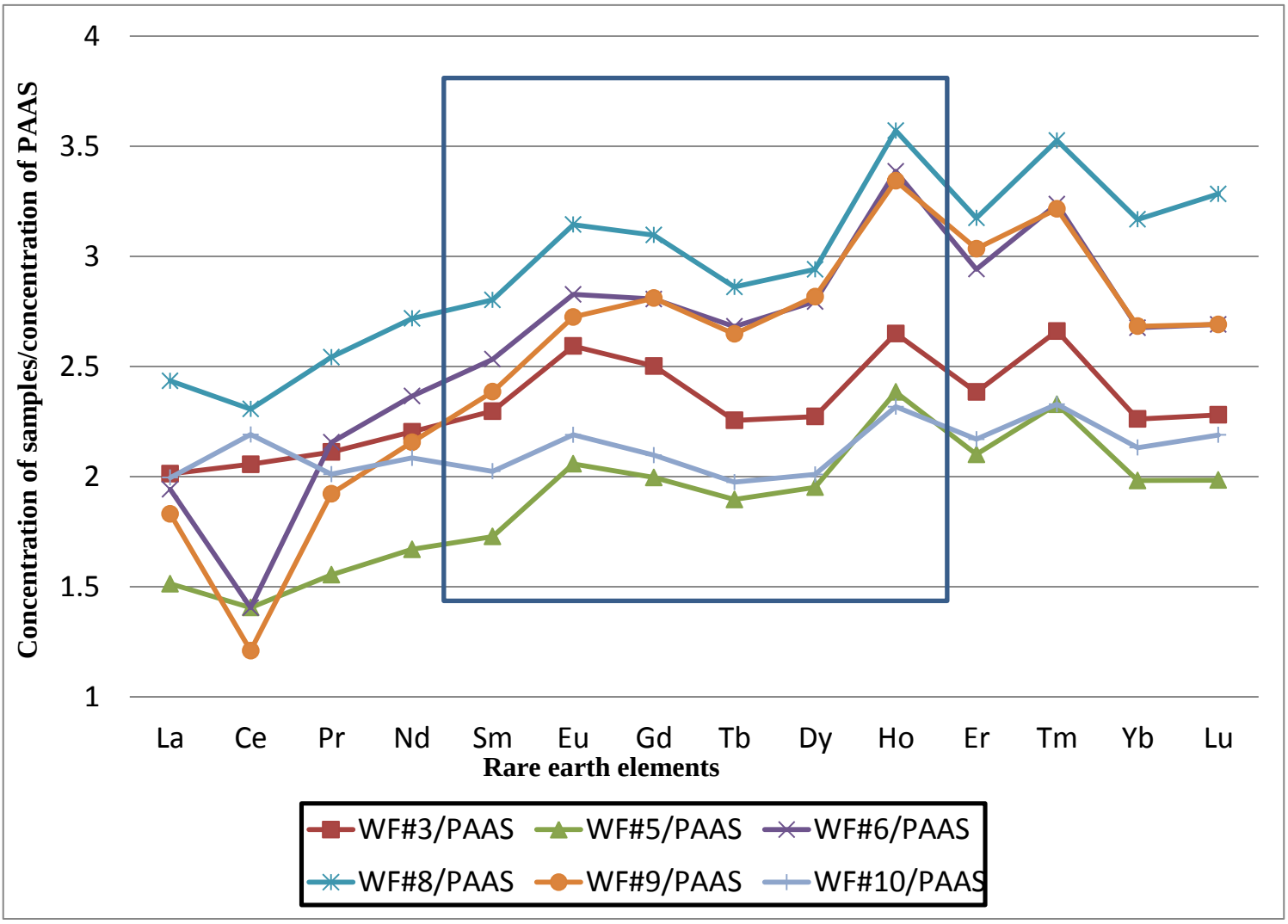

Figure 34 Middle Rare earth enrichment in six samples of the Woodford's shale organic portion.

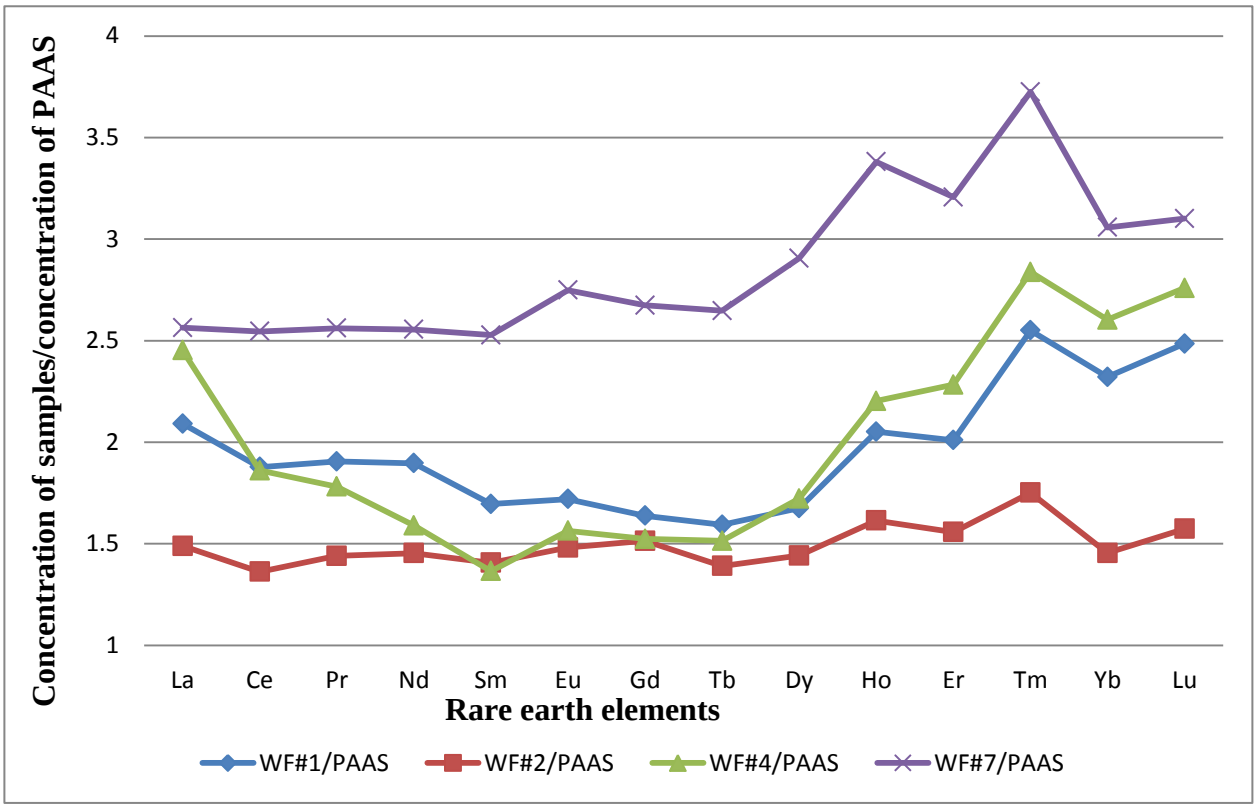

Figure 35 REE distribution patterns of the organic portion of the Woodford shale with flat REE pattern

The MREE enrichment of the organic materials in the Woodford Shale has some underlying cause that probably has a link to the organic material-inorganic sediment system that underwent transformation as it continued to get buried deeper under accumulating younger strata. A key mineralogical system development that happened during the burial history was an abundant formation of the already mentioned apatite nodules (Figure 9, 33). A major geochemical requirement for abundant formations of phosphate nodules was the supply of Phosphorous. It can be reasonably argued that organic matter associated with the Woodford Shale was a prime source of this Phosphorous, which became available when extensive amount of organic matter transformation happened. The P-rich nodules were not products of processes at water-sediment surface at the time of deposition of the sediments, suggesting they formed at some post-burial time that promoted the organic matter transformation, releasing the phosphorous from the organic matter as it is transformed and precipitating in nearby rock. A strong argument that can be put forward for a post-burial event in the formation of the nodules is the recent data that Chaudhuri et al.,2011 reported about REE signatures of several brines that

were collected from the Woodford Shale in Oklahoma. They all have the relative REE distribution patterns with varied but prominent MREE enrichment and positive Eu anomaly.

One may suggest that high REE is incorporated into the organic matter during slow deposition periods in the ocean, as the amount of metal enrichment in a sediment depends upon the diffusion of metal cations from its overlying body, while the sediment system remains open (Lewan and Maynard, 1982), but this study presents and alternative suggestion, with some arguments behind it. First, plant/algal materials have low concentrations of REE (dry weight REEs are generally in few tens to few hundreds ppb at most, and not in ppm levels as we have found in our Woodford Shale organic materials). Therefore, the high concentrations of REE seen in the organic fractions of the Woodford Shale samples are reflections of post-depositional phenomena. The REE concentration range seen here is wide. The range cannot be explained in terms of the degree of maturation of the organic matter or the burial of the organic matter, in part because the organic matter that was deposited in a large sedimentary basin most likely had diverse sources with different amounts of contribution from each to different depositional sites, separated horizontally or vertically. It is well known that ocean organic deposits are varied mixtures of land and ocean derived materials. A correlation scheme for the REE, depicting concentration-burial relationship is possible only when the organic matter comes from the same or an identical source. The distribution patterns of the REEs are to some degree different. These cannot be explained in terms of slow deposition versus rapid deposition effect, as has been claimed by some to explain the concentration variation. This suggestion of the modes of high concentrations of REE and the relative distribution of the REEs in the organic fraction involves intense chemical interactions among the different components within the organic material-inorganic mineral particle-water system. In this scheme, I cannot present evidence to support, an idea that continued input of the REEs from the overlying ocean water as a means of having high REE concentrations in the organic materials or products formed from the organic materials, a concept of which has been used by Lewan and Maynard (1982) to explain the high V and Ni contents in bitumens produced from organic fraction in argillaceous sediments deposited in anoxic or anaerobic environment. The distribution pattern variations are reflections of REE-complexation variations, which can very easily arise from post-depositional effects occurring at different times on way to hydrocarbon liquid/gas generation.

3.2 Analytical Results for Silicate-Carbonate Fraction of the Woodford Shale

Results shown on Table 9A for the silicate-carbonate fraction were analyzed by ICP-AES. Results for major elements ranging from Silicon to Phosphorous are represented in parts per million. Concentrations from Strontium to Copper are represented in parts per billion.

Table 9A Analytical Results of Silicate-Carbonate Fraction

WOODFORD SHALE SAMPLES SILICATE-CARBONATE FRACTION ANALYSIS																	
	Concentrations in mg/L (ppm)										Concentrations in µg/L (ppb)						
Sample	Si	Al	Mg	Ca	Fe	Mn	Ti	Na	K	P	Sr	Ba	V	Ni	Cr	Zn	Cu
WR SC-1	828.01	9003.74	566.19	4505.74	9887.54	85.78	2551.98	436.93	6628.52	205.43	30237.09	217139.23	121412.37	17123.67	67997.56	70317.54	10881.82
WR SC-2	580.98	3892.22	1674.26	13952.13	9638.68	532.52	1517.69	235.38	5698.01	1006.47	42213.18	137444.45	66512.25	9691.94	37542.94	27851.01	3354.90
WR SC-3	715.95	10604.49	322.15	2818.50	13012.00	195.18	1857.22	204.87	5085.57	215.41	14141.24	89880.25	108624.41	31870.80	53538.37	69531.09	11865.57
WR SC-4	958.60	8552.60	170.03	1529.29	12523.45	93.37	1649.43	615.99	s	127.63	11785.28	28203.22	29094 1.17	49533.82	24924 7.24	78653.39	13999.79
WR SC-5	340.10	9805.79	329.55	1834.55	4678.23	108.42	1235.03	259.79	5642.05	131.14	13678.45	56538.43	214237.84	38478.41	40029.96	83969.82	15329.30
WR SC-6	496.54	10375.37	165.16	157.75	6458.14	27.10	1360.44	539.94	6616.95	116.78	8967.29	98142.55	291675 0.00	14144 3.85	61828.75	15457 18.70	58705.55
WR SC-7	714.67	8716.71	162.61	30.58	10347.91	34.51	1962.54	60.86	5082.71	114.80	1447.69	8461.84	499197.58	37925.35	57448.76	11199 1.94	11469.36
WR SC-8	917.50	10433.42	250.08	1011.61	6561.22	77.98	2242.65	359.04	5372.68	337.47	25013.33	44476.50	335913.21	57975.41	85134.58	269064.00	43454.67
WR SC-9	69.87	3526.92	264.52	5356.92	473.47	6.59	166.16	582.27	2216.97	2039.62	34936.44	104143.85	66911.59	6654.56	24821.51	94228.56	2961.28
WR SC-10	711.52	3510.14	1248.47	4047.73	9486.87	122.38	1347.14	95.47	5407.52	99.11	13145.64	81966.54	36461.20	12079.95	29251.18	19637.82	2846.06

The silicate-carbonate fraction of the Woodford Shale was analyzed by ICP-MS to obtain trace metal analytical data and to know REE concentrations in the silicate-carbonate fraction of the shale. Total REE concentrations are found at the bottom of Table 9B. These concentrations are low compared to the REE concentrations in the organic portion of the Woodford Shale. The silicate-carbonate samples are abbreviated to WR-SC with their respective sample number.

Table 9B REE and Trace Element Results of Silicate-Carbonate (WR SC) fraction of Woodford Shale

WOODFORD SHALE SAMPLES SILICATE-CARBONATE (WR SC) FRACTION ANALYSIS (ppm)										
Concentrations expressed in mg/g of inorganic matter (ppm)										
element	**WR SC-1**	**WR SC-2**	**WR SC-3**	**WR SC-4**	**WR SC-5**	**WR SC-6**	**WR SC-7**	**WR SC-8**	**WR SC-9**	**WR SC-10**
Co	4.81	6.71	12.95	5.89	6.91	8.08	4.98	7.56	0.59	3.98
As	10.18	4.80	8.50	5.88	2.88	5.36	4.40	4.06	2.03	1.99
Rb	4.86	3.62	2.34	3.46	3.91	8.52	2.18	3.28	7.16	6.35
Y	1.18	2.75	2.58	1.01	5.41	4.88	0.82	3.49	5.19	0.94
Zr	46.03	20.52	56.86	45.50	38.55	30.51	66.25	95.17	6.85	15.55
Mo	3.42	0.86	32.72	16.67	69.41	142.02	37.99	91.27	3.80	0.73
Cd	0.13	0.03	0.33	1.43	0.79	25.00	1.50	2.22	0.90	0.03
Sn	1.71	1.29	1.36	1.24	1.10	1.12	1.38	1.48	0.21	0.27
Sb	0.30	0.06	0.70	1.39	1.21	10.71	0.78	1.29	0.26	0.04
Cs	0.31	0.15	0.11	0.12	0.14	0.29	0.11	0.14	0.29	0.39
La	7.53	15.64	5.28	2.46	5.74	8.93	0.46	3.48	4.08	6.06
Ce	14.82	27.96	13.04	4.37	11.71	15.01	1.10	7.09	5.66	13.79
Pr	1.86	3.54	1.73	0.52	1.71	3.01	0.14	0.75	0.70	1.49
Nd	6.93	13.57	7.07	1.88	7.13	12.98	0.61	5.02	4.58	5.29
Sm	1.06	2.01	1.33	0.30	1.43	2.27	0.15	1.03	0.92	0.83
Eu	0.17	0.36	0.28	0.06	0.32	0.40	0.03	0.22	0.18	0.14
Gd	0.76	1.67	1.12	0.26	1.43	1.67	0.15	1.03	0.92	0.54
Tb	0.10	0.23	0.17	0.04	0.21	0.23	0.03	0.16	0.14	0.07
Dy	0.58	1.34	1.02	0.32	1.30	1.31	0.19	1.01	0.83	0.41
Ho	0.12	0.27	0.21	0.08	0.28	0.26	0.04	0.21	0.17	0.08
Er	0.40	0.80	0.64	0.28	0.82	0.77	0.14	0.68	0.49	0.22
Tm	0.06	0.10	0.09	0.05	0.11	0.10	0.02	0.10	0.06	0.03
Yb	0.38	0.59	0.58	0.33	0.74	0.65	0.15	0.69	0.41	0.17
Lu	0.06	0.08	0.09	0.05	0.11	0.10	0.02	0.11	0.06	0.02
Pb	4.97	4.95	7.61	46.22	4.47	10.47	2.21	7.27	0.55	3.37
Th	1.18	0.73	1.39	0.98	1.81	2.50	1.25	1.64	0.81	0.71
U	4.93	2.95	28.85	7.09	41.79	68.58	17.27	28.55	5.58	1.20
Eu/Eu*	1.02	1.05	1.21	1.21	1.18	1.09	1.17	1.14	1.02	1.07
Ce/Ce*	0.95	0.91	1.02	0.93	0.89	0.68	1.02	1.05	0.80	1.11
U/Th	4.20	4.07	20.76	7.24	23.05	27.48	13.84	17.38	6.85	1.69
V/Ni	7.09	6.86	3.41	5.87	5.57	20.62	13.16	5.79	10.06	3.02
K/Rb	1363.98	1576.14	2174.90	s	1443.84	776.51	2329.27	1639.82	309.47	851.09
TREE	34.83	68.16	32.65	11.02	33.07	47.70	3.24	21.59	19.18	29.15

3.2.1 REE in silicate-carbonate fraction of the Woodford Shale

Concentrations of total REE in the silicate-carbonate fraction of the Woodford shale samples are comparatively low to the concentrations of REE in the organic matter of the shale. Concentrations in the silicate-carbonate fraction range from 3 to 70 ppm reflecting a concentration 10 times lower than the concentration in the organic portion of the Woodford shale.

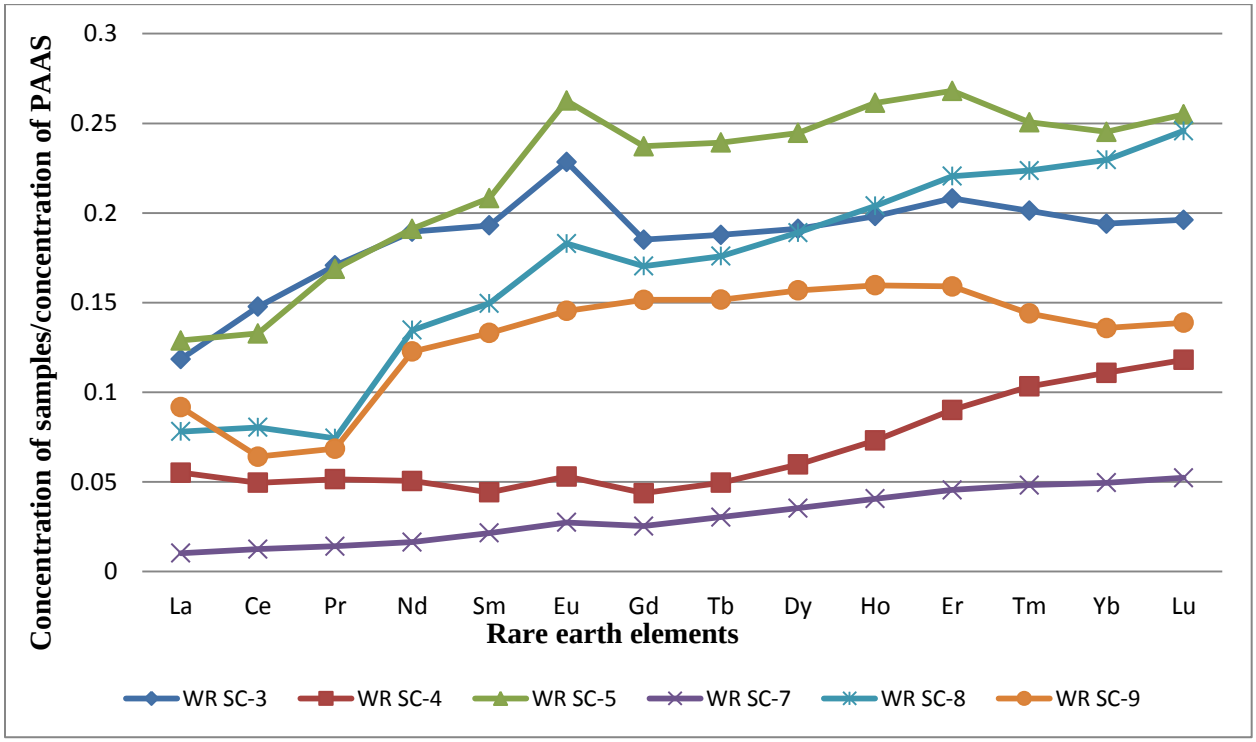

Figure 36 HREE enrichment in 6 silicate-carbonate fraction samples of the Woodford Shale.

The majority of the samples show a HREE enrichment in the silicate-carbonate fraction of the Woodford shale (Figure 36), which can be related to REE patterns inherited from seawater, which also shows a HREE enrichment compared to LREE, although this explanation does not explain the distribution patterns with HREE depletion (Figure 37).

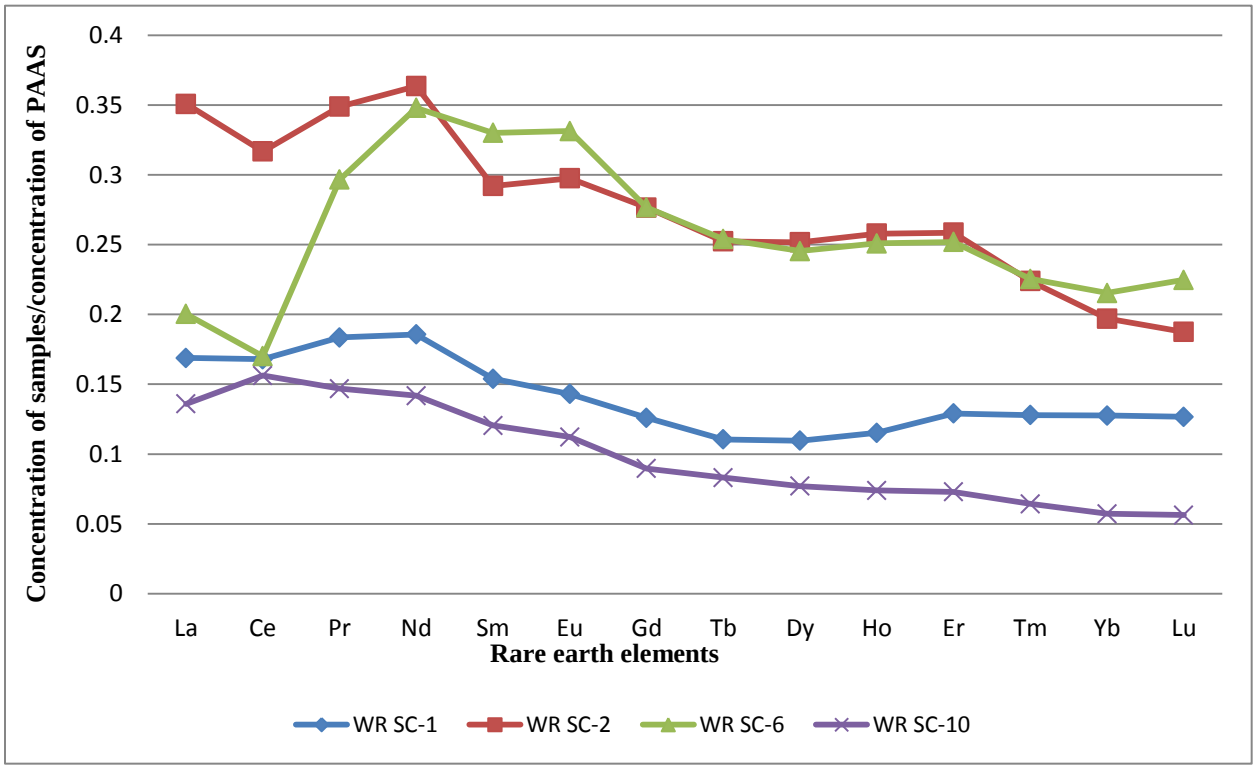

Figure 37 LREE enrichment in 6 silicate-carbonate fraction samples of the Woodford Shale.

Individual distribution patterns for the silicate-carbonate fraction can be found in the Appendix.

3.3 Organic Gecohemical Data on Woodford Shale Samples

The Woodford shale samples were analyzed for Total Organic Carbon (TOC), to know organic richness of the sampled Woodford shale. The weight percent of organic carbon is measured in each of the samples to know the TOC. The total organic carbon concentrations of whole rock samples are given in Table 10. Whole Rock samples were analyzed by SRA-THP/TOC instrumentation in Golden, CO Weatherford Laboratories. TOC levels range from 0.36 to 11.50 wt.%

Table 10 TOC values on the Woodford shale whole rock samples.

WELL NAME	LECO TOC
Shell McCalla Ranch WF#1	1.74
Mobil Sara Kirk WF#2	1.09
Mobil Rahm Lela WF#3	4.62
Shell Guthrie WF#4	6.51
Mobil Dwyer Mt WF#5	6.05
Mobil Cement Ord WF#6	6.54
Amerada Chenoweth WF#7	3.19
Apexco Curtis WF #8	11.50
Jones and Pellow WF#9	6.05
Lonestar Hannah WF#10	0.36

Four Woodford Shale Organic matter samples were analyzed at the Weatherford Laboratories for Organic Elemental data. Knowing H/C and O/C ratios provides insight into knowing the thermal maturity of the samples as well as knowing the Kerogen type.

Table 11 Weight percentage values of different elements in organic matter of the Woodford Shale along with Atomic H/C and O/C ratios.

Sample / Well Name	C Wt. %	H Wt. %	N Wt. %	O Wt. %	S Wt. %	Atomic H/C	Atomic O/C
WF#1 Shell McCalla Ranch	3.52	1.12	0.37	8.38	2.83	3.75	1.80
WF#3 Mobil Rahm Lela	7.84	1.01	0.43	5.70	5.52	1.53	0.55
WF#8 Apexco Curtis	20.94	2.09	0.75	0.75	1.29	1.20	0.03
WF#10 Lonestar Hannah	0.62	0.97	0.07	6.16	2.73	19.35	7.75

The organic matter percentage for each of the rock samples was determined by weighting the samples before the analysis and weighting the crucible used for preparation. After the organic matter separation from the whole rock, the remaining black matter was washed through filtration using Whatman 542 Quantitative Grade filter paper. The filter paper was weighted before the sample was on the paper, and then the filter paper was dried up and weighted to know the exact volume of organic matter per rock sample. The weight percentages for organic matter in the Woodford Shale are shown on Table 8.

Table 12 Organic Matter Percentage of each Rock Sample

Organic Matter Percentages per Whole Rock Sample							
Sample number	Crucible weight	Sample + Crucible	Sample weight	Filter Paper	Org. Matter + Filter	Org. Matter Weight	Org Matter %
WF#1	39.77	40.98	1.21	1.22	1.55	0.33	27.32
WF#2	52.53	53.73	1.21	1.24	1.73	0.50	41.12
WF#3	39.17	40.36	1.19	1.22	1.71	0.49	41.05
WF#4	47.05	48.29	1.24	1.23	1.65	0.42	33.82
WF#5	39.85	40.99	1.14	1.23	1.53	0.30	26.23
WF#6	32.69	33.92	1.23	1.23	1.55	0.32	25.81
WF#7	33.71	34.98	1.27	1.22	1.47	0.25	19.31
WF#8	46.35	47.63	1.28	1.22	1.66	0.45	34.87
WF#9	43.50	44.73	1.23	1.22	1.26	0.036	2.92
WF#10	39.73	40.98	1.25	1.22	1.71	0.50	39.62

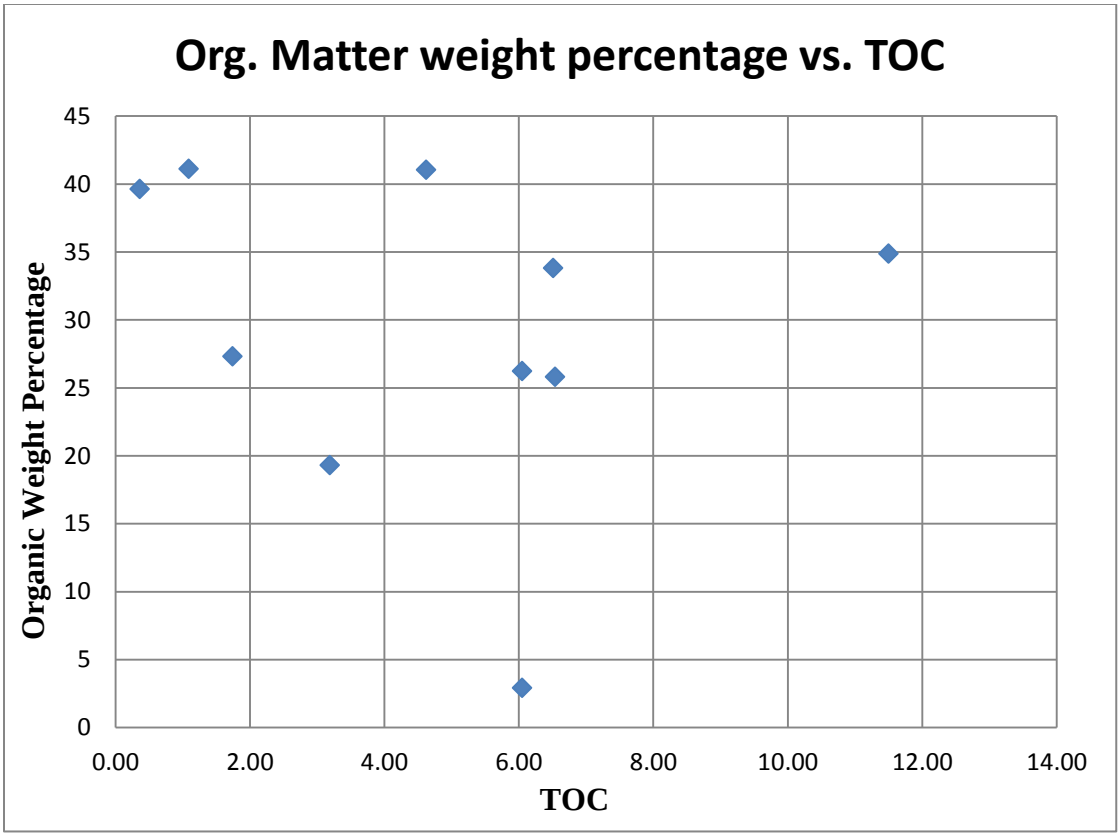

Figure 38 Relationship between organic matter (weight percentage) of the Woodford Shale and TOC of the whole rock.

When plotting the values for Organic matter weight percentage against the TOC values of the Woodford Shale whole rock, a correlation between the two is hard to observe (Figure 38). But a relationship can be found when analyzing the H/C and O/C ratios of each of the samples, analyzing the kerogen type of each sample, and comparing these values to vitrinite reflectance (Figure 39).

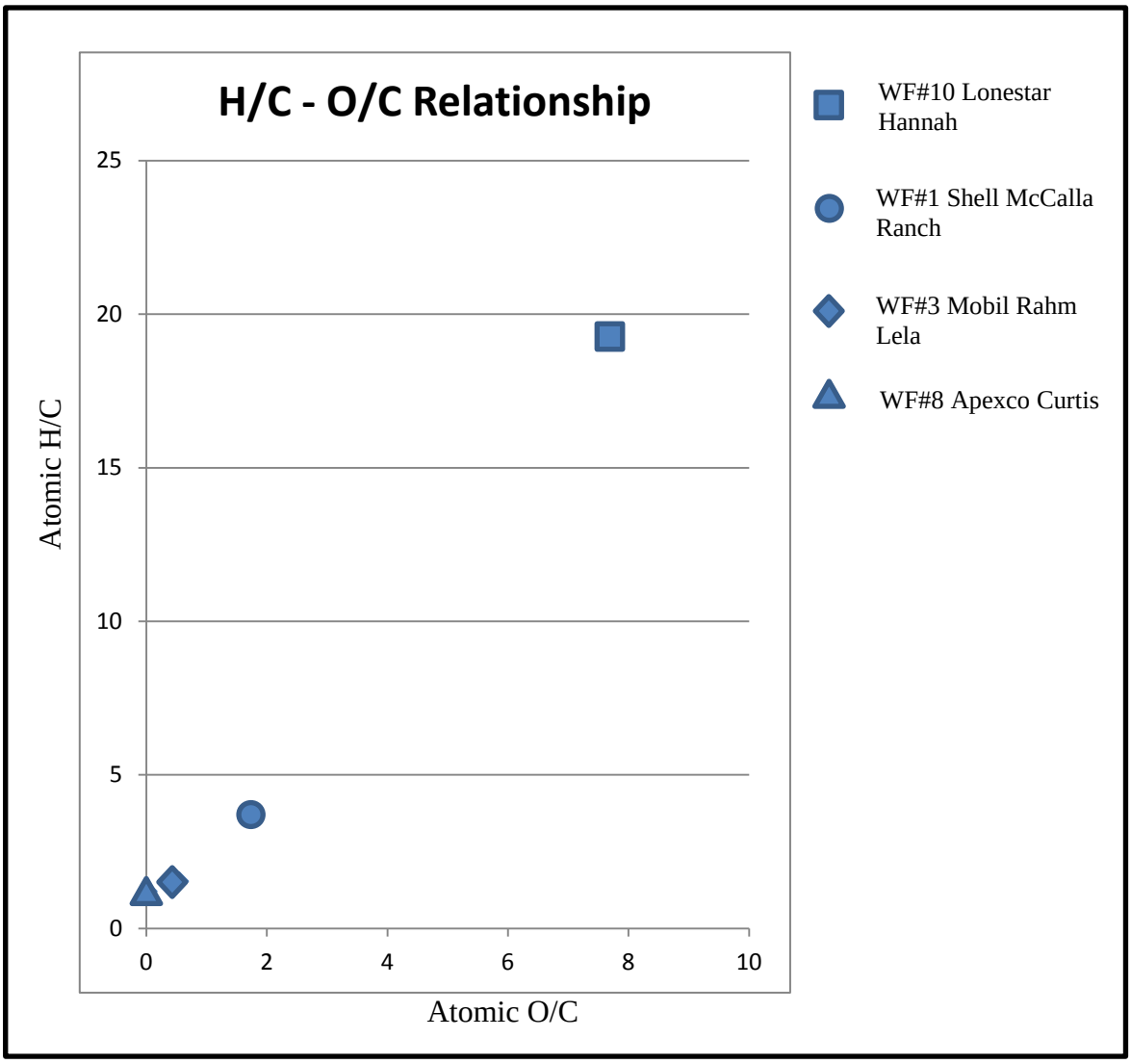

Figure 39 H/C – O/C Diagram

In an effort to compare the organic matter weight percentage measured for each of the samples after the organic matter separation from the Woodford Shale, the H/C-O/C values of 4 samples are plotted in this diagram. This diagram is a modification of Van Krevelen diagram published in 1961.The values of the samples plotted are found in Tables 11 and 13. Through the elemental analysis (carbon, hydrogen, oxygen) of the organic portion of for Woodford shale samples, kerogen type can be inferred. After removing the mineral matter with hydrochloric acid and hydrofluoric acid the organic matter can be analyzed for maturation with this diagram. During maturation, the oxygen is removed as CO_2, and H_2O, the hydrogen as hydrocarbons and H_2O, and the carbon as hydrocarbons and CO_2. When plotting the H/C-O/C ratios, three types of

kerogen can be distinguished. Kerogen type I generally has a high H/C ratio and low O/C ratio. These are called Liptinitic because they consist of Liptinite which is the oil forming, sapropelic material derived from plants and animal lipids. Type III kerogens have a low H/C ratio and high O/C ratio. These are originated from humic materials, resulting in woody and coaly kerogens. Type II kerogens are in the intermediate position which contain liptinite like type I kerogen but with a lower ratio than type I kerogen.

According to the previous explanation, it can be observed that sample WF#10 Lonestar Hannah is in the range of kerogen type I. This sample is also at a deep portion of the basin which explains the high value of maturity (Ro=2), and the high H/C ratio losing hydrogen molecules as the organic matter is overpressured and thermally overmature. The other three samples are considered to be kerogen type II, ranging in their Ro values from 0.53 to 0.75.

Table 13 Atomic H/C-O/C ratios compared to Ro and Org. Matter % Weight.

Sample Name	Depth (ft)	Atomic H/C	Atomic O/C	Org. Matter % Weight	Vitrinite Reflectance (Ro)
#1 Shell McCallla Ranch	12309	3.75	1.80	27.32	0.75
#3 Mobil Rahm Lela	6729	1.53	0.55	41.05	0.55
#8 Apexco Curtis	8520	1.20	0.03	34.87	0.53
#10 Lonestar Hannah	14323	19.35	7.75	39.82	2

No statistical relationship can be seen between vitrinite reflectance and REE concentration values for the organic portion of the Woodford shale samples. As observed on Figure 41, R^2 value for the 10 samples of the Woodford shale does not show a strong relationship between the two variables. R^2 value for this relationship is of 0.0998, which doesn't comply with statistics rules to have a probability of 95%. It is important to note that the only vitrinite reflectance values provided directly by Brian Cardott (OGS) are the ones for samples WF#4, WF#5, WF#8, WF#9, and WF #10. The rest of the vitrinite reflectance values for the samples were obtained from a regional thermal maturity map of Oklahoma published by the OGS. Though the statistical value (R^2) is not being favorable to tie both variables, the hypothesis

should not be discarded; instead the Woodford Shale should be analyzed at the exact intervals of depths for its vitrinite reflectance and its REE concentration in organic matter.

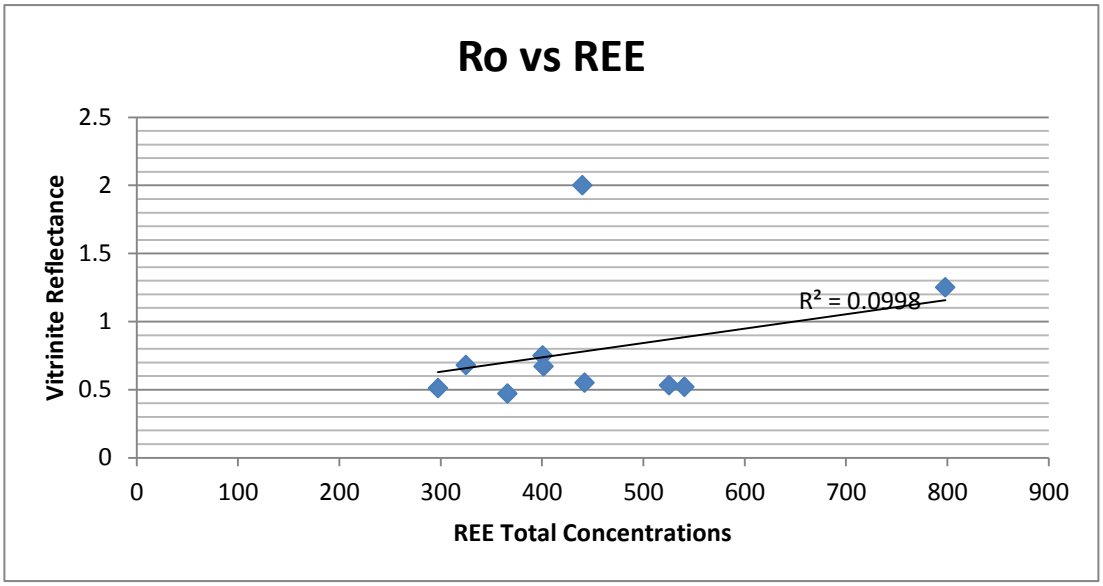

Figure 40 Plot of REE concentrations and Vitrinite Reflectance values

When observing the concentration values of REE in the organic portion of the Woodford shale, it can be observed that the values obtained through this study represent a wide variation of values of REE in organic matter. When comparing these values to values in other studies like the one by Abanda and Hannigan (2006), an even wider variation in total REE concentration can be seen in that studies sample. Studies by Chaudhuri on plant materials and the data currently existing in the literature describing growth of plants on various soils, point to the fact of wide variations in the total REE content among the organic materials. Chaudhuri (personal communication) has noted different types of vegetation grown on the same type of substrate under nearly identical environmental conditions have different total REE contents. With all this mounting evidence, one should expect to find that the organic materials of different sorts that accumulate in different parts of the same sedimentary basin or that accumulate in different sedimentary basins at different times to have different total REE contents at the time of their deposition. It is not therefore surprising to see that the high total REE contents on this study of the Woodford Shale organic material differ from the REE total concentration values that have been reported by Abanda and Hanningan (2006), and by Birdwell (2012).

3.4 Results of Inorganic Components of Oil Samples

3.4.1 Analytical Data for Mississippian Oil Samples

Analytical data for the Mississippian oil samples processed by ICP-AES is represented in Table 14A. Concentrations of metals in Table 14A are in parts per million for the elements ranging from Silicon to Phosphorous and the rest of the elements ranging from Vanadium to Copper have concentration values ranging in parts per billion. Orange cells represent null data due to element's concentration being under instrumentation detection limit.

Table 14A Major element analytical results Mississippian Oil (CR) Samples

Mississippian Oil (CR) Samples

	Concentrations in mg/L (ppm)										Concentrations in µg/L (ppb)					
Sample Name	**Si**	**Al**	**Mg**	**Ca**	**Fe**	**Mn**	**Ti**	**Na**	**K**	**P**	**V**	**Ni**	**Co**	**Cr**	**Zn**	**Cu**
CR-OIL-5 Jester	0.036	0.008	0.029	0.386	0.045	0.001	-	0.735	0.017	0.061	2979.480	1101.211	2.348	0.454	579.385	854.310
CR-OIL-2 Holstein 2-22(1)	0.039	0.019	0.017	0.053	0.021	-	-	0.317	0.006	0.085	2413.266	780.110	2.114	0.423	21.141	8.456
CR-OIL-11 German 1-13H(1)	0.023	0.009	0.008	0.021	0.007	-	-	0.069	0.001	0.062	1101.891	448.227	0.623	0.138	15.218	15.218
CR-OIL-7 McGuire 1-14H(1)	0.073	0.019	0.088	0.481	0.188	-	-	1.632	0.015	0.377	6789.071	2665.417	3.557	0.837	127.622	642.294
CR-OIL-8 Holstein 2-22H(2)	0.041	0.026	0.041	0.131	0.094	-	-	0.300	0.006	0.056	4013.527	1214.176	2.998	0.562	80.570	24.358
CR-OIL-9 German 1-13H(2)	0.030	0.020	0.145	0.586	0.222	0.002	-	6.163	0.067	0.101	3124.171	1200.361	1.819	0.606	198.039	189.956
CR-OIL-12 McGuire (2)	0.061	0.016	0.029	0.054	0.036	-	-	0.269	0.004	0.054	4302.087	1581.017	2.330	0.538	50.191	48.398

Oil sample analytical data is shown for Mississippian Oils. The analytical data for each of the oil families is separated showing first the Mississippian oil data. Location for each of the samples is also shown in Table 14B, as well as the collection date for each of the samples. Orange cells represent the lack of analytical result for a certain element on a certain sample, due that the metal's concentration was under the detection limit of the ICP-MS. Concentrations are represented in parts per billion.

Table 14B REE and trace element analytical results for Mississippian Oil (CR) Samples

MISSISSIPPIAN OIL (CR) SAMPLES (ppb)							
Location	**Payne Co, OK (27-19N-6E) Oct-2011 3260-3290 ft**	**Payne Co, OK (22-19N-3E) Oct-2011**	**Payne, Co, OK (13-18N-4E) Oct-2011 3923-5550ft**	**Payne, Co, OK (14-13N-4E) Oct- 2011**	**Payne Co, OK (22-19N-3E) March 2012**	**Payne, Co, OK (13-18N-4E) March - 2012 3923-5550ft**	**Payne, Co, OK (14-13N-4E) March- 2012**
	CR-OIL-5 Jester 1-27 MISS	**CR-OIL-2 Holstein 2-22H (1) MISS**	**CR-OIL-11 German 1-13H (1) MISS**	**CR-OIL-7 McGuire 1-14H (1) MISS**	**CR-OIL-8 Holstein 2-22H (2) MISS**	**CR-OIL-9 Geman 1-13H (2) MISS**	**CR-OIL-12 McGuire (2) MISS**
Cr	0.386	0.233	0.145	1.151	0.675	0.849	0.825
Co	2.271	2.163	0.645	3.527	3.485	1.740	2.052
As	0.659	0.846	0.297	1.255	1.124	0.768	0.825
Rb	0.031	0.024	0.008	0.069	0.054	0.107	0.025
Sr	10.649	3.087	0.277	47.429	7.870	67.030	2.151
Y	0.139	0.008	0.007	0.016	0.008	0.011	0.003
Zr	0.076	-	-	-	-	-	0.143
Mo	0.239	0.170	0.057	0.879	0.429	0.418	0.335
Cd	0.100	0.009	0.008	0.025	0.005	0.035	0.015
Sn	0.545	0.264	0.090	1.444	0.356	0.546	1.165
Sb	5.430	6.977	3.708	14.541	24.377	26.836	12.297
Cs	0.004	0.004	-	0.004	0.006	0.006	-
Ba	0.810	0.867	0.450	1.695	1.892	4.850	1.595
La	0.052	0.023	0.038	0.063	0.018	0.020	0.075
Ce	0.028	0.032	0.012	0.046	0.026	0.026	0.023
Pr	0.003	0.002	0.001	0.004	0.002	0.003	0.001
Nd	0.014	0.011	0.004	0.019	0.011	0.012	0.004
Sm	0.003	0.001	0.001	0.003	0.001	0.002	0.001
Eu	0.001	0.0003	0.002	0.001	0.001	0.001	0.001
Gd	0.003	0.001	0.0005	0.003	0.001	0.002	0.001
Tb	0.0003	0.0002	0.0001	0.0004	0.0004	0.0004	
Dy	0.002	0.001	0.0003	0.002	0.002	0.002	0.001
Ho	0.0003	0.0002	0.0001	0.0004	0.0004	0.0004	
Er	0.001	0.0004	0.0002	0.001	0.001	0.001	0.0004
Tm	0.0001						
Yb	0.001	0.0003	0.0002	0.001	0.001	0.001	0.0002
Lu	0.0001			0.0002			
Pb	56.575	0.402	11.482	1.824	0.538	2.144	0.968
Th	0.001	0.002	0.001	0.011	0.003	0.002	0.001
U	0.006	0.009	-	0.011	0.003	0.002	-
U/Th	4.765	4.143		0.981	1.125	1.111	
V/Ni	2.706	2.706	2.458	2.547	3.306	2.603	2.721
K/Rb	560.976	260.870	166.667	212.121	103.448	622.642	142.857
TREE	0.107	0.073	0.058	0.144	0.066	0.072	0.108

Table 15 Cerium and europium anomalies in Mississippian oil samples REE Distribution Patterns of Devonian Oils Normalized to the PAAS.

Sample	Ce/Ce*	Eu/Eu*
CR-OIL-5 Jester 1-27 MISS	0.42	1.31
CR-OIL-2 Holstein 2-22H (1) MISS	0.99	1.36
CR-OIL-3 German 1-13H (1) MISS	0.28	12.43
CR-OIL-7 McGuire 1-14H (1) MISS	0.57	1.42
CR-OIL-10 Holstein 2-22H (2) MISS	0.93	2.13
CR-OIL-3 German 1-13H (2) MISS	0.84	2.65
CR-OIL-13 McGuire (2) MISS	0.29	2.94

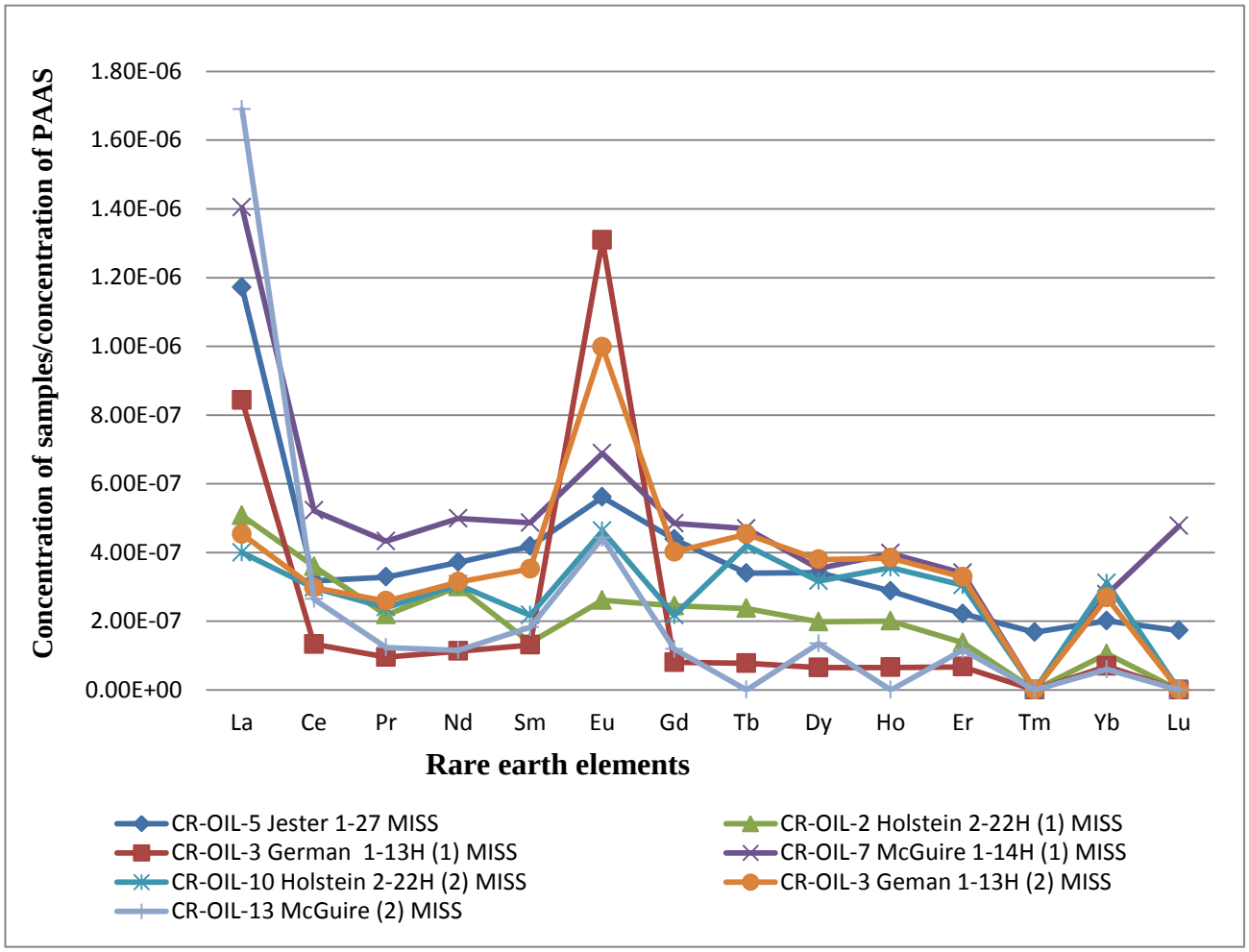

Figure 41 REE Distribution patterns for Mississippian oil samples.

The REE distribution patterns for the Mississippian oil samples show a general LREE enrichment with a minor MREE enrichment. Five out of the seven samples have a Cerium negative anomaly and all of the samples have a Europium positive anomaly.

3.4.2 Analytical Data for Devonian Oil Samples

Table 16A Major element analytical results for Woodford shale Oil (CR) samples

WOODFORD (ICP-AES)

	Concentrations in mg/L (ppm)										Concentrations in µg/L (ppb)					
Num Lab	**Si**	**Al**	**Mg**	**Ca**	**Fe**	**Mn**	**Ti**	**Na**	**K**	**P**	**V**	**Ni**	**Co**	**Cr**	**Zn**	**Cu**
CR-OIL-4 Myers	0.183	0.005	0.016	0.138	0.054	0.001	-	0.199	0.004	0.046	2539.509	899.043	2.219	-	93.347	219.596
CR-OIL-6 Holstein 1-22	0.071	0.006	0.014	0.043	0.008	-	-	0.300	0.004	0.036	806.297	281.383	0.786	0.143	27.853	19.99673
CR-OIL-1 Mehan 5-14	0.051	0.011	0.010	0.056	0.075	-	-	0.024	-	0.075	12569.910	4126.930	9.550	0.749	136.691	1121.611
CR-OIL-12 Holstein 1-22(2)	0.207	0.008	0.151	0.439	0.042	-	-	1.778	0.040	0.293	5640.680	1885.109	4.812	-	92.059	983.353
CR-OIL-9 Mehan 5-14(2)	0.079	0.016	0.019	0.047	0.031	-	-	0.062	0.002	0.031	5670.374	1748.546	3.875	0.465	27.902	49.60415
CR-OIL-8 Mehan 2-14	0.005	0.009	0.019	0.056	0.094	-	-	0.169	0.004	0.320	26549.896	8241.766	19.206	2.448	82.851	5.648914

Analytical data for Devonian oil samples from the Woodford shale are represented in Table 16A. These values are represented in parts per million from Silicon to Phosphorous and from Vanadium to Copper the concentrations are represented in parts per billion. These values were processed through an ICP-AES. Orange cells represent null data due to element's concentration being under instrumentation detection limit.

Table 16B REE and trace element analytical results for Woodford Shale Oil (CR) samples

WOODFORD PRODUCING (CR) WELLS (ppb)						
	Payne, Co, OK (24-19N-5E) Oct-2011 3510-3520 ft	**Payne Co, OK (22-19N-3E) Oct 2011 4274-4300ft**	**Payne Co, OK (14-18N-2E) Oct-2011 4580-4600ft**	**Payne Co, OK (22-19N-3E) March 2012 4274-4300ft**	**Payne Co, OK (14-18N-2E) -March 2012 4580-4600ft**	**Payne Co, OK (14-18N-2E) - March 2012**
	CR-OIL-4 Myers WFORD	**CR-OIL-6 Holstein 1-22 (1) WFORD**	**CR-OIL-1 Mehan 5-14H (1) WFORD**	**CR-OIL-12 Holstein 1-22 (2) WFORD**	**CR-OIL-09 Mehan 5-14 (2) WFORD**	**CR-OIL-8 Mehan 2-14H (2) WFORD**
Cr	0.283	0.114	0.861	1.151	0.481	2.015
Co	2.190	0.884	8.479	5.145	3.970	17.498
As	0.528	0.357	2.228	1.506	1.039	5.743
Rb	0.019	0.010	0.021	0.080	0.016	0.032
Sr	3.780	2.821	0.356	36.886	2.403	1.996
Y	0.080	0.003	0.007	0.004	0.002	0.020
Zr	0.260	-	-	0.146	-	-
Mo	0.341	0.121	0.607	0.462	0.344	0.932
Cd	0.014	0.013	0.008	0.009	0.044	0.020
Sn	0.207	0.293	0.487	0.607	0.093	0.169
Sb	4.759	4.256	10.036	12.386	17.160	12.013
Cs	0.002	-	-	0.002	-	-
Ba	0.972	0.457	0.637	1.737	1.256	0.829
La	0.039	0.006	0.010	0.014	0.012	0.028
Ce	0.041	0.005	0.015	0.019	0.008	0.040
Pr	0.005	0.0004	0.001	0.001	0.001	0.003
Nd	0.022	0.002	0.007	0.007	0.003	0.015
Sm	0.003	0.0005	0.002	0.002	0.001	0.002
Eu	0.001	0.0001	0.0004	0.0004	0.0003	0.001
Gd	0.003	0.0004	0.002	0.001	0.001	0.002
Tb	0.0002		0.0002			0.001
Dy	0.003	0.0003	0.001	0.001	0.001	0.001
Ho	0.0003		0.000			0.0004
Er	0.001	0.0001	0.001	0.0004	0.0003	0.001
Tm						
Yb	0.001	0.0001	0.001	0.0004	0.0002	0.001
Lu						
Pb	10.100	1.821	0.803	0.467	0.347	1.122
Th	0.001	0.000	0.001	0.001	0.001	0.004
U	0.017	0.005	-	0.021	-	0.161
U/Th	32.430	12.800		16.833		45.000
V/Ni	2.824	2.865	3.046	2.992	3.243	3.221
K/Rb	200.000	357.142		500.000	100.000	117.647
TREE	0.119	0.015	0.040	0.046	0.026	0.094

Analytical results from the Devonian Woodford Shale oil samples are found on Table 16B. Total REE concentrations of the samples are found in fractions of parts per billion. The concentrations for each of the elements are in parts per billion values.

Table 17 REE anomalies in distribution patterns for Devonian oil samples

Sample	Ce/Ce*	Eu/Eu*
CR-OIL-4 Myers WFORD	0.68	1.85
CR-OIL-6 Holstein 1-22 (1) WFORD	0.63	1.79
CR-OIL-1 Mehan 5-14H (1) WFORD	1.04	1.07
CR-OIL-12 Holstein 1-22 (2) WFORD	1.03	1.53
CR-OIL-9 Mehan 5-14 (2) WFORD	0.50	1.80
CR-OIL-8 Mehan 2-14H (2) WFORD	0.95	2.02

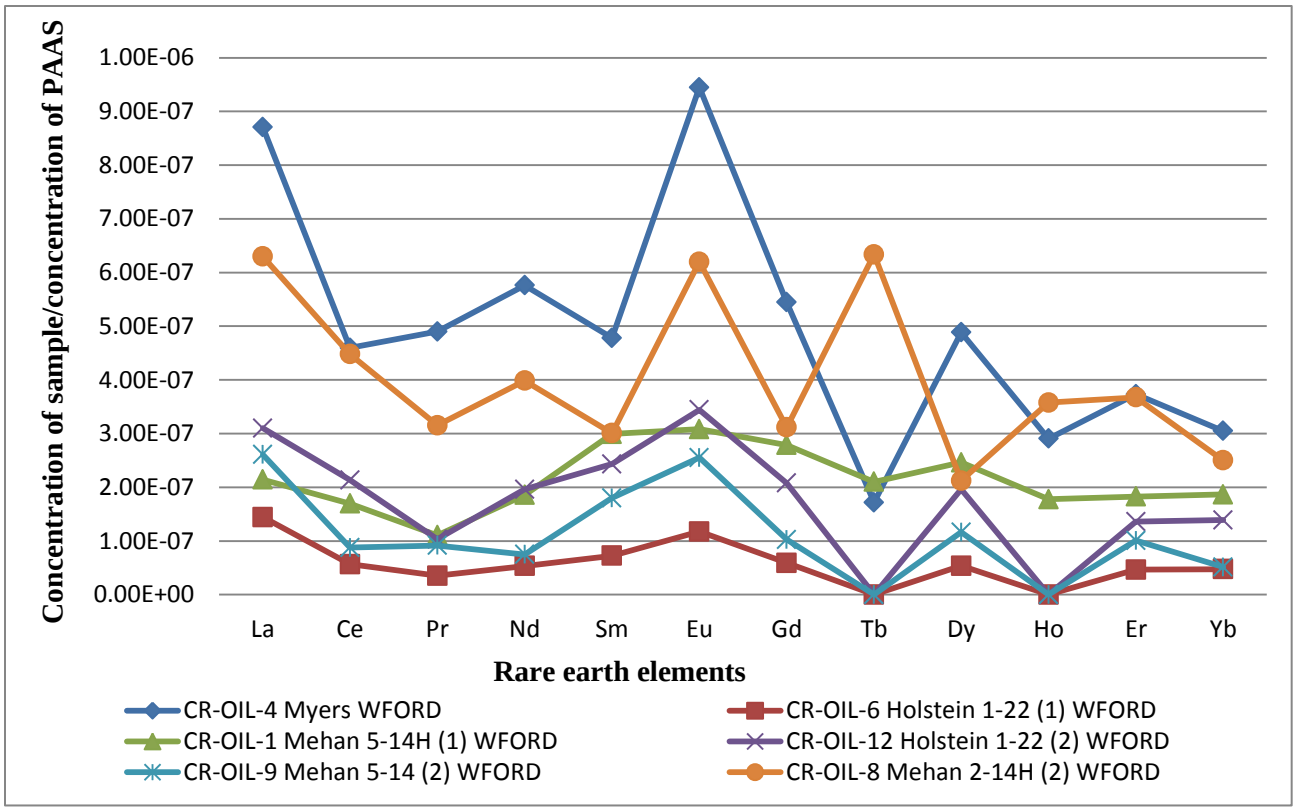

Figure 42 REE Distribution patterns for Devonian oil samples.

The Devonian oil samples have REE distribution patterns with a general LREE enrichement, and a more prominent MREE enrichment is noticeable, when comparing this samples to the Mississippian oil samples. Three out of the six samples have cerium depletion and like the Mississippian oil samples, they show europium enrichment.

Chapter 4 - Discussion

REE in Oil, used as oil – oil correlation tools

As stated on section 1.2 of this study compounds containing Nitrogen, Sulfur and Oxygen represent about 75% of the residuum part of crude oil. Separation of the residuum allowed the study of REE in oil, due to the aromatic structures present in the residuum with space for free radicals capable of complexing metals. REE are analyzed through this study looking at concentrations and distribution patterns normalized to the PAAS in Devonian and Mississippian oil samples.

The analysis is approached by doing an oil to oil comparison between the distribution patterns of the Devonian and Mississippian oil samples. REE distribution patterns could be used as comparison indicators for different oils, in this case comparing differences between stratigraphically different produced oils. The study also focuses on comparing oil samples to themselves over a 3 month collection time difference, with the purpose to see the difference in distribution patterns on a latter hydrofrack flowback collected sample.

When looking at the general distribution patterns of the Devonian oil samples and comparing them to the Mississippian oil samples, a noticeable, striking feature stands out, a heavier MREE enrichment more prominent in the Devonian oils than in the Mississippian oils (Figure 41,42). Samples CR-4, CR-8, CR-6, CR-12, CR-1, CR-9 can be observed with this enrichment which is strikingly noticeable when comparing to the Mississippian oils which only show europium enrichment. Also HREE depletion is present in most of the Mississippian oils (CR-5, CR-2, CR-7, and CR-13) and this trend is not as prominent in the REE distribution patterns for the Devonian oil samples (CR-12, CR-8, CR-4). An absence of carboxyl groups in the Mississippian oils could be the cause of the HREE depletion in these oil samples. Both the Devonian and Mississippian oil samples show a constant feature in their REE distribution patterns, they all show europium enrichment. An oil-oil differentiation can be made when looking at the cerium anomalies in the distribution patterns for both oil types. Two Woodford oil samples show cerium negative anomalies (CR-4, CR-9), and the remaining four Woodford oil REE distribution patterns show no anomaly at all. Five Mississippian oil samples show cerium

negative anomalies in their distribution patterns in varying degrees (CR-13, CR-3, CR-5, CR-11, CR-7), while the remaining three oil samples show no cerium anomaly on their distribution patterns. Cerium depletion in the Mississippian oils is a distinguishing feature that separates the Mississippian oil family from the Devonian oil family. It is interesting to see a cerium depletion in some of the samples which is an indication of the marine plants and marine organic matter's influence as the source of the organic matter for the shale. When looking at europium anomalies in the distribution patterns of both oil families, it can be observed that both oils, the Devonian and the Mississippian samples, show a positive europium anomaly. The individualized distribution patterns for the oil samples are presented in the Appendix. Oil to oil characterization can be made with the study of the REE distribution patterns in different oil families. Stratigraphically different oils have different REE features. Some of the most striking differences were seen on the MREE anomalies, and in the Cerium depletion difference between the two families.

Another approach taken to study the REE signatures through the distribution patterns of both oils was by normalizing the Devonian and Mississippian oil samples to Devonian oil sample Holstein 1-22(1). This sample was chosen to be a standard for the rest of the samples because this sample had the lowest REE concentration values. Differences between the two oil families are present, and these can be observed when observing cerium anomaly trends between in both oil families (Figure 43, and 44). Four samples from the Mississippian oil family show cerium depletion (CR-2, CR4, CR-7, and CR-12) when normalized to Holstein 1-22(1). The rest of the samples have no cerium anomaly and one of them has a cerium positive enrichment (CR-3). The contrast between both oil families is noticeable when observing Ce anomalies on the Devonian oils normalized to Holstein 1-22(1). This oil family has only two oil samples with Cerium depletion (CR-4, and CR-9), with the rest of the oil samples having a positive enriched cerium anomaly, hence showing a distribution pattern difference between Mississippian oil samples and Devonian, where a cerium enrichment is present in the Devonian oils. Europium anomalies don't really indicate a distinction between the two oil families, due to the irregular europium anomalies in both oil families. Another feature that distinguishes both oil families and is observed when comparing the distribution patterns normalized to Holstein 1-22 oil sample is the LREE enrichment and depletions differences. Most of the Mississippian oil samples show a LREE enrichment. Only two samples out of the seven samples have HREE enrichment (CR-8, and CR-

9). This distinguishing feature is not present in the Devonian oil family, where LREE enrichment is found in lower values than in the Mississippian oils and only in two samples (CR-8, CR-9) out of the five. Two of the remaining samples have flat distribution patterns (CR 4, and CR-12), and only one sample present with HREE enrichment. The general distribution trends when compared to a reference material are useful to find REE distribution features in an oil family that can distinguish that certain oil from an oil sample from a different oil family.

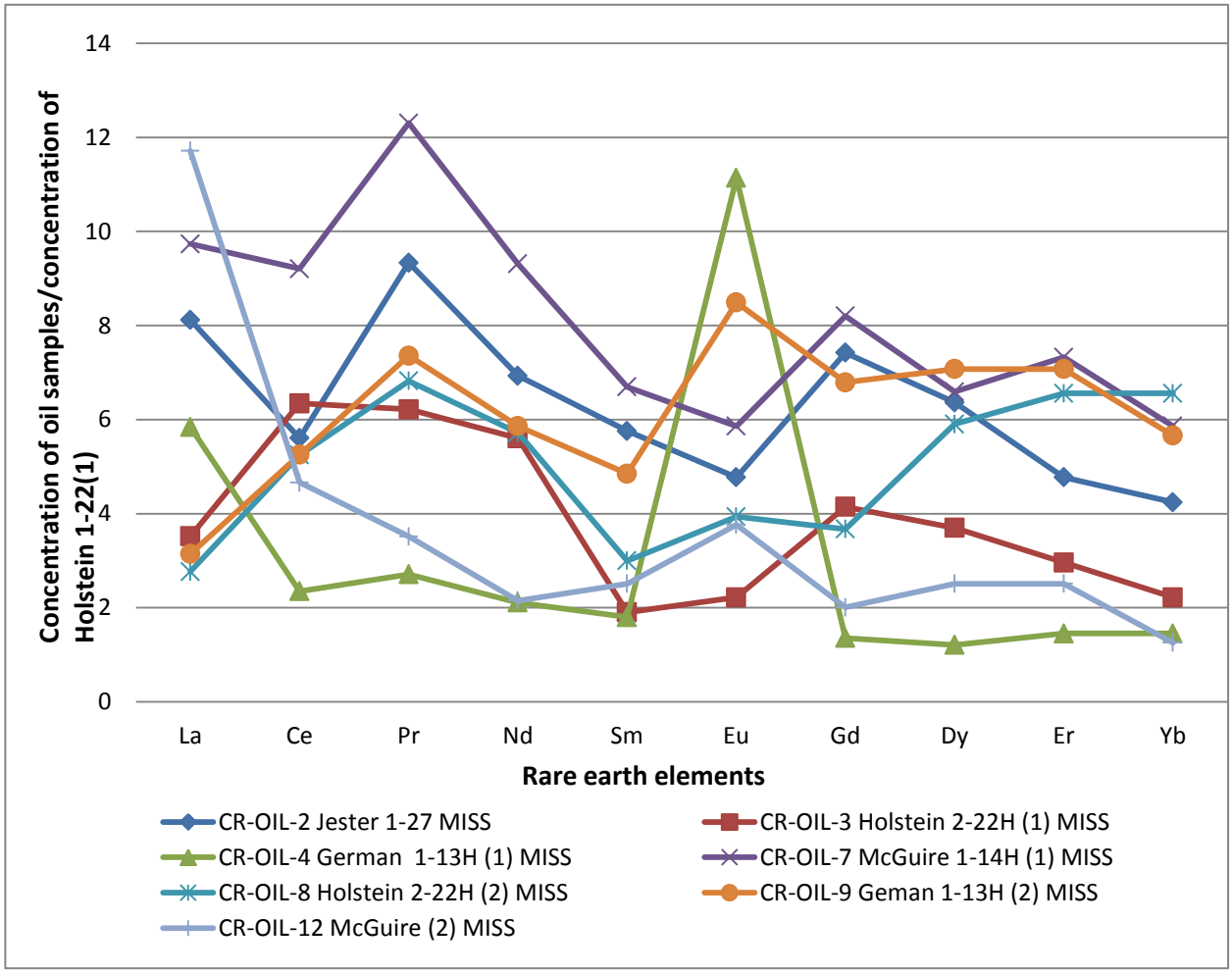

Figure 43 REE distribution patterns for Mississippian oil samples normalized to oil sample Holstein 1-22(1)

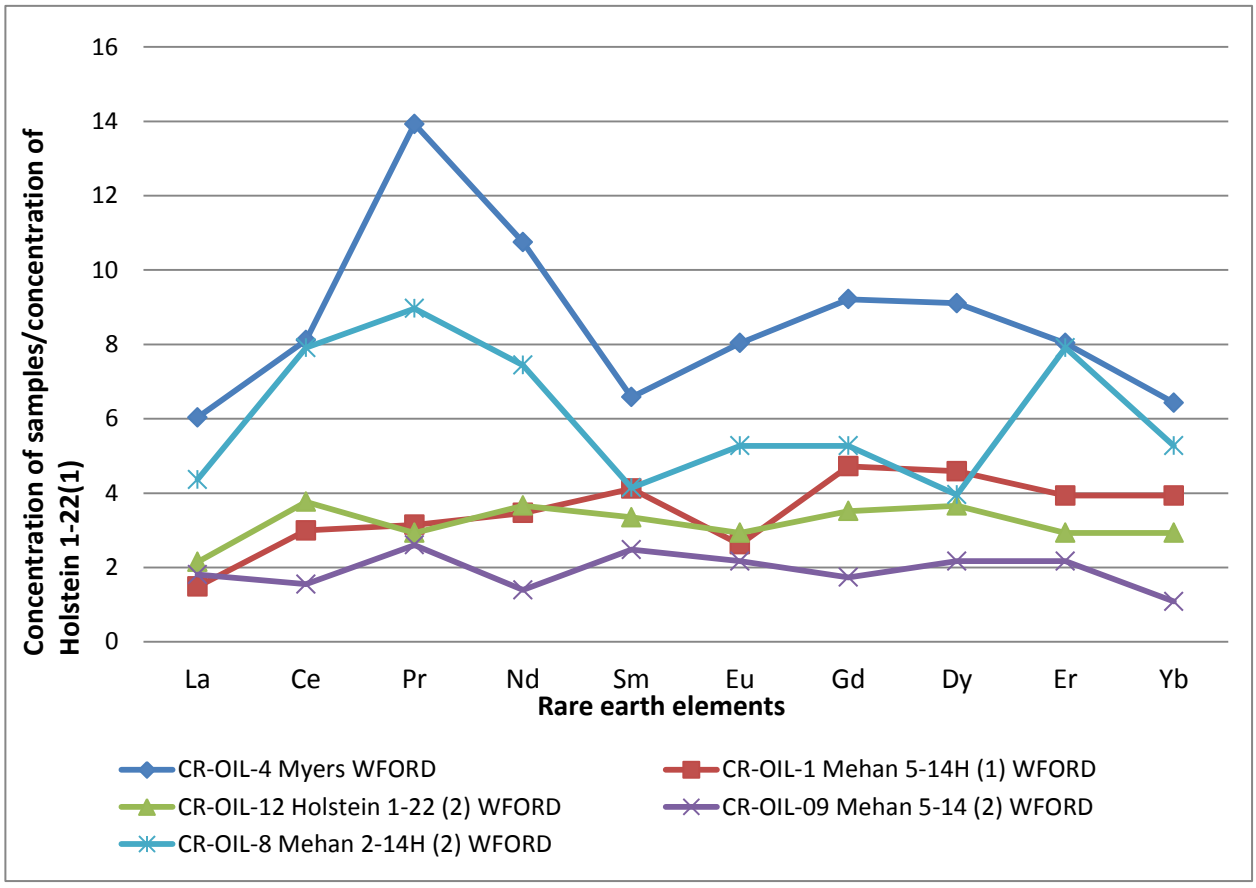

Figure 44 REE distribution patterns for Devonian oil samples normalized to oil sample Holstein 1-22(1)

REE in Oil, to study flowback differences

A number of samples obtained for this study were collected during initial production time and then collected again after several months of production. When observing the distribution patterns of Devonian oil samples and comparing the initial production samples and the samples collected 3 months after initial production, some differences are observed in the MREE trends. Sample Mehan 5-14 (CR-1) has a prominent MREE positive enrichment, and that specific trend decreases when observed in the distribution pattern of the same sample collected three months later (CR-9). Cerium differences are also observed, with no cerium anomaly in the initial production sample (CR-1) and with cerium depletion of 0.49 for the same oil sample collected 3 months after initial production. Very little differences can be observed when analyzing Devonian oil sample Holstein 1-22. The initial production sample (CR-6) has a minor cerium depletion and MREE enrichment. The observable difference between the initial production sample and the

latter sampled oil (CR-12) is the now absent cerium depletion along with a more prominent MREE enrichment.

When observing the distribution patterns on Mississippian oil samples and contrasting the initial production samples from the latter sampled oils, some differences can be observed (Refer to Appendix D for individual REE distribution patterns of oil samples). Sample Holstein 2-22 (CR-2) shows no cerium anomaly. The distribution pattern also shows HREE depletion and a europium enrichment of 1.36. When observing the sample from the same well but on a latter production time, the distribution shows some significant variations. The HREE are not depleted anymore. The most striking feature is the europium positive anomaly increased in the flowback produced oil, with a new europium anomaly value of 2.13. On the samples taken from well German 1-13, the europium anomaly is the only feature that shows variation in this well. On the initial production sample (CR-3), europium anomaly is extremely high with a value 12.42. On the same sample but on a later production date (CR-11), the europium enrichment decreased to a value of 2.65. The final sample that is analyzed for distribution patterns among different production times is the sample coming from well McGuire 1-14. There are no changes in the distribution patterns between the two samples collected from this well at different production dates (CR-7, CR-13)

It is greatly desired to use the REE distribution patterns in the Woodford Shale and in the oil produced from the Woodford shale to correlate oil to its source rock. While samples were collected from the Woodford shale and from oil coming from the Woodford shale, the regional distribution variability between the Woodford shale samples and the oil generated from the Woodford is too great. All the oil samples are coming from Payne County in North-central Oklahoma and the Woodford shale samples are from west Oklahoma. Not only is the geographical distribution of the samples within the basin large, but also the vertical variability in the Woodford Shale samples and along the different members of the core affects the correlation to oil coming from the upper member of the Woodford. For future work, a detailed study over a whole Woodford core section would be interesting to do and comparing the REE data to organic geochemistry data.

Distribution patterns in the graph for the Devonian Oils. The comparison between patterns in oils can be made, but an observable general trend caused by HREE depletion can be made. Values for several rare earths are not present but are represented in the graphs as zeroes

for illustration purposes. The concentrations of the absent rare earths are below the detection limits. The individual distribution patterns provide more descriptive opportunity.

Organic matter correlated to oil samples

When looking at the distribution patterns of the organic portion of the Woodford shale a general HREE enrichment is observed in most of the samples. Organic matter will have different REE distribution patterns, but generally having HREE enrichment. All organic matter has organic functional units, like the phenolic and carboxylic groups. Studies have shown that HREE form stronger bonds with carboxylic groups, hence causing organic matter to have HREE enrichment. It is interesting to note that most of the oil samples from both Devonian and Mississippian units which do not have a flat distribution pattern have LREE enrichment. The silicate-carbonate fraction distribution patterns when normalized to the PAAS show split distribution between the HREE and the LREE, having 6 samples with HREE enrichment and 4 samples with LREE enrichment. Looking at the big picture of oil generation, two hypotheses can be drawn when observing and comparing distribution patterns between organic fraction, silicate-carbonate fraction and oil samples. One assumption made is that all the REE from oil came from the total dissolution of REE from the fraction of organic matter. Nevertheless the oil generated from the Woodford shale must've had contribution of REE from a different portion, along with the REE contribution from organic matter. If organic matter was the only contributor of REE inot the oil generated then the distribution patterns would look similar to the organic matter REE patterns. Oil shows a LREE enrichment, differing from the HREE of organic matter in the Woodford shale. This LREE enrichment in the oil samples might be present due to the silicate-carbonate fraction contributing with the REE content in the oil samples. Another assumption that can be made when observing the differing distribution patterns between organic matter from the Woodford shale and oil from this source bed, is that as the organic matter is being matured and being converted into oil, the LREE are being fractionated easier from the organic matter and complexed into the oil generated. Considering that HREE are strongly complexed into phenolic and carboxylic groups, it is possible the LREE are easier fractionated from the organic matter which doesn't strongly attach the HREE.

Maturity Indicator by considering Potassium/Rubidium ratios

A hypothesis for maturity indication in the source rock is explored by analyzing the Potassium (K) concentrations levels in the organic matter and comparing these concentrations to the K values in the silicate-carbonate fraction and the oils generated from the source bed analyzed. Potassium is found abundantly in organic materials. As the organic matter is transformed under deep burial conditions, the transformation will release K as well as other elements such as silicon, iron and also aluminum which are the general targets of discussion in the smectite to illite transformation. Data presented in the previous chapter shows the concentrations of K in the different portions of the shale and in the oil (Tables 6A, 9A, 14A, 16A). Based upon assumptions regarding average chemistry of smectites and illites, the average shale requires 13.4 % potassium feldspar to provide the necessary K+ (Totten and Blatt, 1996). As the average shale only contains 5% feldspar (Blatt, 1992), an additional source for K is required. It is proposed the overlooked source of K is the organic matter associated with shale, or within adjacent formations. A study by Chaudhuri et al., 2007, showed that when potassium is studied in conjunction with Rubidium, the K/Rb ratio can be a strong geochemical tracer for the source of K in the system. Their study proved that K/Rb ratios are generally much higher in the organic material than the common K bearing silicate minerals like feldspar and mica. The plants can have ratios in the range of 350-10,000, whereas silicate minerals have ratios between 50 and 600. If the hypothesis that the provenance of K is being supplied by the organic matter during burial transformation into the silicate fraction is correct, evidence is needed to establish the release of K by the organic matter. When looking into the K/Rb ratio of the organic matter, it is observed that the ratios are extremely low, indicating a removal of K, showing a contrast in the K/Rb ratios of plant material before transformation, and K/Rb ratio after transformation. The organic matter of the ten Woodford Shale samples show low K/Rb ratios, ranging between 9 and 20, drastically contrasting with K/Rb ratios of plants which have values of ranging from 165 to 47000 (Chaudhuri et al. 2007). This is a remarkable evidence of K being removed from organic matter during the Woodford's burial diagenetic transformation. When observing the K/Rb ratios of the silicate-carbonate fraction of the Woodford shale, high ratios are evident ranging from 300 up to 2000, indicating that K is being released from the organic matter and being supplied to the silicate-carbonate fraction of the Woodford shale. When the K concentration of crude oil is observed, it is noted that the concentrations are noticeably lower than the concentrations of K in

organic matter. It is inferred that any K being released during maturation of the organic matter is not being concentrated in the oil which shows values ranging from 100 to 500.

Chapter 5 - Conclusions

Separating the organic matter from the Woodford shale is a novel approach to study how diagenesis affects the geochemistry of this shale. Through observations and comparison of REE concentration in the organic matter of the Woodford Shale and modern day plant material, clear reflections of post-depositional phenomena are observed. The REE concentration in the organic portion of the Woodford shale is wide, and this range cannot be explained under the scope of maturation of the organic matter. The ranges in REE concentration present are attributed to the deposition of organic matter in a large sedimentary basin that most likely had diverse sources with different amounts of contribution from different depositional sites. REE Distribution patterns of the organic fraction and inorganic fraction of the Woodford Shale, along with observation of REE distribution patterns in oil generated from the Woodford provide insight into knowing the REE chemical complexation in the source rock when undergoing transformation into oil. Different general REE distribution patterns are observed in the different fractions studied in this petroleum system. REE oil distribution patterns have a general LREE enrichment, which indicates the LREE easier fractionation from the organic portion of the Woodford shale, agreeing with the stability constants of REE when being fractionated. REE present higher stability constants in the HREE fraction, and when observing the patterns in this study it can be observed that after the organic matter releases the REE it is left with the HREE and contributes its REE to the oil generated.

Correlation of REE data to maturity (Ro) in the organic portion of the shale was not obtained, but this might be because of the lack of vitrinite reflectance data in the samples. Evidence of phosphate present is available when observing the distribution patterns of REE and the MREE enrichment in the organic portion of the Woodford Shale. HREE enrichment in the organic portion of the Woodford Shale is present because of the HREE complexation with organic functional units. The majority of the samples show a HREE enrichment in the silicate-carbonate fraction of the Woodford shale, which can be related to REE patterns inherited from seawater. Seawater also has HREE enrichment compared to LREE.

When comparing the distribution patterns of the samples a very different pattern is observed for the organic portion of the Woodford shale in sample WF#10. This was the only sample that when plotted in H/C O/C diagram resulted to have kerogen type 1 from terrestrial

origin. This was the only sample to show a positive cerium anomaly and no HREE enrichment among all the samples. REE Distribution patterns show fingerprinting properties when comparing patterns in samples from different provenance or source.

Oil to oil characterization can be made with the study of the REE distribution patterns in different oil families. Stratigraphically different oils have different REE features. Some of the most striking differences were seen on the MREE anomalies, and in the cerium depletion difference between the two oil families.

5.1 Future Work

This is the first study which uses REE in oil and source rock as analytical means to gain insight on oil generation. Being the first study, there is much room for future work to be done with this channel of investigation to keep studying the REE geochemical potential in source bed to oil connection. Future ways to extend this investigation include the characterization of different features in the distribution patterns of the organic matter of the Woodford Shale in specific areas, extending the study over focalized areas where there is gas production, and comparing the study to the distribution patterns in areas where oil is produced. Compare the relationship between REE distribution patterns in gas producing zones, versus REE distribution patterns in condensate producing zones, and also versus REE distribution patterns in oil producing zones.

Having Woodford shale samples of specific hydrocarbon production zones, and studying the oil produced from those Woodford intervals would enhance a better correlation project, where specific Pb istope data would be recommended to be used to link results to REE.

Sampling of oil and shales would be easier when partnering with oil companies who may provide whole rock samples for analysis, and who can also provide localized samples of produced hydrocarbons from the specific intervals the whole rock was producing hydrocarbons. This would be very helpful for research projects as oil companies can provide logs, and can provide conventional geochemical data that could compliment a geochemical study through REE. This would enhance the research providing a link between organic geochemistry and the

use of REE to understand transformation processes in organic matter in the context of existing data and existing production.

Another research perspective that can be approached is by studying the REE in the Woodford Shale or other formations, focusing on the whole vertical extent of the formation and comparing the lithological changes and its effect on REE. The Woodford Shale can reach thicknesses of 600 ft with 3 main lithofacies within the formation, and the formation can be categorized into 11 members. Seeing the vertical variability within one formation and one location could help us understand the effect of burial and transformation in the organic matter as we study the REE distribution patterns.

Approaching the study of REE fractionation from organic matter as it is matured, would be an interesting future research project where REE can be better understood under direct maturation processes. Practicing a stage by stage pyrolysis on the organic matter and studying the REE distribution patterns in the organic matter throughout the different exposure to heat or maturation environments might provide direct data on the REE behavior under organic maturity processes.

Work with modern day marine plant material to work on REE concentrations and K/Rb ratios comparing them to the organic matter of the source rock. Hypothesis have been made in the present study using REE concentrations in terrestrial plants and comparing them to organic matter in the Woodford Shale, but the comparison of the organic matter to modern day marine plant material is desired.

This research project lays ground to develop more geochemical projects in the Petroleum Geology discipline, using similar sample preparation techniques to study metals in oil and in different fractions of source rocks.

Bibliography

Abanda P.A., Hannigan R.E., 2006. Effect of diagenesis on trace element partitioning in shales: Chemical Geology, v. 230, p. 42-59.

Amsden T.W., 1967. Silurian and Devonian strata in Oklahoma: Tulsa Geological Society Digest, v. 35, p. 25-34.

Andrews, R.D., 2009. Production decline curves and payout thresholds of horizontal Woodford wells in the Arkoma Basin, Oklahoma: The Shale Shaker, v. 60, p. 103–112.

Barrat, J.A., Keller, F., Amosse, J., Taylor, R.N., Nesbitt, R.W., 1996. Determination of Rare Earth Elements in Sixteen Silicate Reference Samples by ICP-MS after Tm Addition and Ion Exchange Separation: Geostandards Newsletter, v. 20, issue 1, p. 133-139.

Brewer, J.A., Good, R., Oliver, J.E., Brown, L.D., and Kaufman, S., 1983. COCORP profiling across the Southern Oklahoma aulacogen, overthrusting of the Wichita Mountains and compression with the Anadarko Basin: Geology, v. 11, p. 109–114.

Birdwell, J.E., 2012, Review of Rare Earth Element Concentrations in Oil Shales of the Eocene Green River Formations: U.S. Geological Survey Open-File Report 2012-1016, 20 p.

Blakley, R., Colorado Plateau Geosystems, cpgeosystems.com paleogeography map. http://www2.nau.edu/rcb7/globaltext2.html

Blatt, H., 1992, Sedimentary Petrology, 2nd edition: New York, W.H., Freeman & Co., 514 p.

Brenneman, M. C., Smith, P. V., 1958. The chemical relationships between crude oils and their source rocks, in Weeks, L. G., ed., Habitat of Oil, American Association of Petroleum Geologists, Tulsa, Okla., 1958, p. 818-849.

Byrne, R.H., Liu X., Schijf, J., 1996. The influences of phosphate coprecipitation of rare earth distributions in natural waters: Geochimica et Cosmochimica Acta, v. 60, p. 3341–3346.

Caldwell, C.D., Johnson, P.G., 2013. Anadarko Woodford Shale, Improving Production by Understanding Lithologies/Mechanical Stratigraphy and Optimizing Completion Design: AAPG Woodford Shale Forum, April 2013, Oklahoma City, OK, USA.

Cardott, B.J., Lambert, M., 1985. Thermal Maturation by Vitrinite Reflectance of Woodford Shale, Anadarko Basin, Oklahoma: AAPG Bulletin, v. 69, p 1982-1998.

Cardott, B.J., 2008. Overview of Woodford gas-shale play of Oklahoma, US: Oklahoma Geological Survey, Power Point Presentation, Oklahoma Gas Shale Conference. October 22nd, 2008. http://www.ogs.ou.edu/pdf/AAPG08woodford.pdf

Cardott, B.J., 2012. Introduction to Vitrinite Reflectance as a Thermal Maturity Indicator: Search and Discovery Article # 40928, May 2012.

Cardott, B.J., 2013. Woodford Shale, From Hydrocarbon Source Rock to Reservoir: AAPG Woodford Shale Forum, April 2013, Oklahoma City, OK, USA.

Chaudhuri S., Clauer N., Semhi K., 2007. Plant decay as a major control of river dissolved potassium, A first estimate: Chemical geology, v. 243, p.178-190.

Chaudhuri, S., Totten, M., Clauer, N., Miesse J., Riepl, G., Massie, S., Semhi, K., 2011. Rare-Earth Elements as a Useful Geochemical Tracer in Hydraulic Fracturing Schemes: Shale Shaker, The Journal of the Oklahoma City Geological Society, v. 62, p. 214-223.

Comer, J.B., Hinch, H.H., 1987. Recognizing and quantifying expulsion of oil from the Woodford Formation and age-equivalent rocks in Oklahoma and Arkansas: AAPG Bulletin, v. 71, No. 7, p 844-858.

Comer, J.B., 2008. Reservoir Characteristics and Production Potential of the Woodford Shale: World Oil Magazine. Special Focus: North American Outlook-Unconventional Resources, August 2008.

Condie, K.C., 1993. Chemical Composition and Evolution of the Continental Crust, Contrasting Results From Surface Samples and Shales: Chemical Geology v. 104 p. 1-37.

Cotton F.A., Wilkinson, G., 1962. Advanced Inorganic Chemistry: Interscience Publishers, John Wiley and Sons, New York-London

Davis, H.G., Northcutt, R.A., 1989. The Greater Anadarko basin, an overview of petroleum exploration and development: Proceedings of Anadarko Basin Symposium (1988), Oklahoma Geological Survey Circular 90. p. 13-24.

Davranche, M. O., Pourret, G., Grauau, A., Dia, M., Le Coz-Bouhnik, 2005. Adsorption of REE (III)-humate complexes onto MnO_2, Experimental evidence for cerium anomaly and lanthanide tetrad effect suppression: Geochimica et Cosmochimica Acta v. 69, p. 4825-4835.

Erdman, J.G., Saraceno, A.J., 1962. Investigation of the nature of free radicals in petroleum asphaltenes and related substances by electron spin resonance: Anal Chem., v. 34 (6), p. 694-700

Evans, C.H., 1990. Biochemistry of the Lanthanides. New York: Plenum Press.

Feinstein, S., 1981. Subsidence and thermal history of Southern Oklahoma aulacogen, Implications for petroleum exploration: American Association of Petroleum Geologists Bulletin, v. 65, p. 2521–2533.

Garner, D.L., Turcotte, D.L., 1984. The thermal and mechanical evolution of the Anadarko basin: Tectonophysics, v. 107, p. 1–24.

Ham, W.E., Denison, R.E., Merritt, C.A., 1964. Basement rocks and structural evolution of southern Oklahoma: Oklahoma Geological Survey Bulletin v. 95, p. 302.

Hoffman, P., Dewey, J.F., and Burke, K., 1974, Aulacogens and genetic relation to geosynclines with a Proterozoic example from Great Slave Lake, Canada, *in* Dott, R.H.,Jr., and Shower, R.H., eds., Modern and ancient geosynclinals sedimentation: Society of Economic Paleontologists and Mineralogists Special Publication no. 19, p. 38-55.

Hunt, J.M., 1995. Petroleum Geochemistry and Geology. 2nd edition, New York: W.H. Freeman and Company.

Hycrude, 1986, Beneficiation-hydroretorting of U.S. oil shales: Chicago, IL, Hycrude Corporation, Annual status report, variously paginated, U.S.D.O.E. Grant No. DE-FG21-85LC111066.

Johnson, K.S., Amsden, T.W., Denison, R.E., Dutton, S.P., Goldstein, A.G., Rascoe, B., Jr., Sutherland, P.K., and Thompson, D.M., 1989. Geology of the Southern Midcontinent: Oklahoma Geological Survey, Special Publication 89-2.

Johnson, K.S., Cardott, B.J., 1992. Geologic framework and hydrocarbon source rocks of Oklahoma, in K.S. Johnson and B.J. Cardott, eds., Source rocks in the southern Midcontinent, 1990 symposium: OGS Circular 93, p. 21-37.

Jones, P. J., Philp, R. P., 1990. Oils and source rocks from Pauls Valley, Anadarko Basin, Oklahoma, US: Applied Geochemistry, Vol. 5, No.4, p. 429-448.

Kennedy, C. L., Miller, J.A., Kelso J.B., and Lago, O. K., 1982. The deep Anadarko basin: Tulsa Petroleum Information Corporation, 359 p.

Kidder, D.L., Eddy-Dilek, C.A., 1994. Rare-Earth Element Variation in Phosphate Nodules from Midcontinent Pennsylvanian Cyclothems: Journal of Sedimentary Research, Sedimentary Petrology and Processes, v. A64, p. 584-592.

Lewan M.D., Maynard, J.B., 1982. Factors controlling enrichment of vanadium and nickel in the bitumen of organic sedimentary rocks: Geochimica et Cosmochimica Acta, v. 46, p. 2547-2560.

McCarthy, K., Rojas, K., Niemman M., Peters, K., Stankiewicz, A., 2011. Basic Petroleum Geochemistry for Source Rock Evaluation: Schlumberger Oilfield Review 23, no. 2, p. 32-43.

McLennan, S. M., 1989. Rare earth elements in sedimentary rocks; influence of provenance and sedimentary processes: Reviews in Mineralogy and Geochemistry, v. 21, p. 169-200.

Nagarajan, R., Madhavaraju, J., Armstrong-Altrin, J, Nagendra R., 2011. Geochemistry of Neoproterozoic limestones of the Shahabad Formation, Bhima Basin, Karnataka, southern India: Geosciences Journal, v. 15, No. 1, p. 9-25.

Pearson, R.G., 1963. Hard and soft acids and bases: Journal of American Chemical Society, v. 85, p. 3533–3539.

Pourmand A., Dauphas, N., Ireland, T.J., 2012. A novel extraction chromatography and MC-ICP-MS technique for rapid analysis of REE, Sc and Y, Revising CI-chondrite and Post-Archean Australian Shale (PAAS) abundances: Chemical Geology v. 291, p. 38-54.

Puckette J., 2013. Characteristics of Devonian-Mississippian strata in the Southern midcontinent: AAPG Woodford Shale Forum, April, 2013, Oklahoma City, OK

Rascoe, B., Hyne, N.J., 1988. Petroleum geology of the mid-continent: Tulsa Geological Society Special Publication 3, 162 p.

Rollinson, H.R., 1993. Using Geochemical Data, Evaluation, Presentation, Interpretation. 1st edition, England: Pearson Education Limited.

Sandvik, E.I., Young W.A., Curry, D.J., 1992. Expulsion from hydrocarbon sources, the role of organic absorption: Organic Geochemistry, v. 19, Issues 1-3, p. 77-87.

Smith F.G., 1963. Physical Geochemistry: Addison-Wesley Publishing Company, Reading, Massachusetts, 624 p.

Sorenson R.P., 2005. A dynamic model for the Permian Panhandle and Hugoton fields, Western Anadarko Basin: AAPG bulletin, v. 89, p. 921-938

Sullivan, K.L., 1983. Organic facies variation of the Woodford Shale in western Oklahoma: Master's thesis, University of Oklahoma, Norman, Oklahoma, 101 p.

Taylor, S.R., McLennan, S.M., 1985. The Continental Crust, Its Composition and Evolution: Blackwell Scientific Publications, Carlton, 312 p.

Thompson, L. C., 1979. Complexes, *in* Gschneider, K.A., Jr., and L. Eyring (eds.), Handbook on the Physics and Chemistry of Rare Earths: Amsterdam, North-Holland Publishing Company, p. 209–298.

Topp, N. E., 1965. The Chemistry of Rare Earth Elements: Amsterdam, Elsevier Publishing Company, 345 p.

Totten, M. W., Blatt H., 1996. Sources of silica from the illite to muscovite transformation during late-stage diagenesis of shales, Siliciclastic diagenesis and fluid flow, Concepts and Applications: Society of Economic Paleontologists and Mineralogists, Special Publication No. 55, p. 85-92.

Wang, D.H., Philp R.P., 1997. Geochemical Study of Potential Source Rocks and Crude Oils in the Anadarko Basin, Oklahoma: AAPG bulletin, v. 81, No. 2, p. 249-275.

Walper, J. I., 1977. Paleozoic tectonics of the southern margin of North America: Gulf Coast Association of Geological Societies Transactions, v. 27, p. 230–241.

Wood, S. A., 1990. The aqueous geochemistry of the rare-earth elements and yttrium: Chemical Geology, v. 82, p. 159–186.

Wyttenbach A., Furrer, V., Schleppi, P., Tobler, L., 1997. Rare earth elements in soil and in soil-grown plants: Plant and Soil, v. 199, p. 267-273.

Appendix A - Woodford Shale Core sampled

Figure 45 WF#1 Shell McCalla Ranch, Plug Depth 12309 ft.

Figure 46 WF#2 Mobil Sara Kirk, Plug Depth 5567 ft.

Figure 47 WF#3 Mobil Rahm Lela, Plug Depth 6279 ft.

Figure 48 WF#6 Mobil Cement Ord, Plug Depth 17581 ft.

Figure 49 WF#7 Amerada Chenoweth, Plug Depth 6513 ft.

Figure 50 WF#10 Lonestar Hannan, Plug Depth 14323 ft.

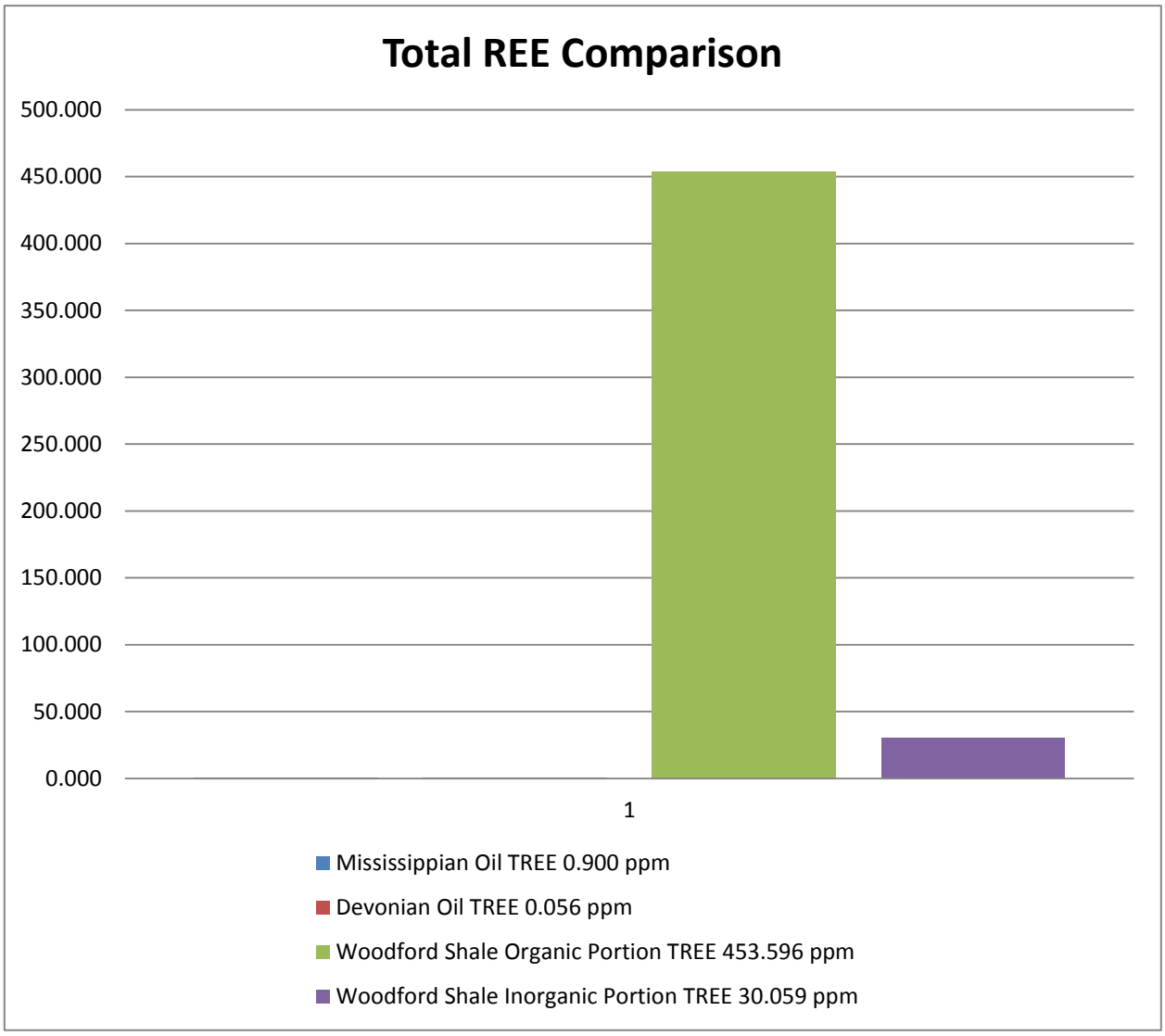

Figure 51 Histogram showing REE concentration averages for the oil samples, organic and inorganic portion of the Woodford Shale.

Appendix B - REE Distribution Patterns in Organic Matter of all the Woodford Shale Samples Normalized to PAAS

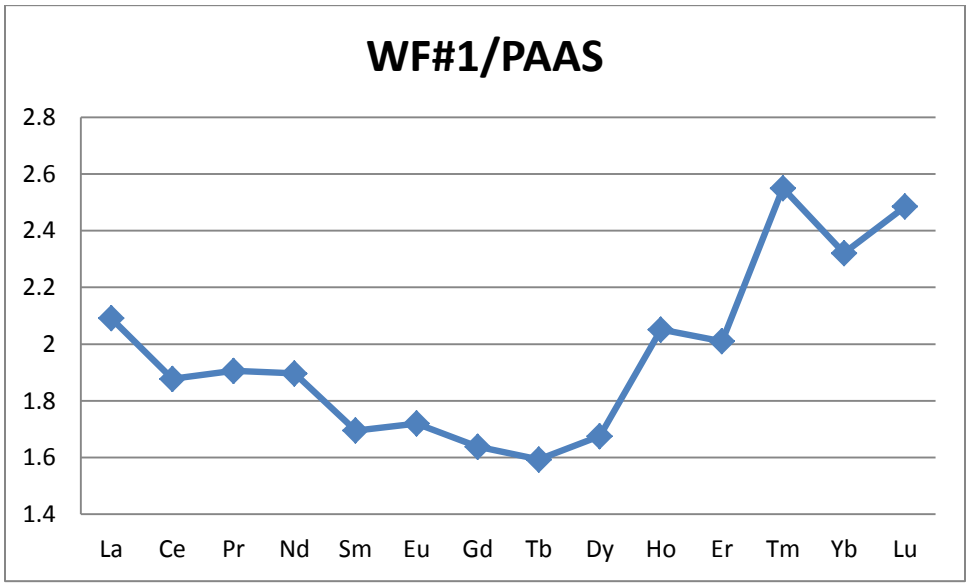

Ce/Ce*= 0.94
Eu/Eu*= 1.03

Heavy Rare Earth Element enrichment
Holmium, Thulium enrichment
MREE depletion

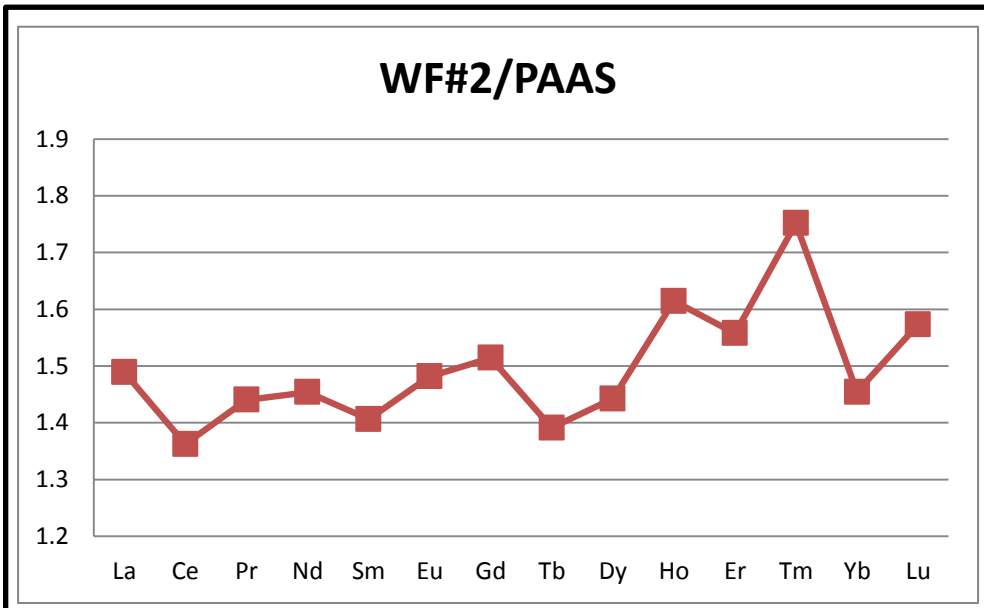

Ce/Ce*= 0.93
Eu/Eu*= 1.01

Heavy Rare Earth Element enrichment
Holmium, Thulium enrichment

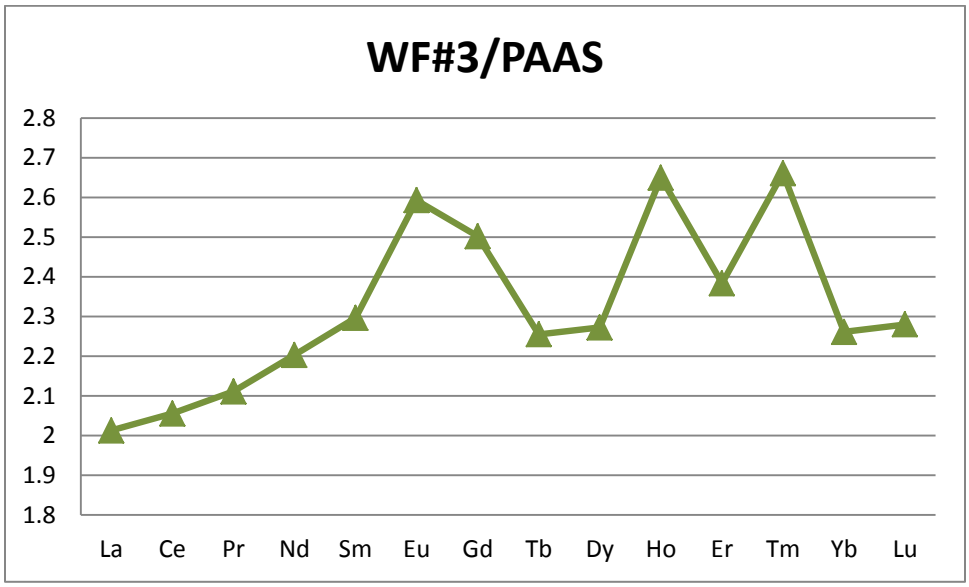

Ce/Ce*= 0.99
Eu/Eu*= 1.08

Heavy Rare Earth Element enrichment
Holmium, Thulium enrichment
MREE enrichment

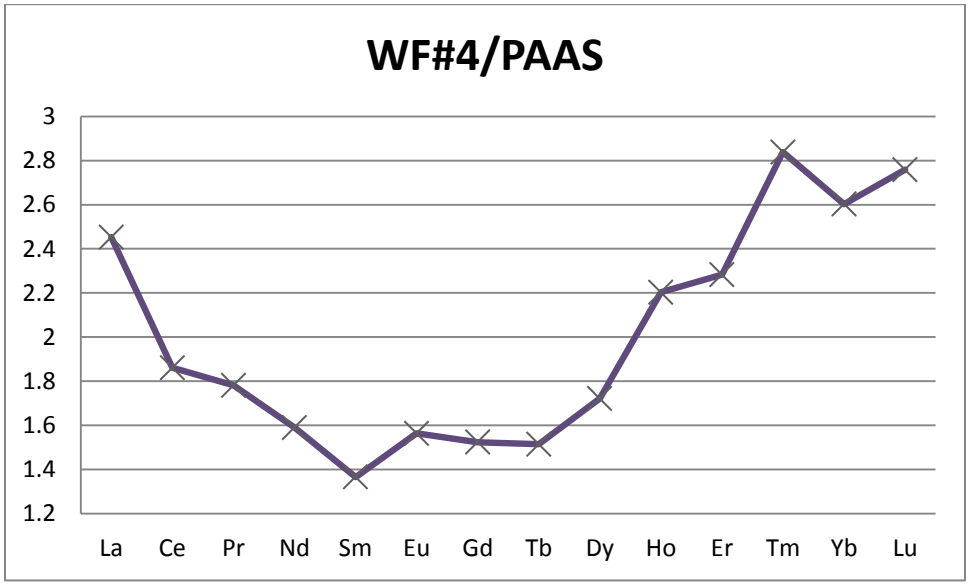

Ce/Ce*= 0.87
Eu/Eu*= 1.08

Heavy Rare Earth Element enrichment
Holmium, Thulium enrichment
MREE depletion

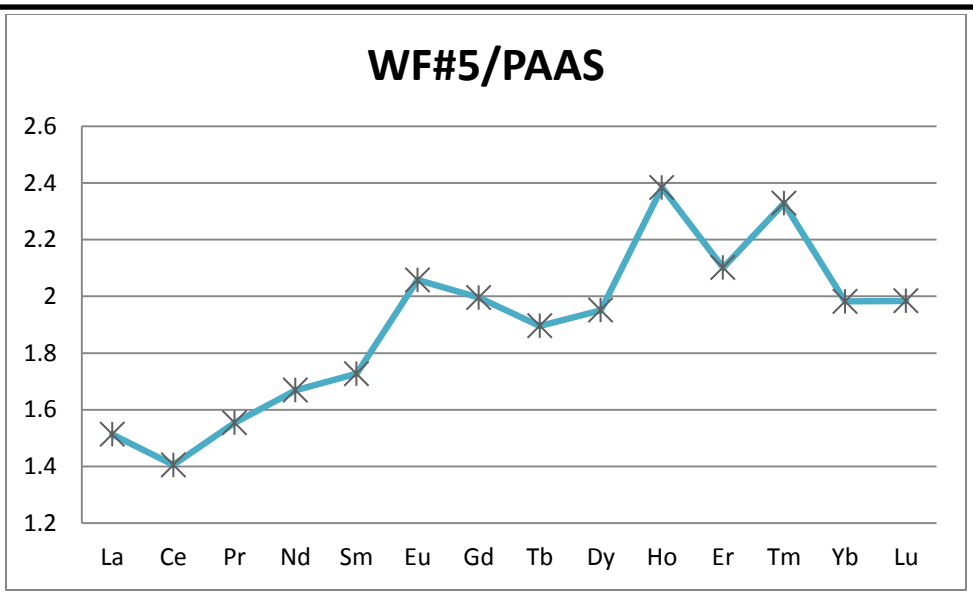

Ce/Ce*= 0.92
Eu/Eu*= 1.11

Heavy Rare Earth Element enrichment
Holmium, Thulium enrichment
MREE enrichment

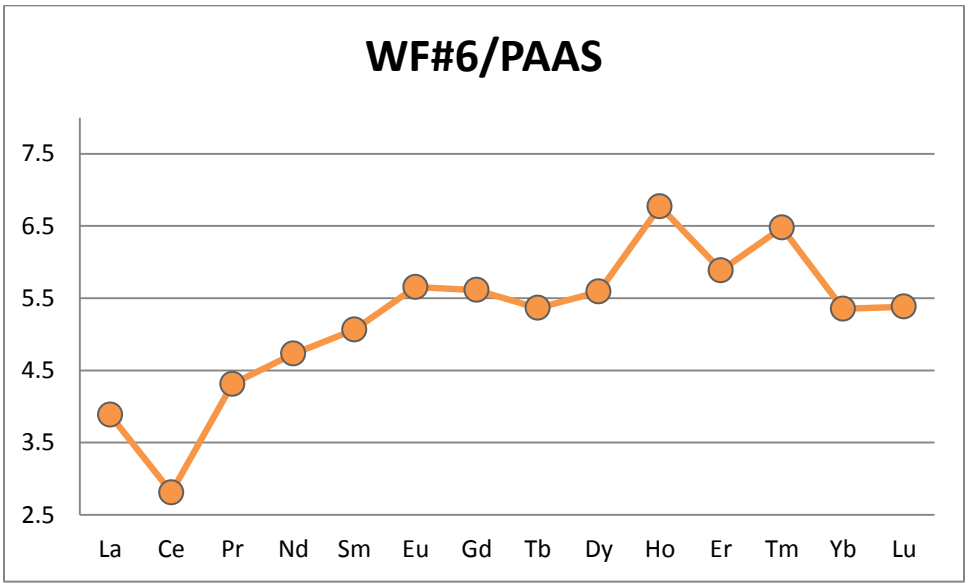

Ce/Ce*= 0.69
Eu/Eu*= 1.06

Heavy Rare Earth Element enrichment
Holmium, Thulium enrichment
MREE enrichment

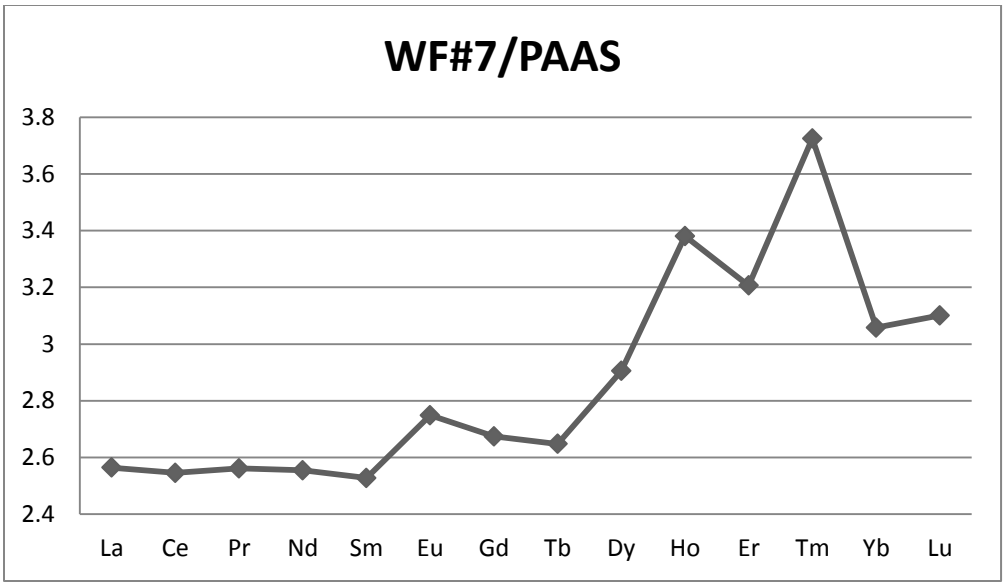

Ce/Ce*= 0.99
Eu/Eu*= 1.06

Heavy Rare Earth Element enrichment
Holmium, Thulium enrichment
No MREE trend

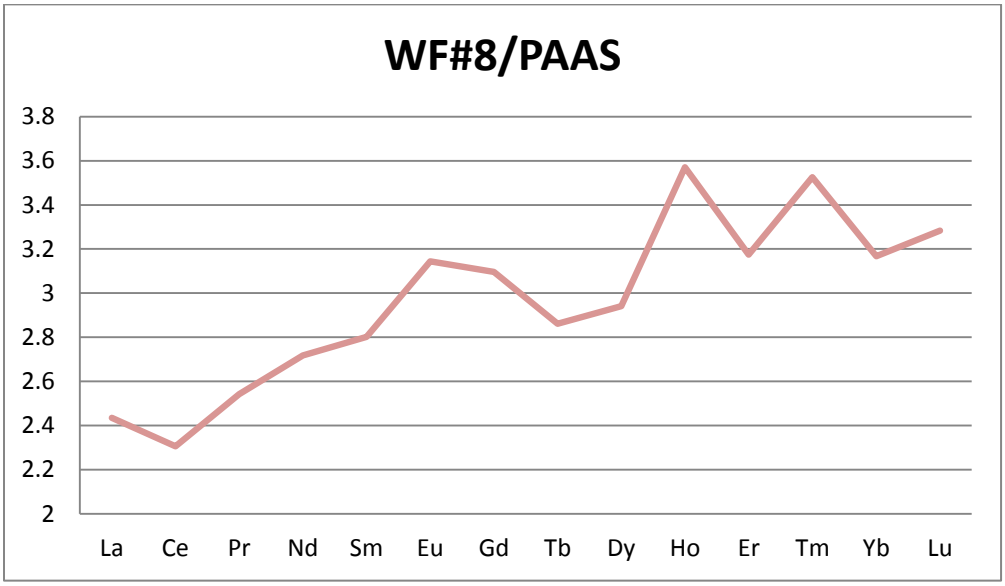

Ce/Ce*= 0.93
Eu/Eu*= 1.06

Heavy Rare Earth Element enrichment
Holmium, Thulium enrichment
MREE enrichment

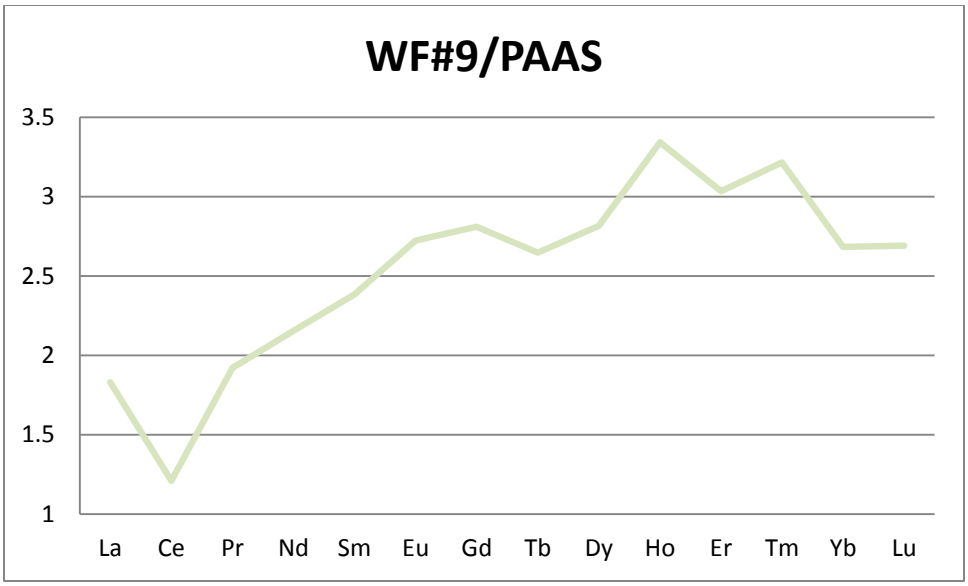

Ce/Ce*= 0.64
Eu/Eu*= 1.05

Heavy Rare Earth Element enrichment
Holmium, Thulium enrichment
MREE enrichment

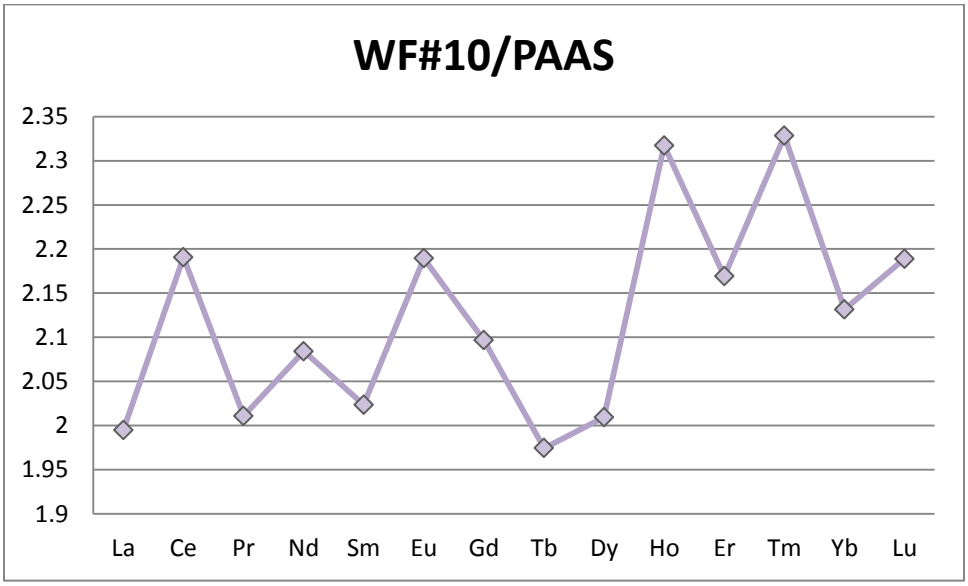

Ce/Ce*= 1.09
Eu/Eu*= 1.06

Heavy Rare Earth Element enrichment
Holmium, Thulium enrichment
No MREE trend

Phosphates influencing mree

Appendix C - REE Distribution Patterns of Inorganic Fraction of the Woodford Shale

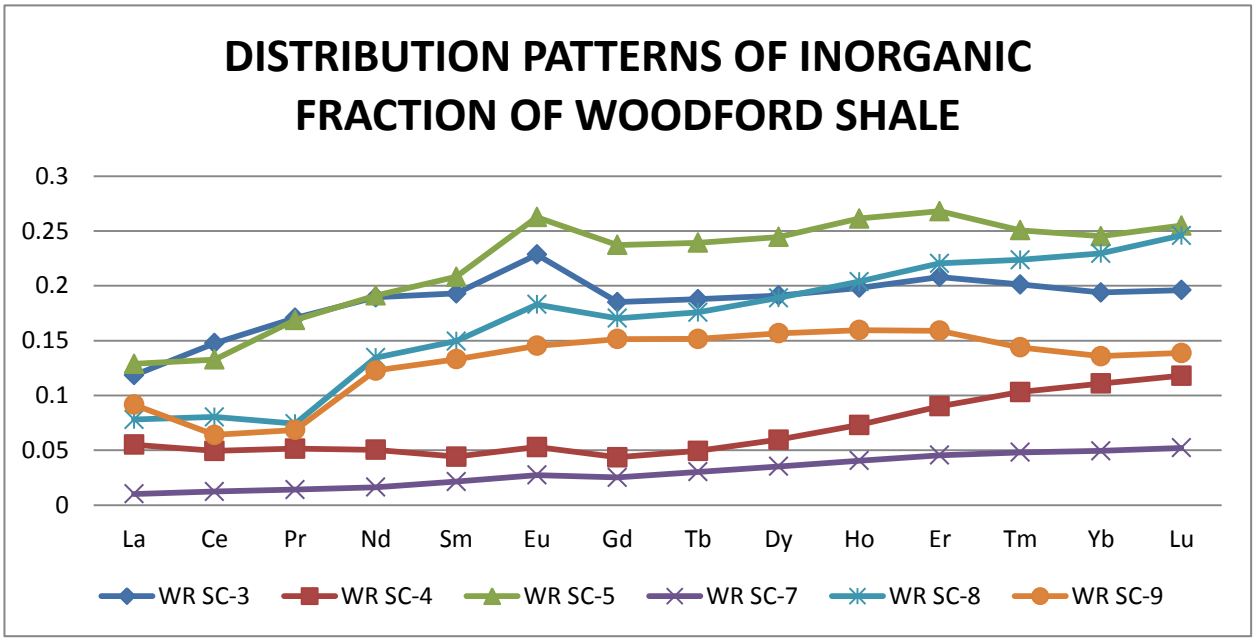

Figure 52 Distribution patterns of the Inorganic Fraction of the Woodford Shale.

This graph show the distribution patterns of the rare earth elements of the inorganic fraction of the Woodford Shale samples with a HeavyRare Earth element enrichment.

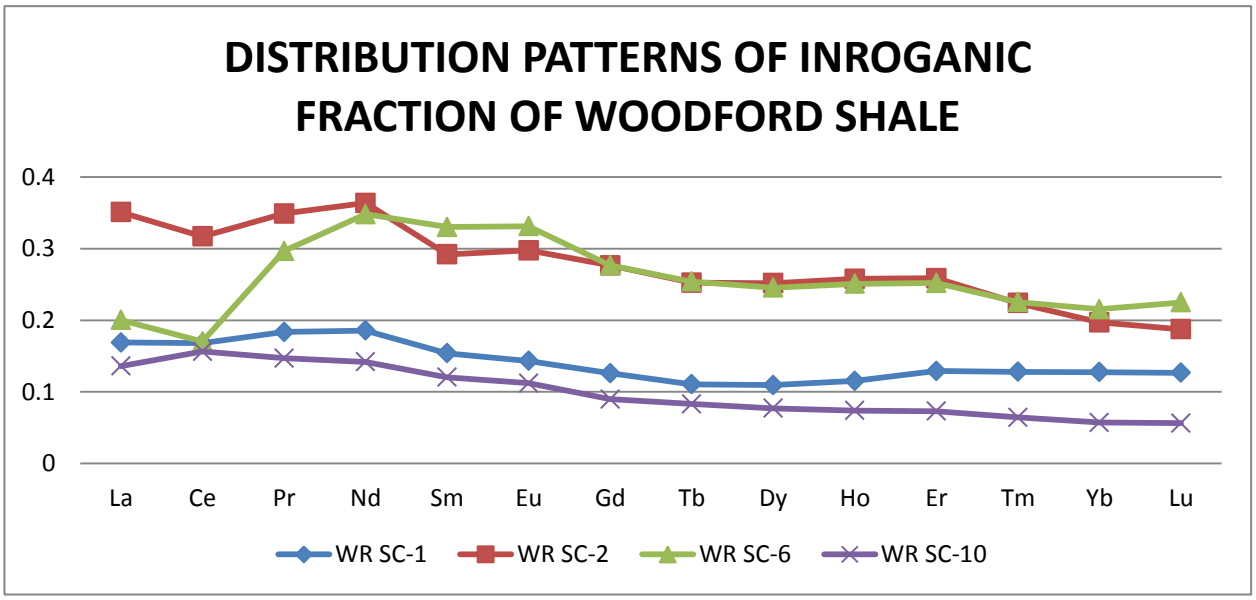

Figure 53 Distribution patterns of the Inorganic Fraction of the Woodford Shale.

The previous graph shows the distribution patterns of the inorganic portion of the Woodford Shale, where comparing with Figure #5, the samples show a consistent trend of heavy rare earth depletion. Individual distribution patterns are shown for the 10 samples in the following figures.

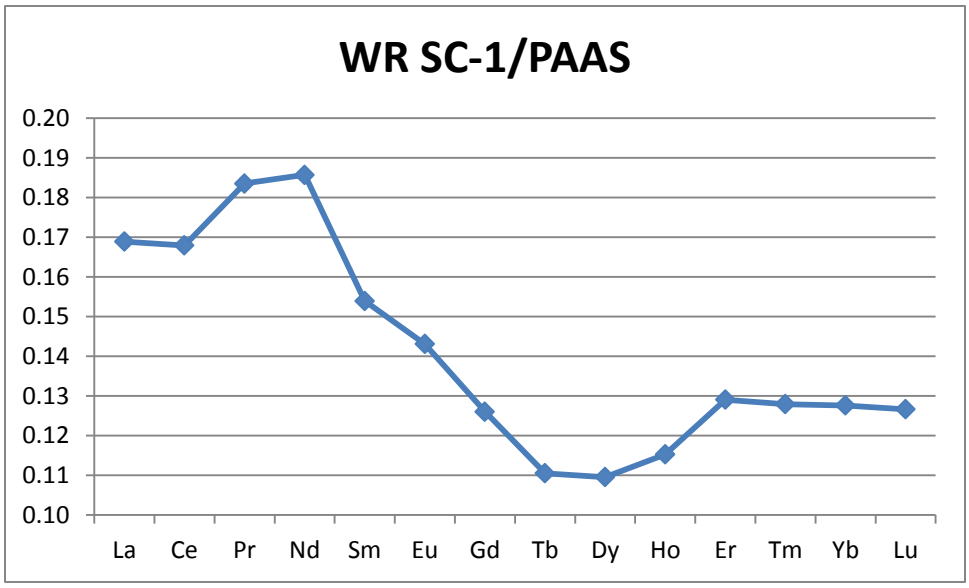

Ce/Ce*= 0.95
Eu/Eu*= 1.02

Light Rare Earth Element enrichment
MREE depletion

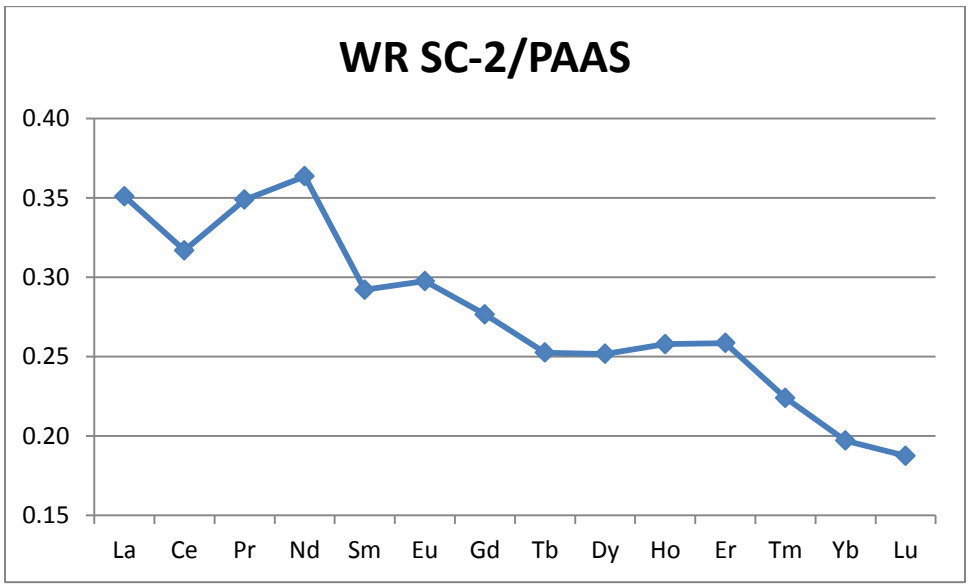

Ce/Ce*= 0.91
Eu/Eu*= 1.05

Light Rare Earth Element enrichment

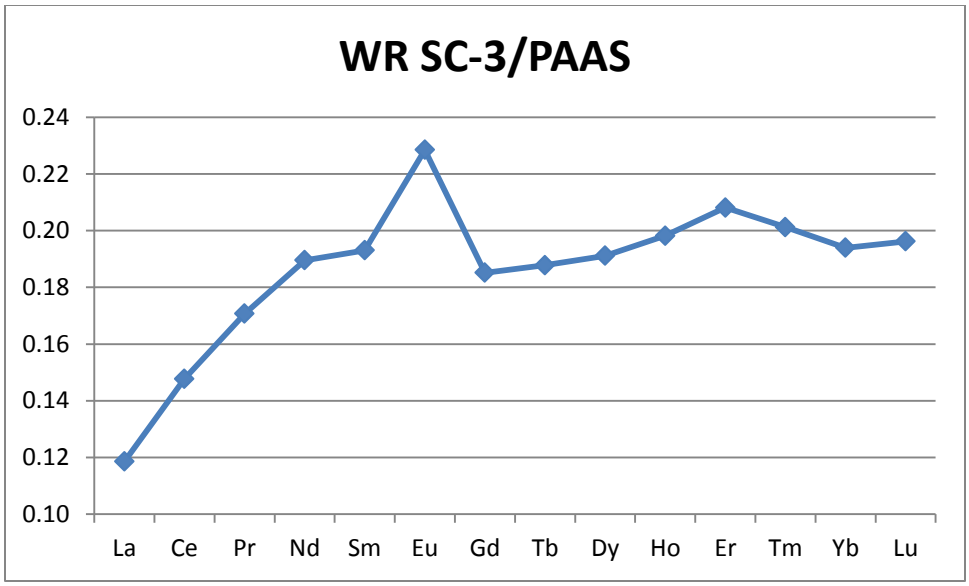

Ce/Ce*= 1.02 Heavy Rare Earth Element enrichment
Eu/Eu*= 1.21

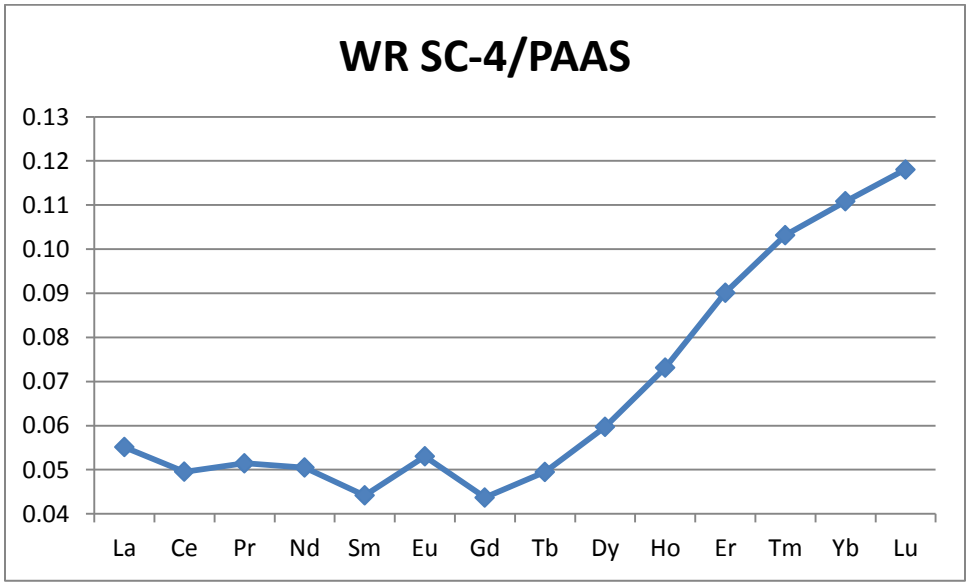

Ce/Ce*= 0.93 Heavy Rare Earth Element enrichment
Eu/Eu*= 1.21

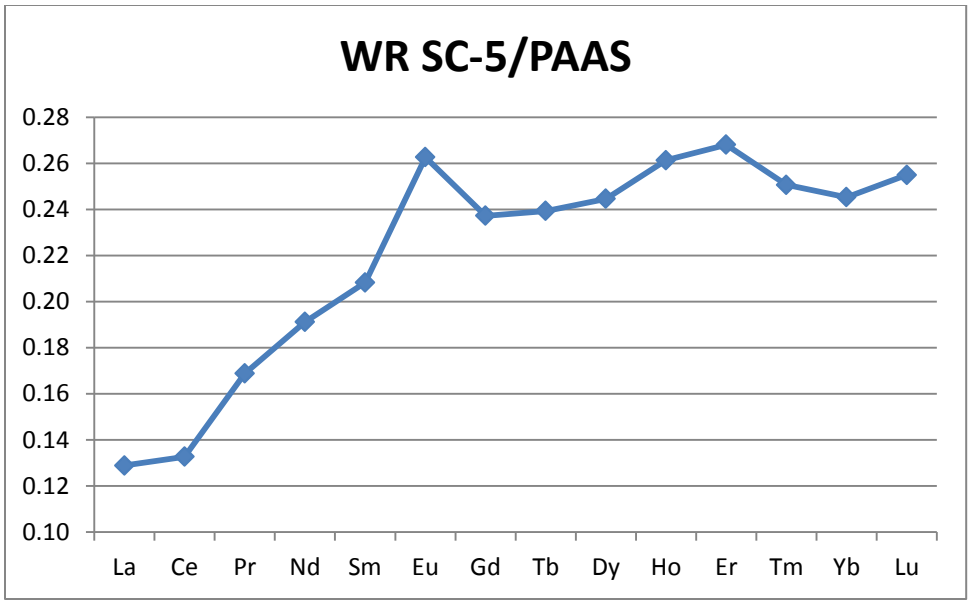

Ce/Ce*= 0.89 Heavy Rare Earth Element enrichment
Eu/Eu*= 1.18 MREE enrichment

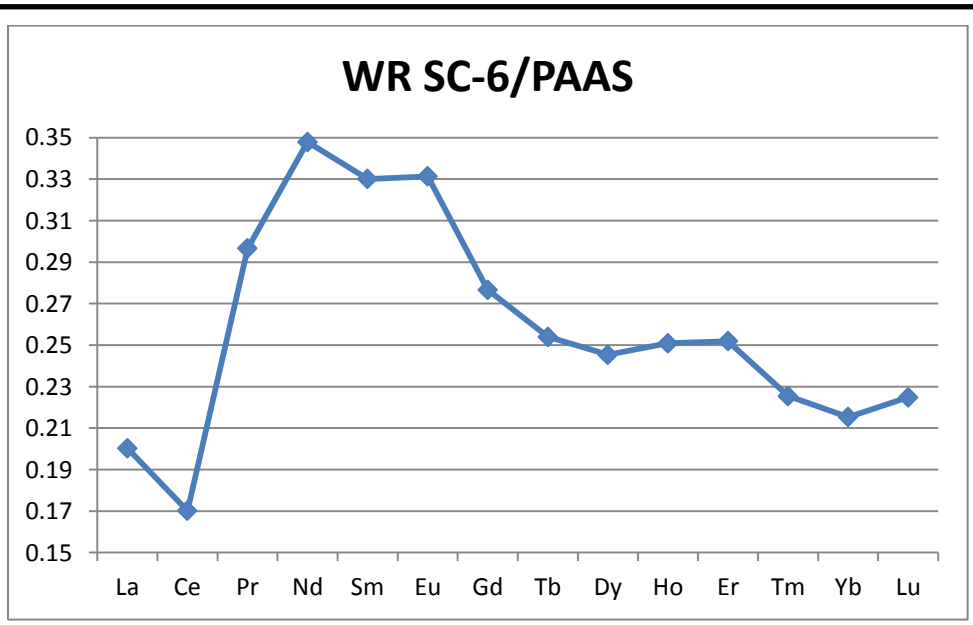

Ce/Ce*= 0.68 Light Rare Earth Element enrichment
Eu/Eu*= 1.09 MREE enrichment

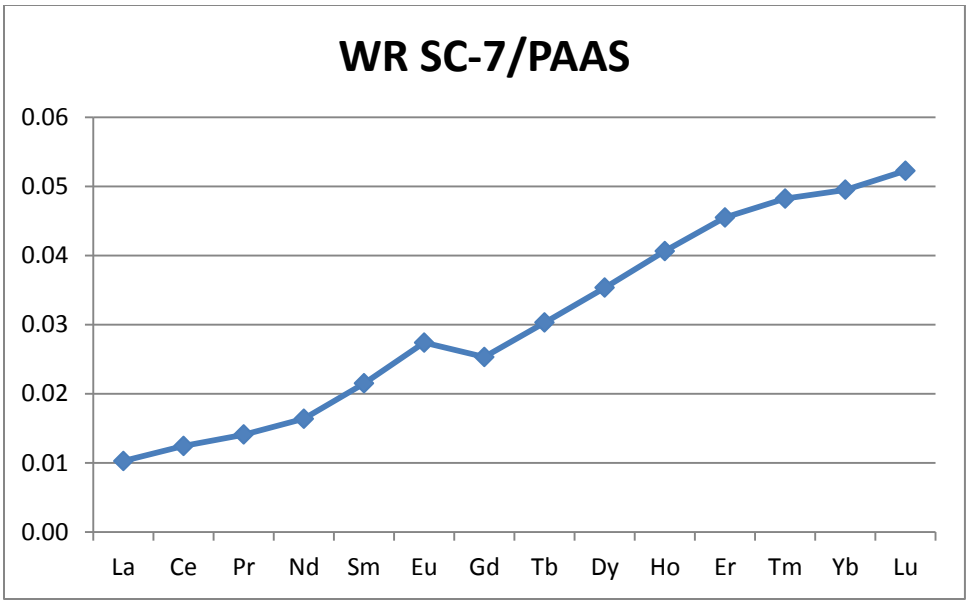

Ce/Ce*= 1.02 Heavy Rare Earth Element enrichment
Eu/Eu*= 1.17 MREE enrichment

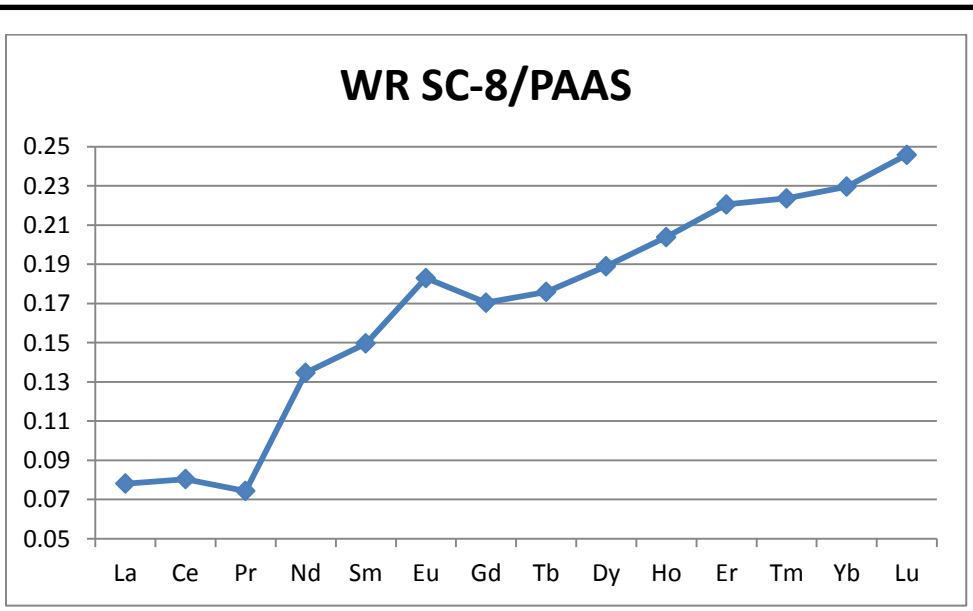

Ce/Ce*= 1.05 Heavy Rare Earth Element enrichment
Eu/Eu*= 1.14

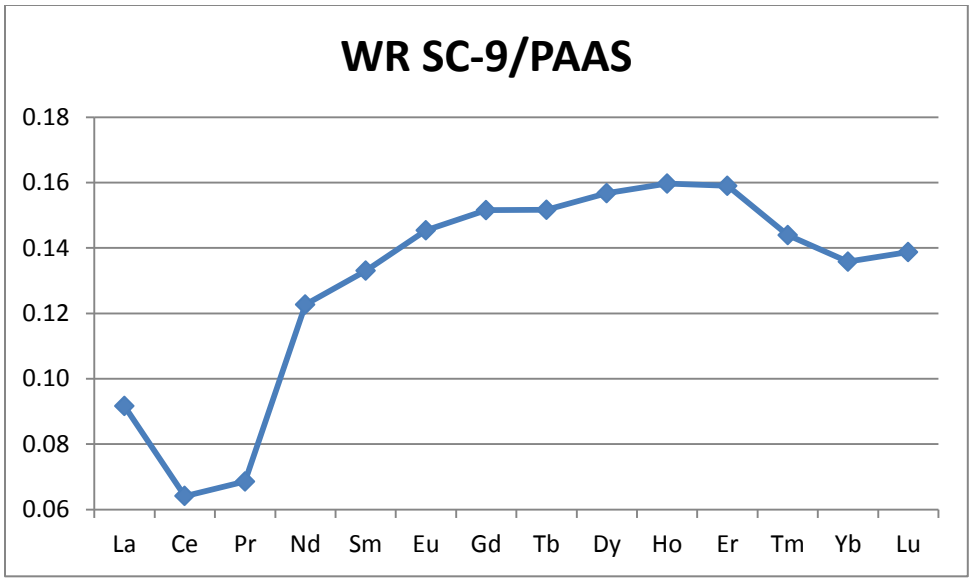

Ce/Ce*= 0.79 Heavy Rare Earth Element enrichment
Eu/Eu*= 1.02 Middle Rare Earth Element enrichment

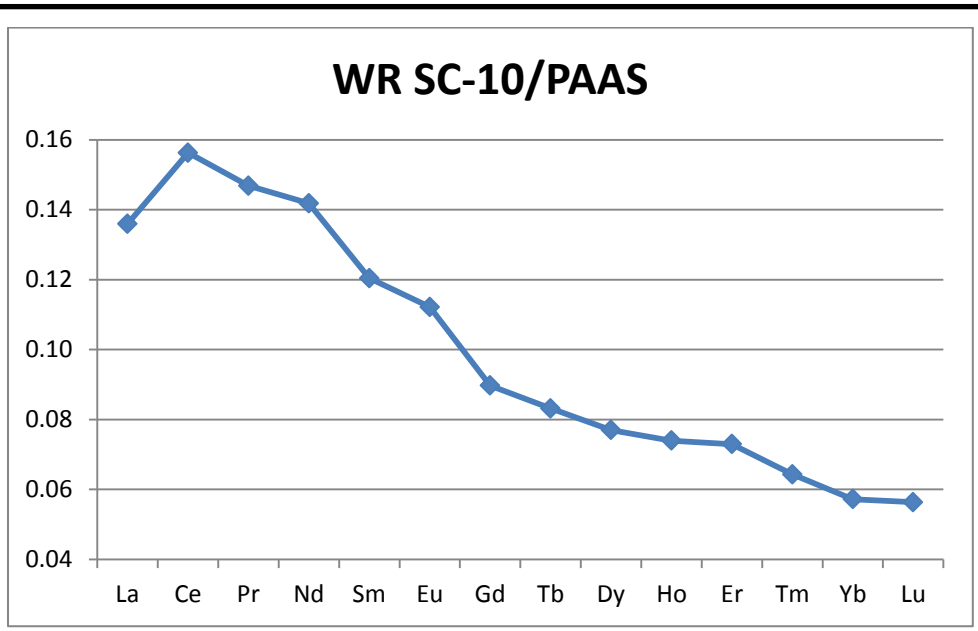

Ce/Ce*= 1.11 Light Rare Earth Element enrichment
Eu/Eu*= 1.07

Total Rare Earth Element Concentration in Inorganic Portion of Woodford Shale

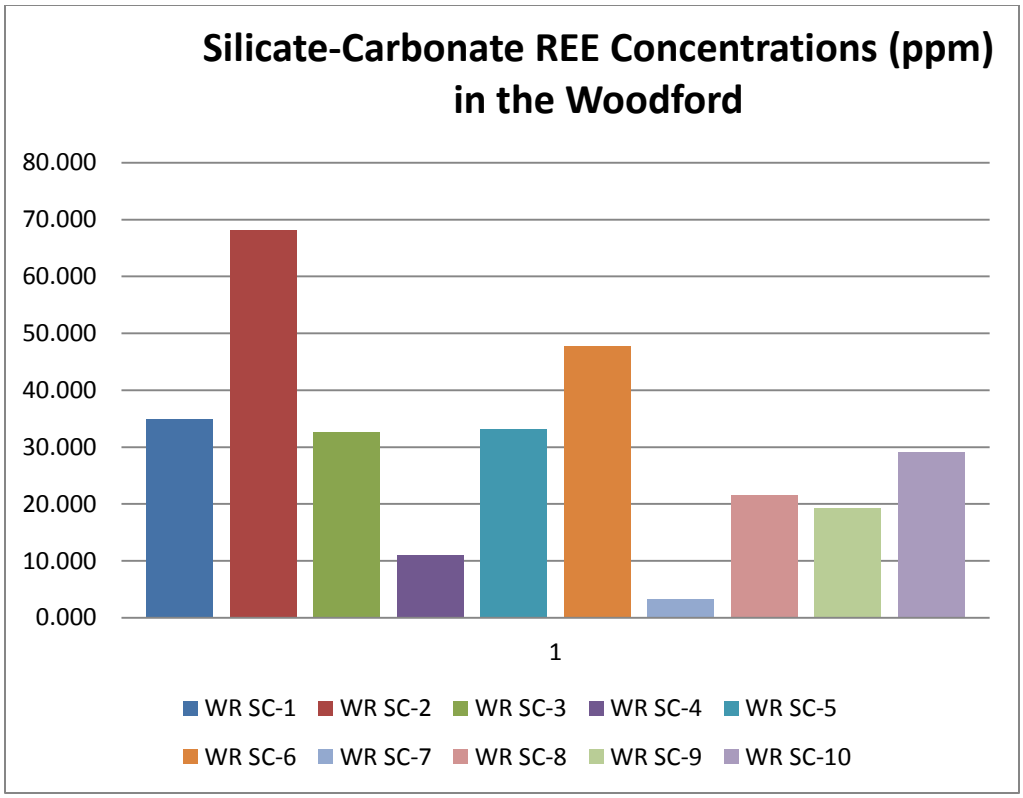

Figure 54 REE concentrations in Rock matrix

Appendix D - REE Distribution patterns in oil

Mississippian Oil

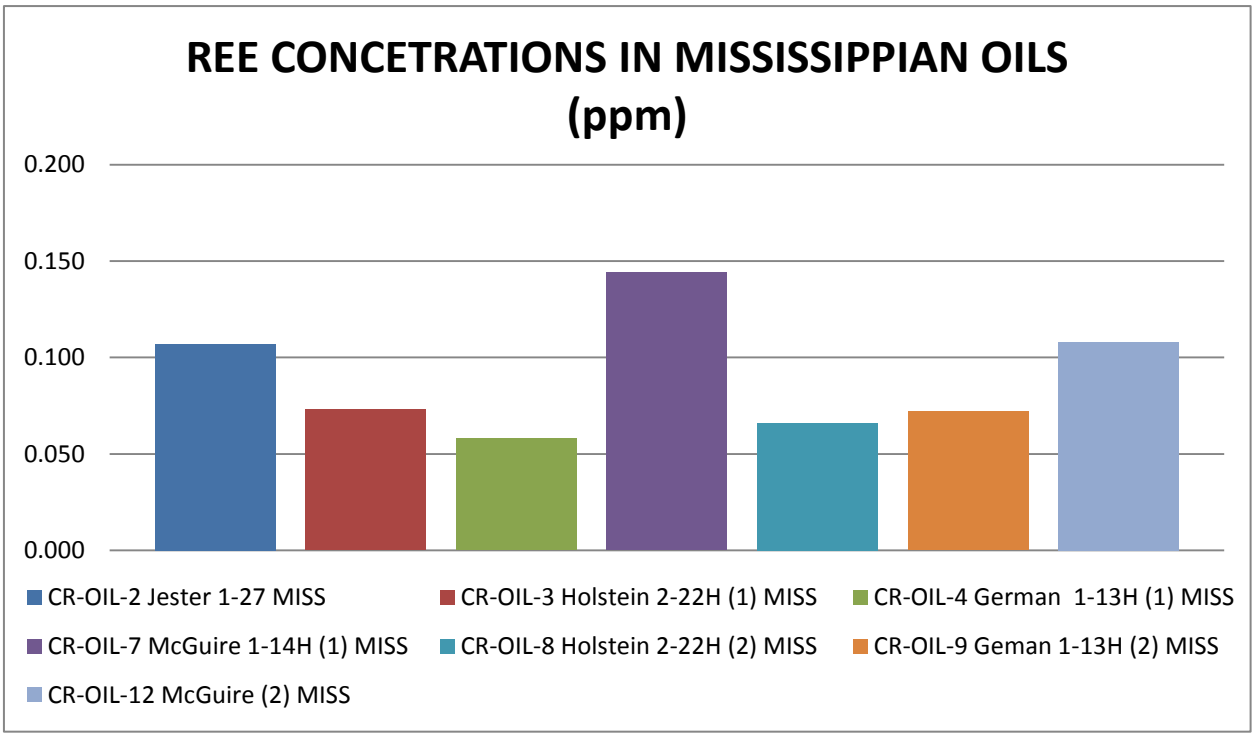

Figure 55 REE concentration in Mississippian oils

The REE concentrations are for the Devonian samples are indicated on Figure 41, and the REE concentrations for the Mississippian oils are shown in Figure 40. It is noticeable that the REE concentrations vary from one oil family to the other, showing higher REE concentration levels in Mississippian oils than in the Devonian oils. Mississippian oils show an average of Total REE of 0.087 ppm, and the Devonian show a lower REE concentration average of 0.057 ppm

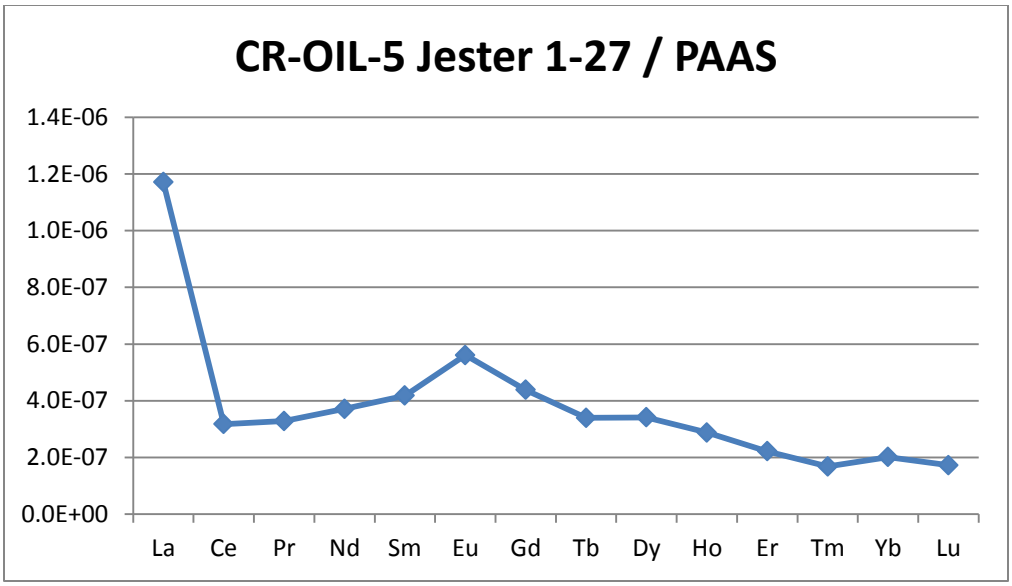

Ce/Ce*= 0.42 Light Rare Earth Element enrichment
Eu/Eu*= 1.31 Middle Rare Earth Element enrichment

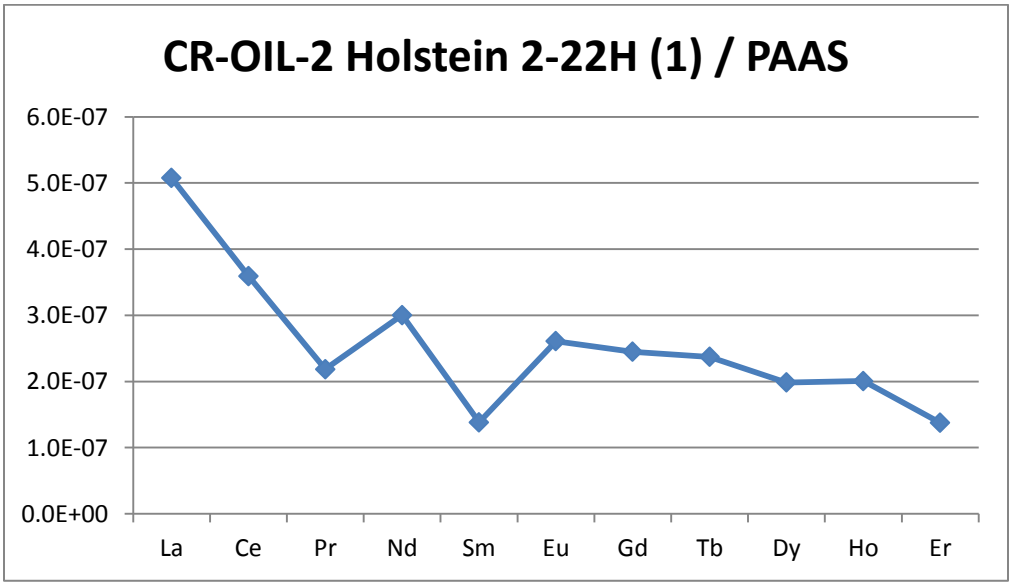

Ce/Ce*= 0.99 Light Rare Earth Element enrichment
Eu/Eu*= 1.36

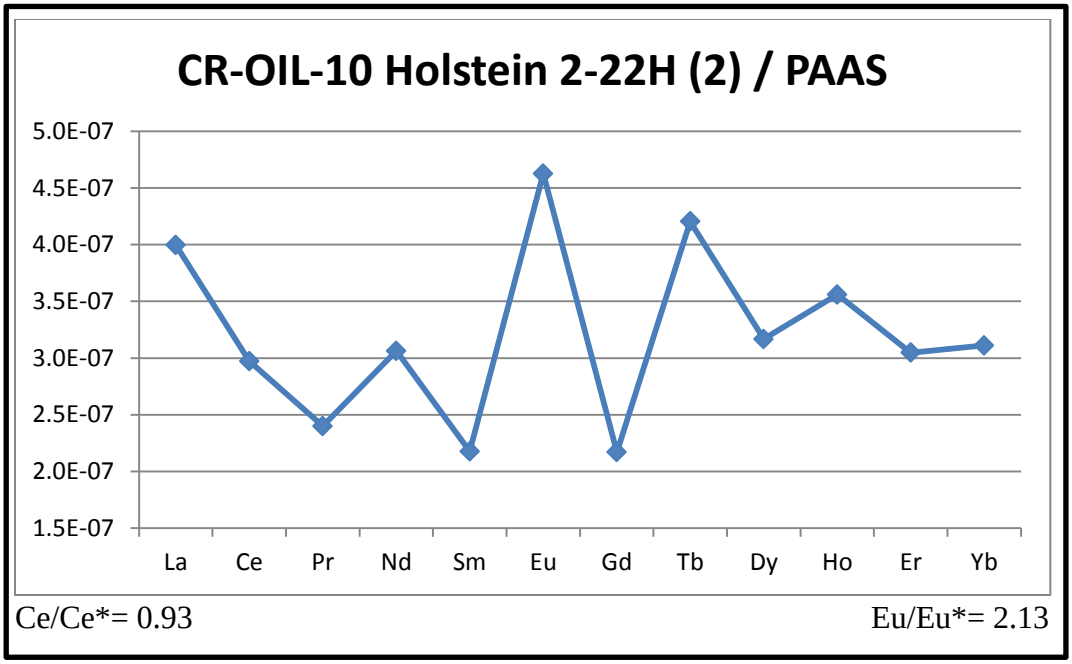

Ce/Ce*= 0.93 Eu/Eu*= 2.13

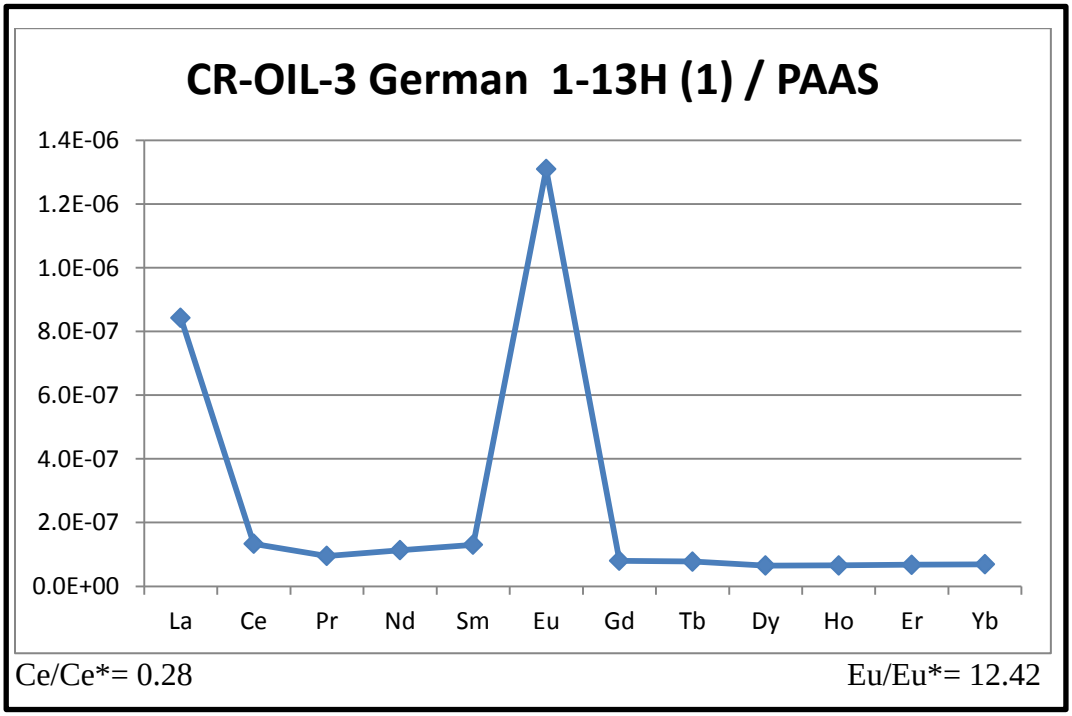

Ce/Ce*= 0.28 Eu/Eu*= 12.42

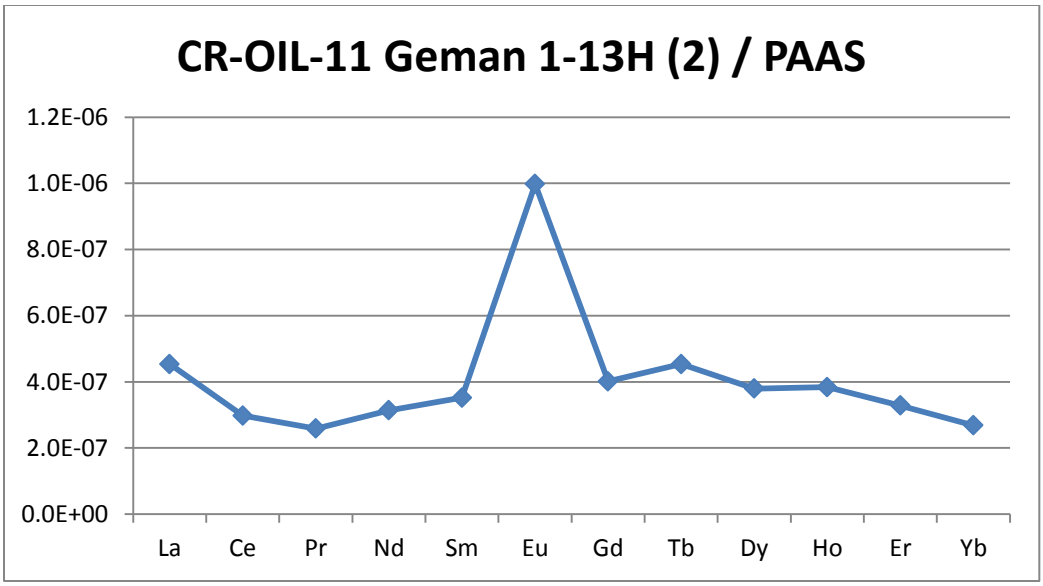

Ce/Ce*= 0.83
Eu/Eu*= 2.65

Middle Rare Earth Element enrichment

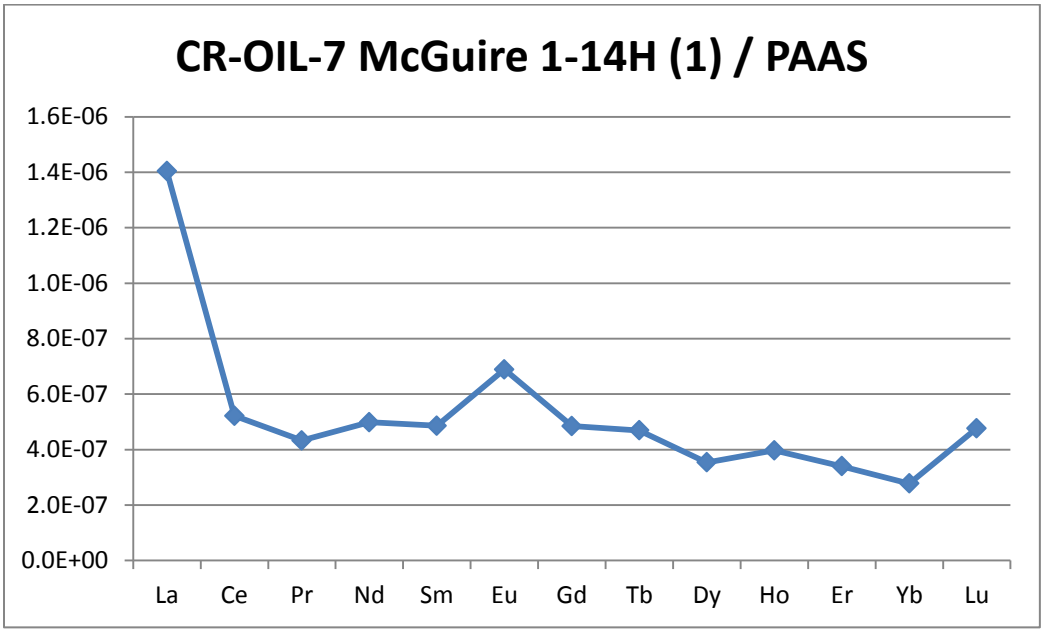

Ce/Ce*= 0.57
Eu/Eu*= 1.42

Light Rare Earth Element enrichment
Middle Rare Earth Element enrichment

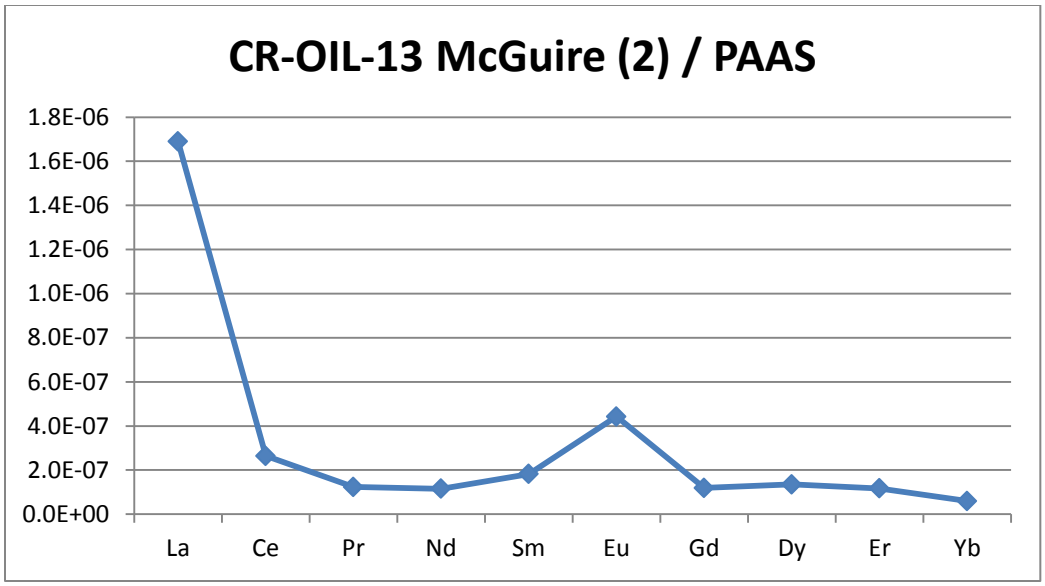

Ce/Ce*= 0.29 Light Rare Earth Element enrichment

Eu/Eu*= 2.94 Middle Rare Earth Element enrichment

Devonian Oil

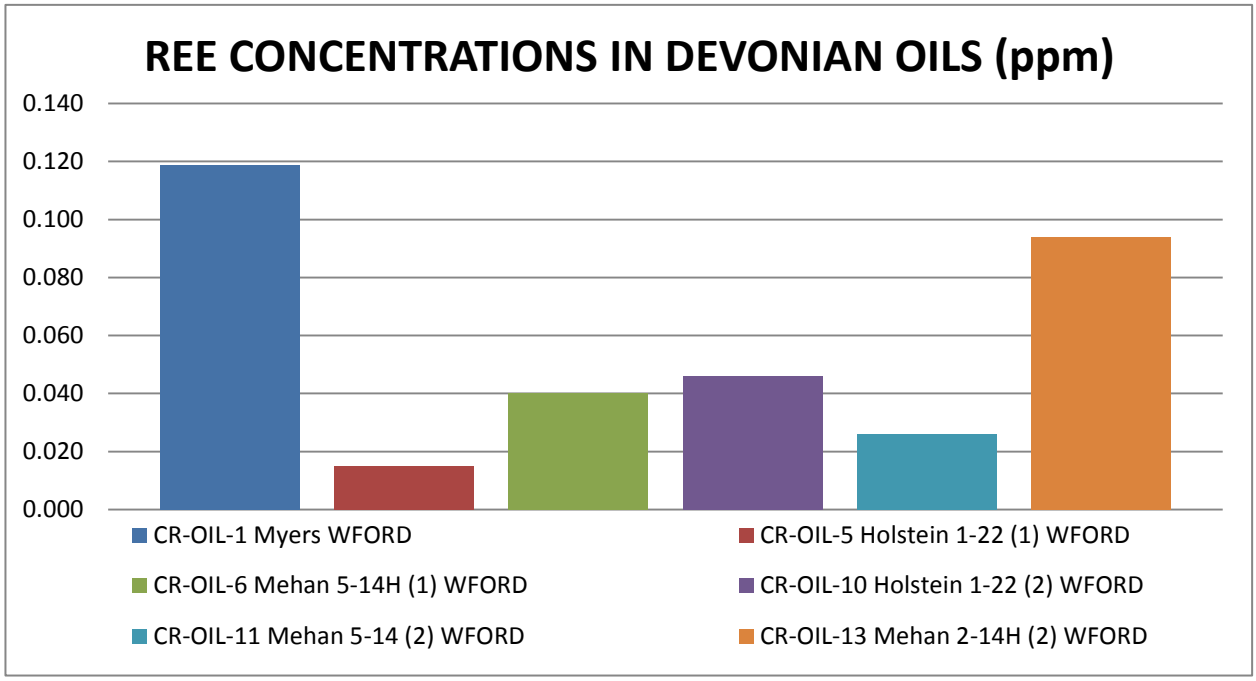

Figure 56 REE concentration in Devonian oils

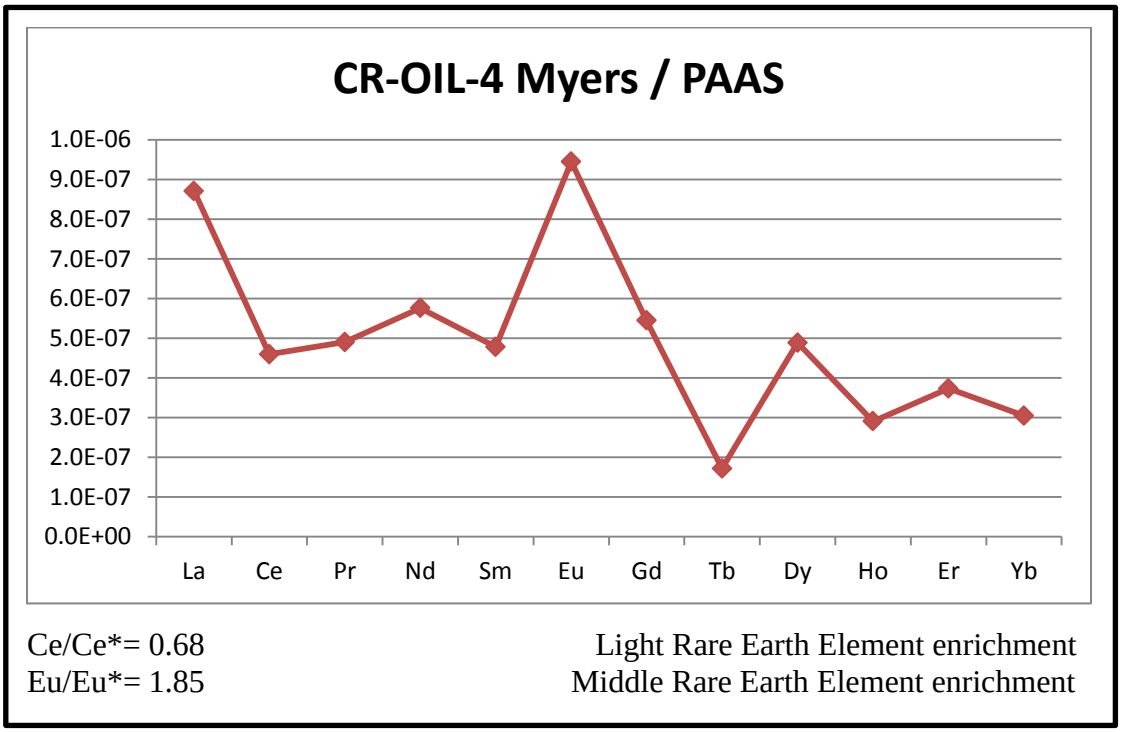

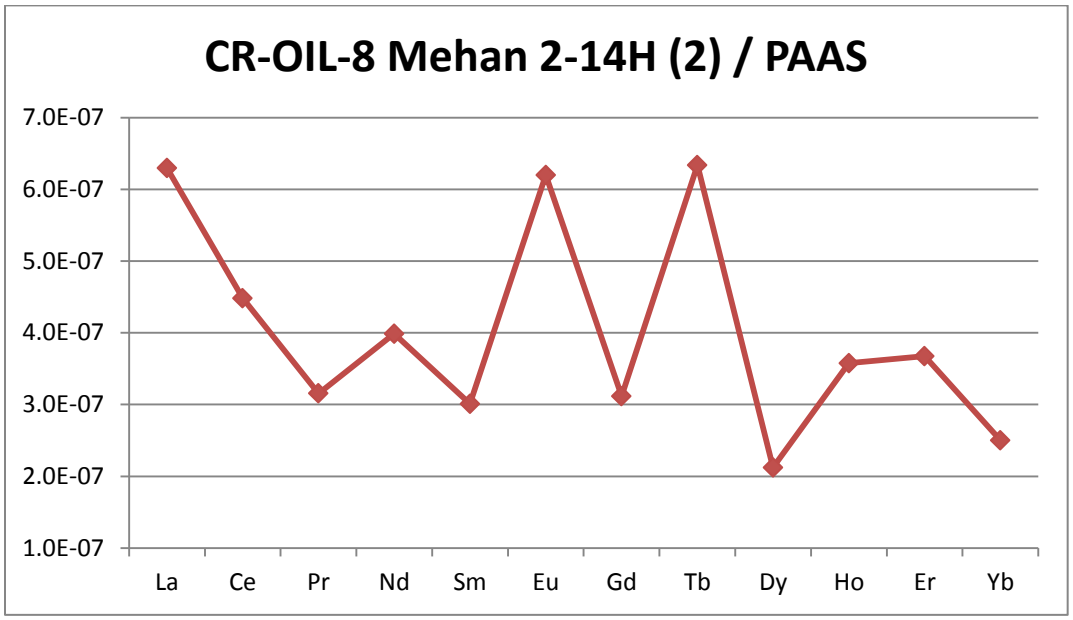

Ce/Ce*= 0.95 Light Rare Earth Element enrichment
Eu/Eu*= 2.02

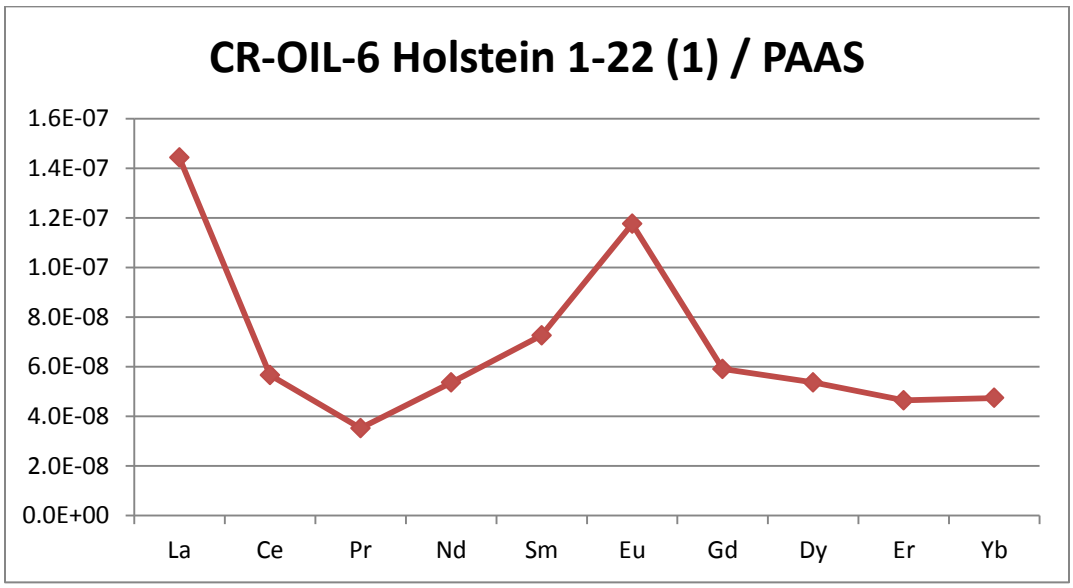

Ce/Ce*=0.63 Light Rare Earth Element enrichment
Eu/Eu*= 1.79 Middle Rare Earth Element enrichment

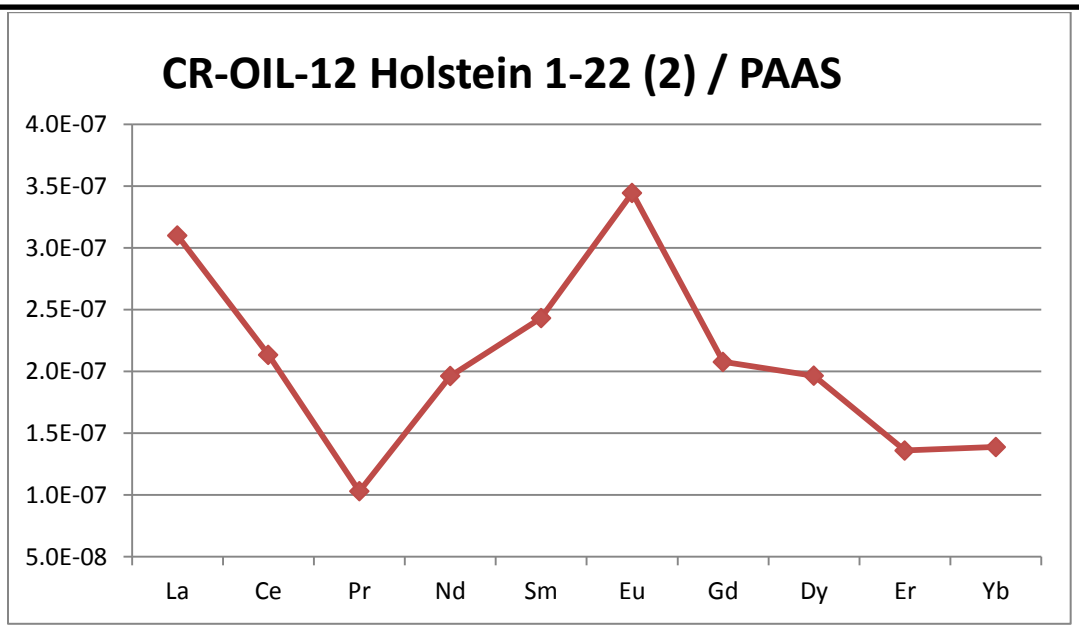

Ce/Ce*=1.03 Light Rare Earth Element enrichment
Eu/Eu*= 1.53 Middle Rare Earth Element enrichment

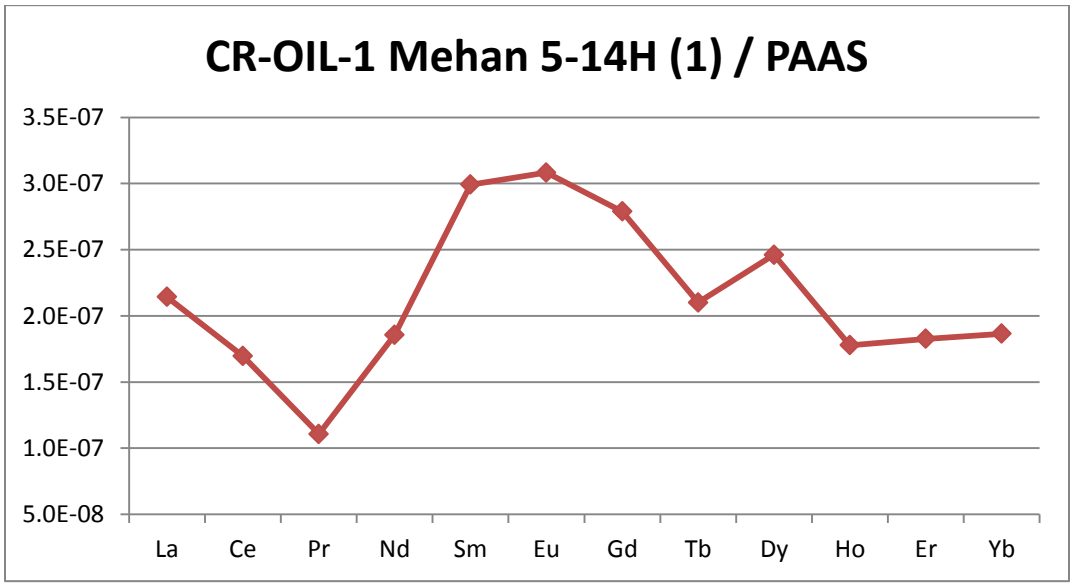

Ce/Ce*=1.04 Heavy Rare Earth Element enrichment
Eu/Eu*= 1.06 Middle Rare Earth Element enrichment

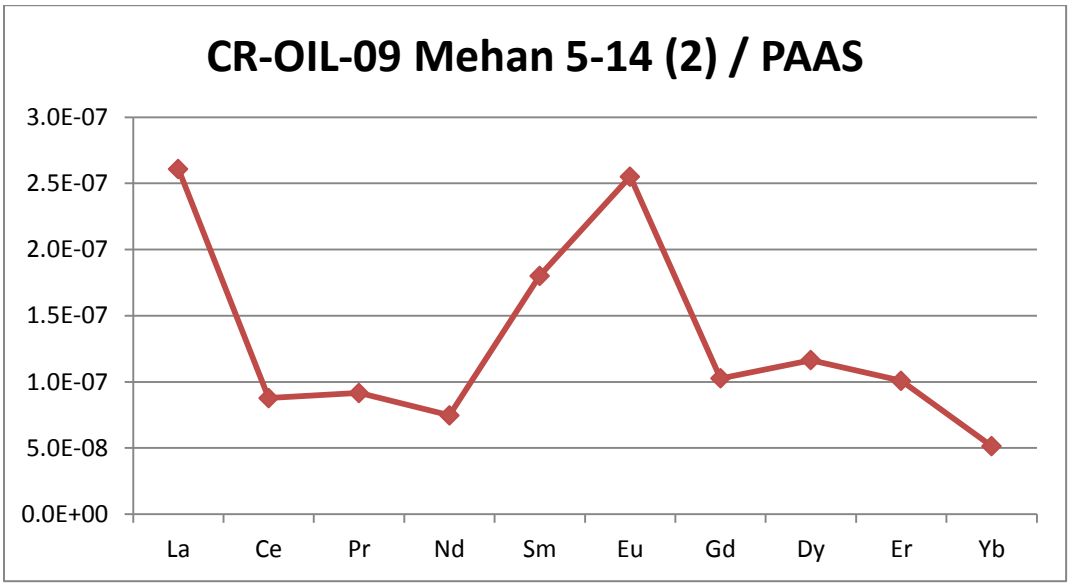

Ce/Ce*=0.49

Eu/Eu*= 1.06

Middle Rare Earth Element enrichment